National Oceanography Centre
NATURAL ENVIRONMENT RESEARCH COUNCIL

National Oceanography Centre

Internal Document No. 17

Airflow distortion at instrument sites on the ODEN during the ACSE project.

B I Moat[1], M J Yelland[1] & I M Brooks[2]

2015

[1]National Oceanography Centre, Southampton
University of Southampton Waterfront Campus
European Way
Southampton
Hants SO14 3ZH
UK

[2]Institute for Climate & Atmospheric Science
University of Leeds
Leeds
LS2 9JT
UK

Author contact details
Tel: +44 (0)23 8059 7739
Email: ben.moat@noc.ac.uk

DOCUMENT DATA SHEET

AUTHOR
MOAT, B I, YELLAND, M J & BROOKS, I M

PUBLICATION DATE 2015

TITLE
Airflow distortion at instrument sites on the ODEN during the ACSE project.

REFERENCE
Southampton, UK: National Oceanography Centre, Southampton, 114pp.
(National Oceanography Centre Internal Document, No. 17)
(Unpublished manuscript)

ABSTRACT

Wind speed measurements obtained from anemometers mounted on ships are prone to systematic errors caused by the distortion of the air flow around the ship's hull and superstructure. This report describes the results of simulations of the air flow around the ODEN made using the computational fluid dynamics (CFD) software VECTIS. The airflow distortion at anemometer sites used during the ACSE project has been quantified at a wind speed of 7 ms-1 for a wide range of wind directions: every 10 degrees from bow on to 120 degrees off the bow, and an additional run was undertaken at 150 degrees off the bow. The anemometers used in this study were located in the bows of the ship. The vertical displacements of the airflow at the anemometer sites and at a location of an aerosol intake are included. Wind speed profiles above a motion-stabilised doppler lidar were also obtained.

For bow-on flows the anemometers in the bows of the ship experienced relatively small flow distortion. At these sites the flow was decelerated by about 3% of the free stream wind speed. Over the full range of relative wind directions the flow to the METEK sonic is generally accelerated with the largest wind speed biases at flows directly over the beam. The vertical displacement of the airflow increases from around 3 m for flows directly over the bow, to around 6 m for flows over the ship's beam as the lockage of the airflow by the ship becomes greater.

The vertical displacement at the aerosol intake location varied from 6m for flows directly over the bow, to around 16 m for flows over the ship's beam. The ship imposes a significant obstacle to the flow and forces a strong vertical velocity in the lowest few tens of meters above the lidar.

KEYWORDS

ISSUING ORGANISATION
National Oceanography Centre
University of Southampton Waterfront Campus
European Way
Southampton SO14 3ZH
UK

Page intentionally left blank

LIST OF TABLES

AIRFLOW DISTORTION AT INSTRUMENT SITES ON THE *ODEN* DURING THE ACSE PROJECT

B. I. Moat, M. J. Yelland and I. M. Brooks

December 2015

1. INTRODUCTION

Wind speed measurements from ship-based anemometers are biased by the distortion of the airflow by the ship's hull and superstructure. For example, previous computational fluid dynamics (CFD) modelling has shown that anemometers located on the foremast platform of the RRS *Charles Darwin* experience a flow distortion of up to 14 % of the freestream or undisturbed wind speed for flows directly over the bow (Yelland et al. 1998). The effect is less severe for wind speed measurements made from the foremast platform of the RRS *Discovery* as the ship is more streamlined in shape (Yelland et al. 2002). This report describes an investigation of the airflow around the *Oden*. The study used a CFD model to simulate the airflow over the ship in order to quantify the effects of airflow distortion on wind speed measurements made at various instrument sites. Corrections are derived for instrument sites used during the ACSE project between July and October 2014.

The VECTIS code is described in Section 2 and the ACSE instrument positions are detailed in Section 3. The effects of flow distortion are dependent on the anemometer location and vary with changes in relative wind direction (Yelland et al., 2002). Therefore the airflow over the ship was simulated for flows directly over the bow (a wind direction of 0 degrees), and at 10, 20, 30, 40, 50, 60, 70, 80, 90, 100, 110, 120 and 150 degrees over the starboard bow. Effective anemometer positions were created to enable the wind speed bias for winds over the port bow to be calculated from the VECTIS simulations of the airflow over the starboard bow: since the ship is roughly symmetrical, an instrument position on the starboard side of the ship could be mirrored to an "effective" positions on the port side. The wind speed bias, the angles of deflection of the flow and the vertical displacement of the flow were calculated for all the sensor locations, and the results are discussed in Section 4.

2. DESCRIPTION OF THE *ODEN* MODELS

VECTIS (Ricardo, 2015) is a commercial three-dimensional Reynolds Averaged Navier-Stokes solver, which has been used successfully since 1994 to model the airflow over many research ships (Yelland et al. 1998; 2002; Moat and Yelland, 2008). These VECTIS simulations (version 2015.1) only reproduce the steady state mean flow characteristics using the standard k-ε (Launder and Spalding, 1974) turbulence closure model to parameterise the turbulence. Except when the anemometer is in the wake of an upstream obstacle, VECTIS simulations of the airflow over detailed ship geometries are accurate to within 2 % (Yelland et al., 2002) for well-exposed anemometer locations on research ships. The full-scale 3-dimensional geometry was created using the software package FEMGV (Version 7.2 - TNO Diana, 2010). The geometry was exported from FEMGV in ABAQUS format and converted into a VECTIS surface definition file using VECTIS translators (APPENDIX C). The

numerical representation of the geometry was very detailed (Figure 1) and reproduced the actual geometry to within 0.1 m. The general ship dimensions are 107.9 m in overall length and 31 m in breadth. A computational domain was defined around the geometry with the ship in the centre. The width of the domain increased with the ship's orientation to the flow to prevent spurious increases in wind speed created by the blockage of the ship in the domain. For all flows direction the computational volume was 1000 m long (-500 m < x < 500 m), 1800 m wide (-900 m < y < 900 m) and 250 m high (0 m < z < 250 m). In general, the ratio of the frontal area of the ship to the area of the inlet gave a blockage by the ship of less than 0.01.

The number of computational cells within the domain was around 5 to 6 million. The time taken for each simulation to converge was about 12 hours using 8 x 3.3 GHz Xeon cores on a Linux workstation. This fast convergence time was obtained using the steady-state rather than the time-marching solver (Moat and Yelland, 2006). The cell sizes varied throughout the computational domain with high-resolution cells in the vicinity of the foremast (cells of around 0.10 m) and much lower resolution cells in areas well away from the ship where the flow did not vary very rapidly.

The vertical profile of the velocity at each domain inlet was specified as a fully logarithmic boundary layer profile with a wind speed at a height of 10 m of 7 ms^{-1};

$$U10_n = \frac{U*}{k_v} ln\left(\frac{10}{z_0}\right) \quad (1)$$

where k_v is the von Karman constant (value 0.4), z_o is the roughness length and u* is the friction velocity calculated from the Smith (1980) drag coefficient relationship. The domain floor was allocated a small roughness length (order 10^{-4} m) in order to maintain the profile downwind of the inlet. All results presented in this report were obtained by comparing the wind speed at a particular anemometer position with the free stream wind speed profile 850 m abeam of the anemometer position to arrive at a percentage wind speed bias for that position.

3. THE INSTRUMENT LOCATIONS

During ACSE the ships foremast was instrumented with: a METEK uSonic-3 sonic anemometer from University of Leeds, UK., and a CSAT sonic anemometer from the University of Stockholm. The METEK and CSAT anemometers where both located on the centreline of the ship, this results in a symmetric wind speed bias and vertical displacement for flows over either beam. Wind profiles were also obtained from a Doppler Lidar. Additional wind speed measurements were made from the ship's weather station and ship's anemometer. Future science campaigns on the Oden will be obtaining air samples for aerosols measurement. The origin of the air upstream is important for aerosols measurements and is contained in this report. The instrument positions are indicated in Figure 1 and the co-ordinates are shown for the model with a flow directly over the bow. The instrument locations relative to the foremast and the bridge are shown schematically in Figures 2 and 3. The ship model geometry was created from the general arrangement plans and has a draught of 7.5 m. The instrument positions were calculated based on their position relative to the deck, which equates to a height above the waterline of 20.58m for the METEK (as shown in Figure 1 and throughout the rest of the report). In the VECTIS co-ordinates system, the instrument positions for the METEK and CSAT

are detailed in Table 1. The ship's weather station, ship's anemometer, and Lidar are detailed in Table 2. The aerosol intake is discussed in Section 4.3.

Relative Wind Direction (degrees)	METEK sonic (x, y, z)	CSAT sonic (x, y, z)
0 (bow-on)	(52.26, 0.0, 20.58)	(53.83, 0.0, 16.03)
±10	(51.47 ,9.08, 20.58)	(53.01, 9.35, 16.03)
±20	(49.11, 17.87, 20.58)	(50.58, 18.41, 16.03)
±30	(45.26, 26.13, 20.58)	(46.62, 26.92, 16.03)
±40	(40.03, 33.59, 20.58)	(41.24, 34.60, 16.03)
±50	(33.59, 40.03, 20.58)	(34.60, 41.24, 16.03)
±60	(26.13, 45.26, 20.58)	(26.92, 46.62, 16.03)
±70	(17.87, 49.11, 20.58)	(18.41, 50.58, 16.03)
±80	(9.08, 51.47, 20.58)	(9.35, 53.01, 16.03)
±90	(0.0, 52.26, 20.58)	(0.0, 53.83, 16.03)
±100	(-9.08, 51.47, 20.58)	(-9.35, 53.01, 16.03)
±110	(-17.87, 49.11, 20.58)	(-18.41, 50.58, 16.03)
±120	(-26.13, 45.26, 20.58)	(-26.92, 46.62, 16.03)
±150	(-45.26, 26.13, 20.58)	(-46.62, 26.92, 16.03)

Table 1. Instrument positions in the VECTIS co-ordinate system for the METEK and CSAT sonics. The z value is the height of the anemometer above the sea surface. A schematic of the locations is shown in Figures 2 and 3.

Relative Wind Direction (degrees)	Weather station (x, y, z)	Ship's anemometer (x, y, z) PORT (x, y, z) STARBOARD	Lidar (x, y, z)
-150 (port)	(-12.61, 8.34, 26.32)	(-8.57, 7.84, 35.98) (-11.07, 3.50, 35.98)	(-24.29, 20.70, 13.39)
-120 (port)	(-6.75, 13.53, 26.32)	(-3.50, 11.07, 35.98) (-7.84, 8.57, 35.98)	(-10.68, 30.07, 13.39)
-110 (port)	(-4.30, 14.49, 26.32)	(-1.53, 11.51, 35.98) (-6.23, 9.80, 35.98)	(-5.30, 31.46, 13.39)
-100 (port)	(-1.71, 15.02, 26.32)	(0.49, 11.60, 35.98) (-4.43, 10.73, 35.98)	(0.24, 31.91, 13.39)
-90 (beam-on port)	(0.92, 15.09, 26.32)	(2.50, 11.34, 35.98) (-2.5, 11.34, 35.98)	(5.78, 31.38, 13.39)
-80 (port)	(3.53, 14.70, 26.32)	(4.43, 10.73, 35.98) (-0.49, 11.60, 35.98)	(11.14, 29.90, 13.39)
-70 (port)	(6.03, 13.87, 26.32)	(6.23, 9.80, 35.98) (1.53, 11.51, 35.98)	(16.16, 27.51, 13.39)
-60 (port)	(8.34, 12.61, 26.32)	(7.84, 8.57, 35.98) (3.5, 11.07, 35.98)	(20.70, 24.29, 13.39)
-50 (port)	(10.40, 10.97, 26.32)	(9.20, 7.08, 35.98) (5.37, 10.29, 35.98)	(24.60, 20.32, 13.39)
-40 (port)	(12.15, 8.99, 26.32)	(10.29, 5.37, 35.98) (7.08, 9.20, 35.98)	(27.75, 15.74, 13.39)
-30 (port)	(13.53, 6.75, 26.32)	(11.07, 3.50, 35.98) (8.57, 7.84, 35.98)	(30.07, 10.68, 13.39)
-20 (port)	(14.49, 4.30, 26.32)	(11.51, 1.53, 35.98) (9.80, 6.23, 35.98)	(31.46, 5.30, 13.39)
-10 (port)	(15.02, 1.71, 26.32)	(11.60, -0.49, 35.98) (10.73, 4.43, 35.98)	(31.91, -0.24, 13.39)
0	(15.09, 0.92, 26.32)	(11.34, 2.5, 35.98) (11.34, -2.5, 35.98)	(31.38, 5.78, 13.39)
10 (starboard)	(14.7, 3.53, 26.32)	(10.73, 4.43, 35.98) (11.60, -0.49, 35.98)	(29.90, 11.41, 13.39)
20 (starboard)	(13.87, 6.03, 26.32)	(9.80, 6.23, 35.98) (11.51, 1.53, 35.98)	(27.51, 16.16, 13.39)
30 (starboard)	(12.61, 8.34, 26.32)	(8.57, 7.84, 35.98) (11.07, 3.50, 35.98)	(24.29, 20.70, 13.39)
40 (starboard)	(10.97, 10.40, 26.32)	(7.08, 9.20, 35.98) (10.29, 5.37, 35.98)	(20.32, 24.60, 13.39)
50 (starboard)	(8.99, 12.15, 26.32)	(5.37, 10.29, 35.98) (9.20, 7.08, 35.98)	(15.74, 27.75, 13.39)
60 (starboard)	(6.75, 13.53, 26.32)	(3.5, 11.07, 35.98) (7.84, 8.57, 35.98)	(10.68, 30.07, 13.39)
70 (starboard)	(4.30, 14.49, 26.32)	(1.53, 11.51, 35.98) (6.23, 9.80, 35.98)	(5.30, 31.46, 13.39)
80 (starboard)	(1.71, 15.02, 26.32)	(-0.49, 11.60, 35.98)	(-0.24, 31.91, 13.39)

		(4.43, 10.73, 35.98)	
90 (starboard)	(-0.92, 15.09, 26.32)	(-2.5, 11.34, 35.98) (2.50, 11.34, 35.98)	(-5.78, 31.38, 13.39)
100 (starboard)	(-3.53, 14.70, 26.32)	(-4.43, 10.73, 35.98) (0.49, 11.60, 35.98)	(-11.14, 29.90, 13.39)
110 (starboard)	(-6.03, 13.87, 26.32)	(-6.23, 9.80, 35.98) (-1.53, 11.51, 35.98)	(-16.16, 27.51, 13.39)
120 (starboard)	(-8.34, 12.61, 26.32)	(-7.84, 8.57, 35.98) (-3.50, 11.07, 35.98)	(-20.70, 24.29, 13.39)
150 (starboard)	(-13.53, 6.75, 26.32)	(-11.07, 3.50, 35.98) (-8.57, 7.84, 35.98)	(-30.07, 10.68, 13.39)

Table 2. Instrument positions in the VECTIS co-ordinate system. The z value is the height of the anemometer above the sea surface. A schematic of the locations is shown in Figures 2 and 3.

4. CFD RESULTS

4.1 Introduction

This section summarises the results of all eight models. Each model had converged when the residuals of velocity (U, V, W), turbulent kinetic energy (K), rate of dissipation of K (E) and pressure (P) were less than 10^{-6}. As an example, Figure 4 shows the residuals for the 90 degree beam-on model. Once the models had converged post-processing files were written for the extraction of data throughout the computational volumes. The flow at the sides and ends of the tunnel were examined to check that the flow was undisturbed by the presence of the ship and could therefore be used to estimate the free stream flow (Section 4.2). The vertical displacement of the flow at the instrument sites was quantified along with the angle of the deflection of the flow away from the horizontal ("tilt") and the angle of deflection on the horizontal plane ("twist") (Section 4.3). The absolute wind speed bias was calculated as well as the wind speed bias accounting for the vertical displacement of the air (Section 4.4).

4.2 The free stream flow

The flow in the computational volume was examined to check that free stream conditions existed at the sides and ends of the tunnel, i.e. that the presence of the ship did not cause a significant blockage of the flow to these regions. As an example, Figure 5a shows the variation in velocity along the tunnel for all simulations. The data were extracted on a plane 50 m in from the tunnel wall, i.e. towards one side of the tunnel, between $-500 \text{ m} < x < 500 \text{ m}$ and at heights z of 10 m, 30 m and 50 m. This shows a change in the free stream velocity for the bow-on run of 0.039 ms^{-1} at a height of 10 m and 0.0005 ms^{-1} at a height of 30 m. These small changes indicate the ship caused a minimal blockage of the flow at the sides of the tunnel. However, since the changes are not zero, the free stream velocity for a particular instrument site is estimated from the vertical profile of the velocity directly abeam of the instrument site, rather than at the inlet or outlet of the tunnel. Examination of the free stream velocity close to the sides of the tunnel in the other models showed that the geometry likewise caused a minimal blockage of the flow.

Figure 5b shows the vertical profiles of wind speed at the tunnel inlet (x=500 m) and outlet (x=-500 m) for the bow-on simulation, and Figure 5c) shows the difference between the profiles for all

simulations. Above a height of about 5 m the difference between the profiles is less than 0.3 m/s. These figures show that the shape of the wind speed profile changes slightly along the tunnel. Because of this change, the free stream velocities are estimated using the vertical profiles of velocity abeam of the anemometer site, rather than the profiles at the tunnel inlet or outlet.

4.3 The vertical displacement at the aerosol intake location

The vertical displacement of the flow reaching the aerosol intake is calculated by tracing a streamline from the intake location upwind to the domain inlet (Table 3). The vertical displacement Δz increases from 6.5m for flows directly over the bow (bow-on) to 17m for flows directly over the beam. The height the flow originated is 15.1m above the sea surface for bow-on flows. This decreases to 5m for flows directly over the beam. The vertical displacement is greater for flows over the starboard side as the aerosol intake is set back further from the upwind leading edge of the ship when compared to equivalent flows over the port side.

Relative Wind Direction (degrees)	Aerosol intake (x, y, z)	Vertical displacement Δz (m)	Height the airflow originated (z-Δz) (m)
-120 (port)	(-7.16, 24.54, 21.58)	12.80	8.78
-110 (port)	(-2.79, 25.41, 21.58)	12.68	8.90
-100 (port)	(1.67, 25.51, 21.58)	12.55	9.03
-90 (beam-on port)	(6.07, 24.83, 21.58)	12.24	9.34
-80 (port)	(10.29, 23.40, 21.58)	11.24	10.34
-70 (port)	(14.20, 21.26, 21.58)	10.17	11.41
-60 (port)	(17.67, 18.47, 21.58)	9.47	12.11
-50 (port)	(20.61, 15.12, 21.58)	8.63	12.95
-40 (port)	(22.92, 11.31, 21.58)	7.73	13.85
-30 (port)	(24.54, 7.16, 21.58)	7.05	14.53
-20 (port)	(25.41, 2.79, 21.58)	6.45	15.13
-10 (port)	(25.51, -1.67, 21.58)	5.93	15.65
0	(24.83, 6.07, 21.58)	6.49	15.09
10 (starboard)	(23.40, 10.29, 21.58)	6.68	14.90
20 (starboard)	(21.26, 14.20 , 21.58)	6.75	14.83
30 (starboard)	(18.47, 17.67, 21.58)	7.32	14.26
40 (starboard)	(15.12, 20.61, 21.58)	8.43	13.15
50 (starboard)	(11.31, 22.92, 21.58)	10.13	11.45
60 (starboard)	(7.16, 24.54, 21.58)	12.37	9.21

70 (starboard)	(2.79, 25.41, 21.58)	14.05	7.53
80 (starboard)	(-1.67, 25.51, 21.58)	-	-
90 (starboard)	(-6.07, 24.83, 21.58)	16.51	5.07
100 (starboard)	(-10.29, 23.40, 21.58)	-	-
110 (starboard)	(-14.20, 21.26, 21.58)	19.50	2.08
120 (starboard)	(-17.67, 18.47, 21.58)	18.88	2.70

Table 3. Aerosol intake positions in the VECTIS co-ordinate system, the vertical displacement and the height the flow originated (z– Δz). The z value is the height of the anemometer above the sea surface. A schematic of the locations is shown in Figures 2 and 3.

4.4 The vertical displacement and angle of flow at the other sensor locations

The vertical displacement of the flow reaching an instrument site is calculated by tracing a streamline from the instrument location upwind to the inlet (Table 6). The vertical displacement Δz for the METEK anemometer increases from around 3.1 m for bow-on flows to around 6 m for flows directly over the beam. The vertical displacement Δz for the CSAT anemometer is similar to the METEK anemometer, and increases from 3.4 m for bow-on flows to around 6 m for flows directly on the beam. The vertical displacement at the weather station site (Table 9) is far larger than at the well-exposed foremast sites. The airflow is raised about 12 m for bow-on flows, which increases to about 16 m for flows directly over the starboard side. The vertical displacement for the weather station has been included as a guide for future positioning of sensors in this area. However, for a number of relative wind directions the vertical displacement at the sensor sites is not reliable as the sensors are in a recirculation region with severe flow distortion. The vertical displacement for the ships anemometers on the main mast has not been calculated.

The path of the streamlines to the METEK sonic CSAT anemometer for each relative wind direction simulated is shown in Figure 6. The influence of the ship on the streamlines is similar for both sites. The vertical displacement increase dramatically for relative wind directions beyond 60 degrees for both sites. The vertical displacement $\Delta z_{t=2}$ at a position two seconds upstream of the anemometer locations was also calculated for the METEK sonic and CSAT anemometers (after Yelland et al. 2002). The co-ordinates of the streamlines were written to file and the vertical displacement using a position at 2 seconds upstream was calculated. The speed and deflection of the streamline was taken into account in the calculation. Compared to the full vertical displacements (Δz), the vertical displacement at 2 seconds upstream ($\Delta z_{t=2}$) was around 1.50 m less for bow-on flows at the METEK site (full displacement 3.1 m compared to 1.6 m for the two-second displacement) and around 4.4 m for beam on flows. For bow-on flows at the CSAT site the vertical displacement at 2 seconds upstream ($\Delta z_{t=2}$) was around 1.3 m less for bow-on flows at the METEK site (full displacement 3.4 m compared to 2.1 m for the two-second displacement) and around 4.3 m for beam on flows. The vertical displacements for each relative wind direction simulated are summarised in Tables 6 and B.1.

For relative wind directions within 60 degrees of the bow the angle of the flow from the horizontal ("tilt" of the flow) is greater at the CSAT site than at the METEK site (Table 7), 13.4 degrees and 8.2 degrees for a flow directly over the bow decreasing to 5.6 and 4.6 degrees at 60 degrees. For flows at relative wind directions greater than 60 degrees the tilt is greater at the METEK site. The tilt decreases at both anemometer locations with increasing relative wind direction for flows over the bow to flows directly over the beam (±90 degrees). For flows at relative wind directions greater than 90 degrees the tilt increases. This behaviour is linked to the flat (or blunt) bow shape and large superstructure influencing the flow.

The horizontal deflection ("twist") of the streamlines is shown in Figure 7. A positive deflection of the flow indicates a rotation of the flow in a clockwise direction, e.g. for flows over the starboard side the substructure presents a large blockage to the flow and deflects the streamlines towards the bow. This means that the measured relative wind direction appear to come from further aft, i.e. the "twist" angle should be subtracted from the measured relative wind direction. The deflection increases with increases in relative wind direction, and the flow is deflected more at the CSAT sonic site than the METEK sonic site. The twist at the weather station location (Table 9) are larger than at the foremast anemometer locations due to its close proximity to the superstructure. The flow angles are shown in Table B.1 and summarised in Tables 7, 8, 9 and 10.

4.5 Wind speed bias

The free stream velocity has small, predictable gradients and can be estimated accurately at any given point on the vertical profile. In contrast, the flow at an instrument site can suffer from severe flow distortion and from large gradients in the velocity field. In addition, it is not always possible to define the mesh so that the instruments are at the exact centres of the computational cells (see Moat et. al., 1996). Therefore the velocity at an instrument site is estimated from lines of data extracted in all three directions. Figures 9 to 77 show the lines of data through the instrument sites for all wind directions, and the results are summarised in Tables 3, 4 and B.1. The wind speed error at an instrument site (height z) is expressed as a percentage of the free stream speed at height z and also as a percentage of the free stream wind speed at which the airflow originated (at height $z - \Delta z$, where Δz is the full vertical displacement of the flow) with a positive error indicating an acceleration of the flow. In addition the wind speed error at an instrument site (height z) is expressed as a percentage of the free stream wind speed at a height two seconds upstream of the anemometer site (at height $z - \Delta z_{t=2}$). The change in the percentage wind speed bias (at height $(z - \Delta z)$, $(z - \Delta z_{t=2})$ and at the height z of the sensor) with relative wind direction for each sensor is summarised in Tables 3 and 4.

The airflow distortion at the METEK sonic anemometer site varies from decelerations of 3 % for winds directly over the bow to accelerations of around 12% for winds 120 degrees off the bow (Figure 8). These large accelerations are caused by the presence of the upwind foremast extension at this relative wind direction. The wind speed at the CSAT anemometer site is reduced by 5.5% for bow-on flows and is accelerated by up to 16 % for winds 120 degrees off the bow. Vertical planes of velocity through the METEK and CSAT sites are shown for all relative wind directions in Figures A1 to A23. Similarly, horizontal planes of velocity through both sites are shown in Figures A24 to A50.

The wind speed bias and vertical displacement for all sensors is plotted in Figure 8. The rates of change of the wind speed bias with relative wind direction and vertical displacement for both the anemometers are relatively smooth. This suggests that the wind speed bias and vertical displacement may be parameterised for all relative wind directions between ±120 degrees.

The airflow distortions at the ships weather station (Table 9) located on the port side of the monkey island are greater than those on the foremast. The wind speed was generally decelerated over much of the relative winds directions modelled, quite severely decelerated for flows greater than 70 degrees off the bow were the anemometer would be in the down stream wake region of the monkey Island container labs. The vertical displacement was calculated for these instruments, but is only intended as a guide for any future anemometer deployments (Table 9).

The ships anemometers (Table 10) where located either side of the ship's main mast. The wind speed was accelerated over the range relative wind directions used in this study, typically 2% to 10% (Table 10 and Figures 57 to 84).

4.6 Lidar wind speed profiles

Wind profiles were obtained from a Doppler Lidar located on the top on the port container top (Figure 1). Wind speed profiles were extracted from the model at all relative wind directions and shown in Figure 85. Each wind speed profile was normalised by the free stream profile 850m directly abeam of the Lidar site.

The ship imposes a significant obstacle to the flow and forces a strong vertical velocity in the lowest few tens of meters above the lidar, which varies with relative wind direction. This effect is slightly asymmetric about the bow because the lidar is situated towards the port side. More details are available from Achtert et al., (2015).

5. SUMMARY

During ACSE campaign the foremast of the *ODEN* was instrumented with: a METEK uSonic-3 sonic anemometer from University of Leeds, UK., and a CSAT sonic anemometer from the University of Stockholm. Additional wind speed measurements were made from the ship's weather station and ship's anemometers. Wind profiles were obtained from a Doppler Lidar. Future science campaigns on the *ODEN* will be obtaining air samples for aerosols measurement. The height the air originated is contained in this report.

The wind speed bias for all relative wind directions are summarised in Table B1. For bow-on flows the anemometers in the bows of the ship experienced relatively small flow distortion. At these sites the flow was decelerated by about 3% of the free stream wind speed. Over the full range of relative wind directions the flow to the METEK sonic is generally accelerated with the largest wind speed biases at flows directly over the beam. The airflow distortions at the ships weather station (Table 9) located on the port side of the monkey island are greater than those on the foremast. The wind speed was generally decelerated over much of the relative winds directions modelled, quite severely decelerated for flows greater than 70 degrees off the bow were the anemometer would be in the down stream wake region of the monkey Island container labs. The ships anemometers (Table 10) where

located either side of the ship's main mast. The wind speed was accelerated over the range relative wind directions used in this study, typically 2% to 10%.

The vertical displacement of the airflow increases from around 3 m for flows directly over the bow, to around 6 m for flows over the ship's beam as the blockage of the airflow by the ship becomes greater. The vertical displacement of the airflow was used to obtain the height at which the airflow originated a long way upstream and also from a point 2 seconds upstream (after Yelland et al., 2002). The free stream wind speed at these two heights was used to determine the wind speed bias at the anemometer locations. These measurements are required if data from the anemometer are to be used to calculate the wind stress via the dissipation method (Yelland et al., 1998). The results are summarised in Table *. The vertical displacement at the aerosol intake location varied from 6m for flows directly over the bow, to around 16 m for flows over the ship's beam.

The ship imposes a significant obstacle to the flow and forces a strong vertical velocity in the lowest few tens of meters above the lidar. More details are available from Achtert et al., (2015).

.

	Relative wind direction (degrees)													
	0	±10°	±20°	±30°	±40°	±50°	±60°	±70°	±80°	±90°	±100°	±110°	±120°	±150°
METEK	-3.10	-2.95	-2.20	-0.93	0.48	2.41	4.44	6.45	7.94	8.46	8.90	10.67	12.39	-
	(-3.81)	(-3.67)	(-2.99)	(-1.78)	(-0.48)	(1.25)	(3.03)	(4.67)	(5.65)	(5.37)	(5.67)	(6.10)	(5.32)	-
CSAT	-5.53	-4.87	-3.56	-1.29	0.90	3.46	6.27	9.00	10.98	11.73	12.59	13.99	16.33	-
	(-6.72)	(-6.09)	(-4.90)	(-2.72)	(-0.69)	(1.60)	(4.02)	(6.15)	(7.11)	(6.66)	(5.02)	(3.37)	(0.61)	-

Table 4. The percentage **wind speed bias** at the sensor location accounting for the height the airflow was raised ΔU_z (i.e. at height z - Δz). The values in brackets indicate the wind speed error using a free stream velocity from a location 2 seconds upstream of the anemometer site ΔU_{zt2}, i.e. z - Δzt=2 (after Yelland et al., 2002). The anemometers were on the centreline of the ship, which results in a symmetric wind speed bias.

	Relative wind direction (degrees)													
	0	±10°	±20°	±30°	±40°	±50°	±60°	±70°	±80°	±90°	±100°	±110°	±120°	±150°
METEK	-4.50	-4.36	-3.68	-2.44	-1.13	0.59	2.37	3.98	4.92	4.60	4.88	5.24	4.39	-10.37
CSAT	-8.14	-7.50	-6.32	-4.11	-2.03	0.28	2.74	4.87	5.77	5.31	4.10	2.47	-0.33	-29.58

Table 5. The percentage **wind speed bias** at the sensor location ΔU. The anemometers were on the centreline of the ship, which results in a symmetric wind speed bias.

	Relative wind direction (degrees)													
	0	±10°	±20°	±30°	±40°	±50°	±60°	±70°	±80°	±90°	±100°	±110°	±120°	±150°
METEK	3.10	3.08	3.20	3.20	3.32	3.60	3.93	4.43	5.15	6.03	7.4	8.77	10.30	-
	(1.63)	(1.60)	(1.60)	(1.52)	(1.47)	(1.47)	(1.44)	(1.47)	(1.52)	(1.58)	(1.79)	(1.99)	(2.17)	-
CSAT	3.40	3.40	3.50	3.47	3.51	3.68	3.90	4.35	5.10	5.96	7.14	8.35	10.34	-
	(2.06)	(2.03)	(2.02)	(1.92)	(1.82)	(1.74)	(1.64)	(1.60)	(1.64)	(1.64)	(1.56)	(1.54)	(1.63)	-

Table 6. The variation of the **vertical displacement** (ΔZ, meters) with changes in relative wind direction. The values in brackets indicate the vertical displacement at a location 2 seconds upstream of the anemometer site ΔZ_{t2}, i.e. Δzt=2 (after Yelland et al., 2002). A negative relative wind direction indicates a flow over the port side.

	Relative wind direction (degrees)													
	0	±10°	±20°	±30°	±40°	±50°	±60°	±70°	±80°	±90°	±100°	±110°	±120°	±150°
METEK	8.21	7.83	7.50	6.60	5.92	5.31	4.63	4.14	3.90	4.22	5.18	5.95	6.53	11.11
CSAT	13.44	12.92	12.17	10.54	8.93	7.27	5.56	4.05	3.39	2.93	3.24	3.92	4.95	10.78

Table 7. The variation of the angle of the flow to the horizontal **(tilt)** at the sensor site (degrees). A negative relative wind direction indicates a flow over the port side.

	Relative wind direction (degrees)													
	-150°	-120°	-110°	-100°	-90°	-80°	-70°	-60°	-50°	-40°	-30°	-20°	-10°	0
METEK	-1.12	-8.68	-9.33	-9.93	-9.37	-8.14	-7.77	-6.93	-6.08	-4.96	-3.59	-2.10	-0.97	-0.01
CSAT	-0.60	-12.58	-13.00	-12.82	-11.07	-9.47	-9.23	-8.27	-7.40	-6.10	-4.47	-2.81	-1.38	-0.03
	Relative wind direction (degrees)													
	0	10°	20°	30°	40°	50°	60°	70°	80°	90°	100°	110°	120°	150°
METEK	-0.01	0.97	2.10	3.59	4.96	6.08	6.93	7.77	8.14	9.37	9.93	9.33	8.68	1.12
CSAT	-0.03	1.38	2.81	4.47	6.10	7.40	8.27	9.23	9.47	11.07	12.82	13.00	12.58	0.60

Table 8. The variation in the horizontal **twist** (tan-1(v/u)) of the flow at the sensor site (degrees). A negative twist indicates a flow, which has moved anti-clockwise due to the presence of the ship. A negative relative wind direction indicates a flow over the port side.

Relative wind direction	ΔU_z (%)	ΔU (%)	ΔZ (m)	Tilt (degrees)	Twist (degrees)
-110 (port)	-	-66.89	-	-5.8	-68.9
-100 (port)	-	-63.17	-	-16.4	-59.0
-90 (port-beam)	-48.71	-52.25	13.42	-0.4	-16.7
-80 (port)	-48.95	-51.95	12.26	6.7	-16.4
-70 (port)	-	-40.73	-	11.9	-18.4
-60 (port)	-6.47	-12.49	12.98	17.5	-16.0
-50 (port)	1.27	-5.13	12.87	21.46	-14.1
-40 (port)	1.74	-4.15	12.21	26.2	-10.9
-30 (port)	6.09	0.27	11.80	30.5	-5.4
-20 (port)	5.94	0.72	11.12	31.6	-0.6
-10 (port)	9.14	3.99	10.85	29.5	1.5
0 bow-on	-2.27	-7.69	11.91	30.4	1.1
10 (starboard)	6.74	1.52	11.07	30.3	2.8
20 (starboard)	6.91	1.47	11.32	31.2	4.2
30 (starboard)	5.27	-0.60	11.94	27.2	4.0
40 (starboard)	6.25	-0.01	12.33	25.3	9.2
50 (starboard)	3.01	-3.92	13.29	21.8	12.7
60 (starboard)	-4.58	-11.28	13.58	15.5	16.1
70 (starboard)	-	-40.73	-	11.9	18.4
80 (starboard)	-46.18	-52.18	17.27	4.9	15.4
90 (starboard beam)	-40.16	-46.15	16.35	-2.8	13.1
100 (starboard)	-	-63.70	-	-15.1	39.1
110 (starboard)	-86.92	-90.17	23.76	28.4	25.5

Table 9 The percentage wind speed bias at the **weather station site** accounting for the height the airflow was raised ΔU_z (i.e. at height z - ΔZ), the percentage wind speed bias at the sensor location ΔU, the variation of the vertical displacement (ΔZ, meters), the variation of the angle of the flow to the horizontal (tilt) and the variation in the horizontal twist (tan-1(v/u)) of the flow. A negative relative wind direction indicates a flow over the port side. Gaps in the data indicate where no measure of vertical displacement could be made. No estimates at 120 and 150 degrees to the wind were calculated as the flow distortion at these anemometer sites are too severe to be corrected.

	Ships PORT anemometer			Ships STARBOARD anemometer		
Relative wind direction	ΔU (%)	Tilt (degrees)	Twist (degrees)	ΔU (%)	Tilt (degrees)	Twist (degrees)
-150 (port)	7.02	13.5	-4.3	9.76	7.7	-11.8
-120 (port)	3.96	17.6	3.9	6.03	18.0	0.2
-110 (port)	3.61	16.5	5.1	6.00	16.9	4.4
-100 (port)	2.86	15.8	5.1	7.11	14.3	4.9
-90 (port-beam)	3.74	13.8	5.5	6.73	11.8	5.4
-80 (port)	2.61	13.2	5.8	6.59	10.7	6.4
-70 (port)	2.78	12.2	5.2	7.20	9.4	5.4
-60 (port)	2.23	11.9	3.8	7.07	9.8	4.3
-50 (port)	2.78	10.8	1.6	6.12	9.7	2.3
-40 (port)	2.88	10.8	0.2	6.30	10.0	2.0
-30 (port)	3.50	10.3	-1.5	5.56	10.7	1.1
-20 (port)	4.30	10.2	-2.8	5.61	10.3	0.5
-10 (port)	4.22	9.2	-2.0	4.40	9.7	0.5
0 bow-on	5.03	15.1	3.9	4.97	14.8	-4.4
10 (starboard)	4.40	9.7	0.5	4.22	9.2	-2.0
20 (starboard)	5.61	10.3	0.5	4.30	10.2	-2.8
30 (starboard)	5.56	10.7	1.1	3.50	10.3	-1.5
40 (starboard)	6.30	10.0	2.0	2.88	10.8	0.2
50 (starboard)	6.12	9.7	2.3	2.78	10.8	1.6
60 (starboard)	7.07	9.8	4.3	2.23	11.9	3.8
70 (starboard)	7.20	9.4	5.4	2.78	12.2	5.2
80 (starboard)	6.59	10.7	6.4	2.61	13.2	5.8
90 (starboard beam)	6.73	11.8	5.4	3.74	13.8	5.5
100 (starboard)	7.11	14.3	4.9	2.86	15.8	5.1
110 (starboard)	6.00	16.9	4.4	3.61	16.5	5.1
120 (starboard)	6.03	18.0	0.2	3.96	17.6	3.9
150 (starboard)	9.76	7.7	-11.8	7.02	13.5	-4.3

Table 10 The percentage wind speed bias, tilt and twist at the **port** and **starboard ships** anemometer sites on the main mast. A negative relative wind direction indicates a flow over the port side.

6. ACKNOWLEDGEMENTS.

This work was supported by the Natural Environment Research Council NERC (grant NE/K011820/1).

7. REFERENCES

Achtert, A., I. M. Brooks, B. J. Brooks, B. I. Moat, J. Prytherch, P. O. G. Persson, and M. Tjernström, 2015: Measurement of wind profiles by motion-stabilised ship-borne Doppler lidar, *Atmos. Meas. Tech.,* 8, 4993-5007. doi: 10.5194/amt-8-4993-2015.

TNO Diana, 2010: Femgv user's manual Pre and post processing release 7.2, TNO DIANA BV Schoemakerstraat 97, 2628 VK Delft, The Netherlands.

Launder, B. E., and D. B. Spalding, 1974: The numerical computation of turbulent flows, *Computer Methods in Applied Mechanics and Engineering*, **3**, 269 - 289pp.

Moat, B. I., M. J. Yelland, and J. Hutchings, 1996: Airflow over the RRS Discovery using the Computational Fluid Dynamics package VECTIS, Southampton Oceanography Centre, Southampton, UK. SOC Internal Report No. 2, 41 pp.

Moat, B. I. and M. J. Yelland, 2006: Validation of the VECTIS steady state solver, NOC internal document No. 4, National Oceanography Centre, UK., 15 pp [available from: http://eprints.soton.ac.uk/41394/]

Moat, B. I. and M. J. Yelland, 2008: Going with the flow: state of the art marine meteorological measurements on the new NERC research vessel, *Weather*, 63(6), 158-159.

Moat, B. I., M. J. Yelland, R. W. Pascal and J. Prytherch, 2014: Metadata for the WAGES instrumentation deployed on the RRS James Clark Ross between May 2010 and August 2013. NOC internal document No. 13, National Oceanography Centre, UK., 146 pp.

Ricardo, 2015, VECTIS 2015.1 user guide, Ricardo software, Shoreham-by-sea, Sussex, UK, 1129pp.

Yelland, M. J., B. I. Moat, P. K. Taylor, R. W. Pascal, J. Hutchings and V. C. Cornell, 1998: Wind stress measurements from the open ocean corrected for air flow distortion by the ship. *Journal of Physical Oceanography,* 28, 1511 – 1526.

Yelland, M. J., B. I. Moat, R. W. Pascal and D. I. Berry, 2002: CFD model estimates of the airflow over research ships and the impact on momentum flux measurements, *Journal of Atmospheric and Oceanic Technology*, 19, 1477-1499.

8. FIGURES

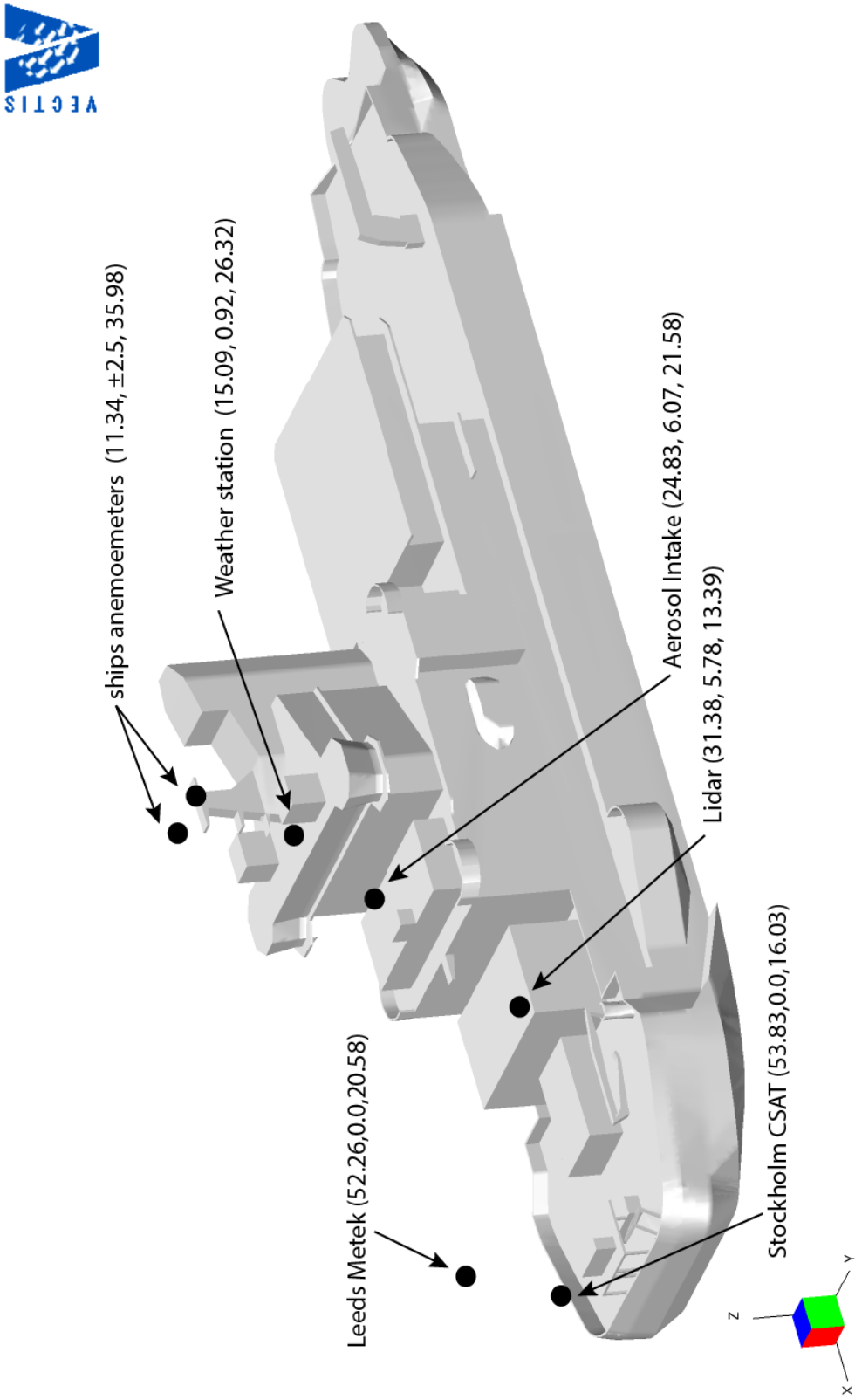

Figure 1. The *ODEN* geometry. The x, y and z co-ordinates of the instruments are shown.

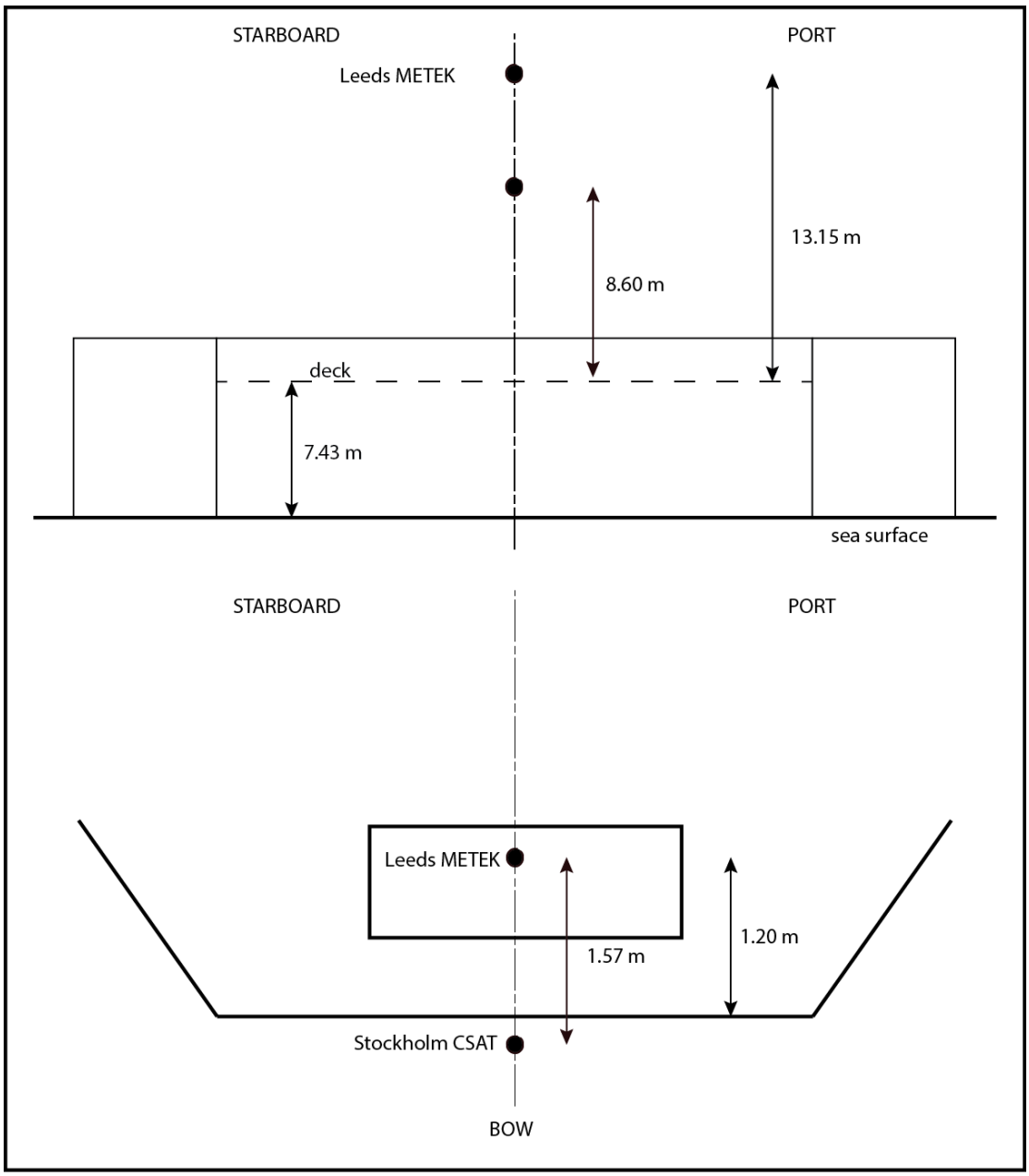

Figure 2. Schematic of the instrument positions relative to the bow.

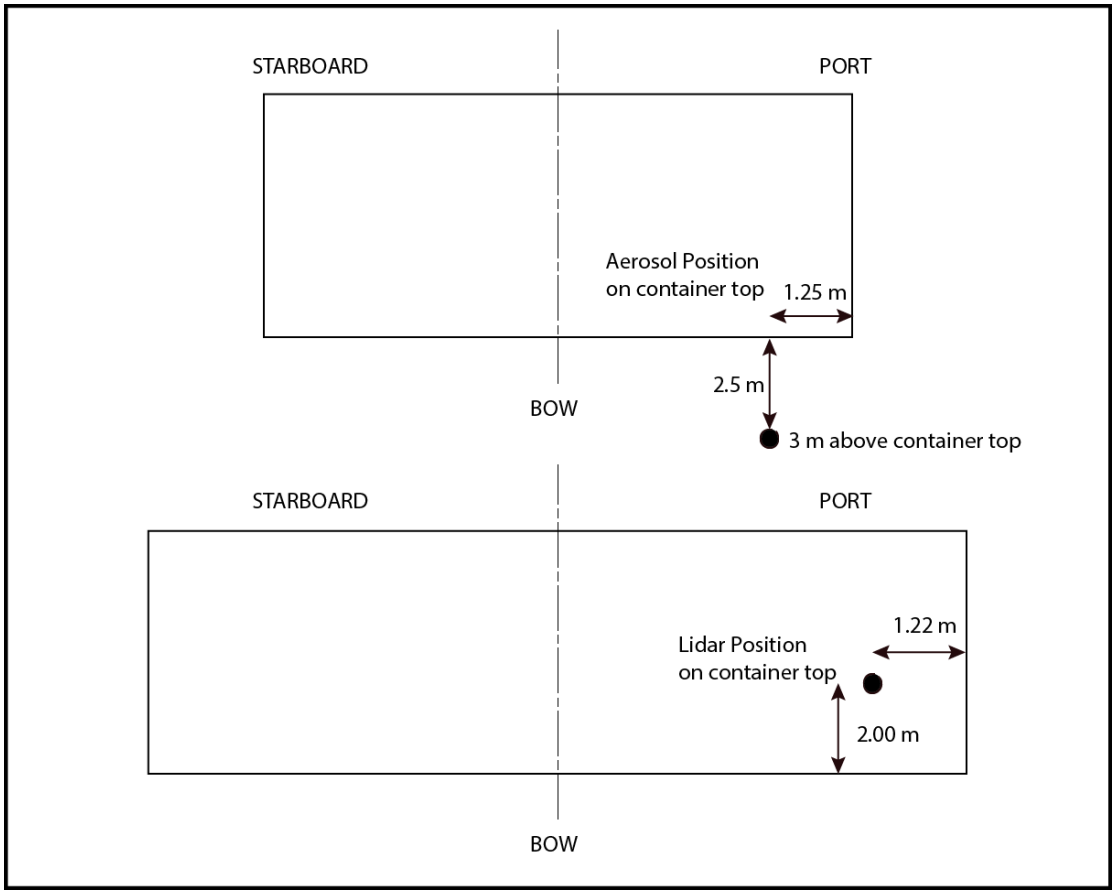

Figure 3. Schematic of the instrument positions of the Doppler Lidar and aerosol intake.

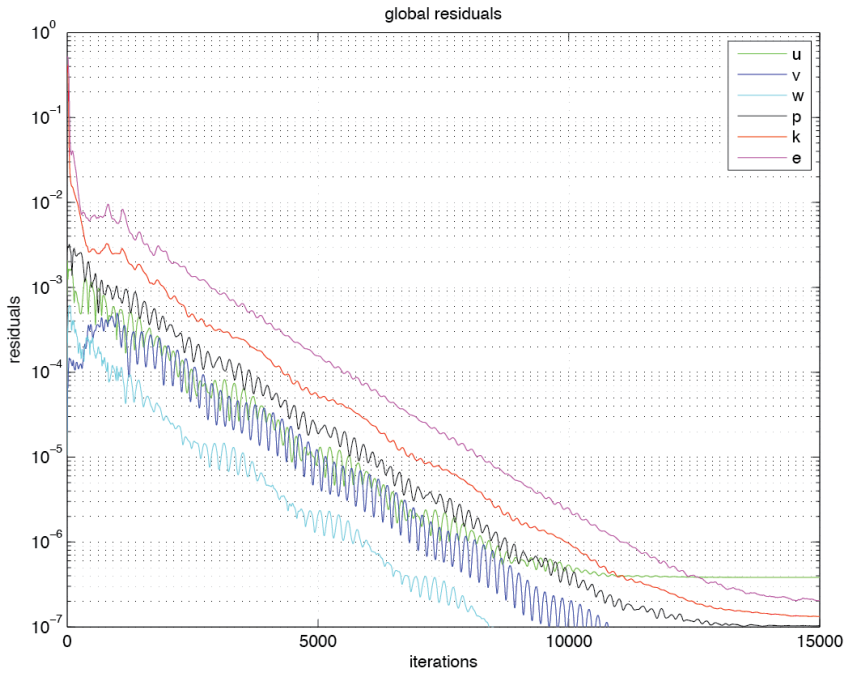

Figure 4. The CFD model convergence for the beam-on simulation (90 degrees). The residuals of velocity u (along stream), v (across stream), w (vertical), and p (pressure), k (turbulent kinetic energy) and e (rate of dissipation of k) are shown.

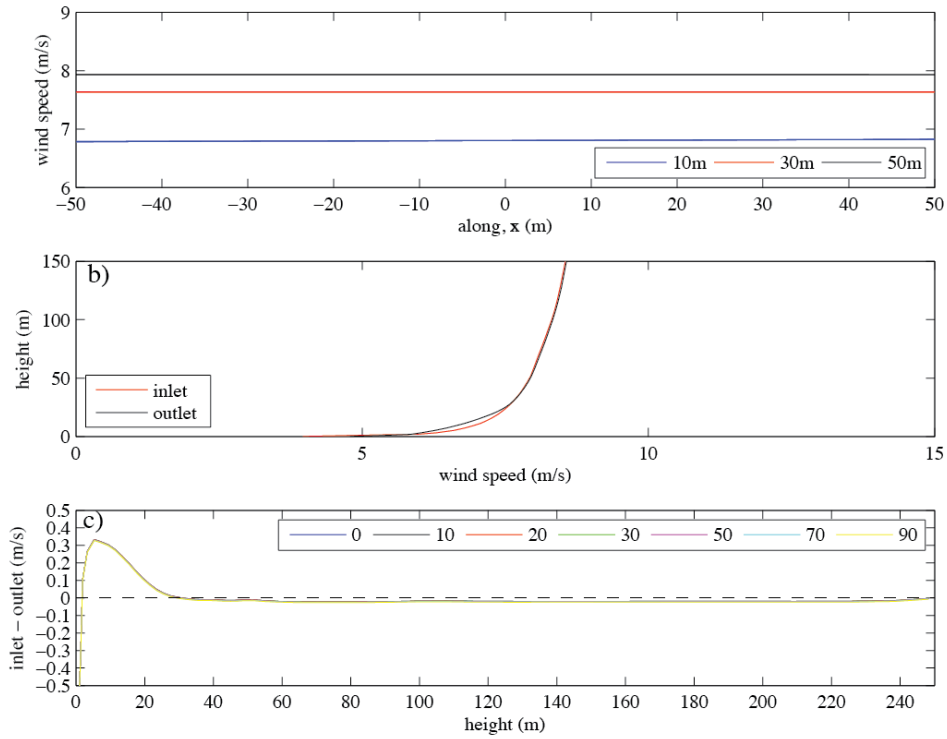

Figure 5. a) Lines of velocity data along the length of the tunnel for all CFD simulations. The data were obtained at heights of 10, 30 and 50 m, in the free stream region on the port side of the models b). The inlet and outlet velocity profile for the bow-on flow c). The difference between the inlet and outlet velocity for all wind direction runs as shown in the key.

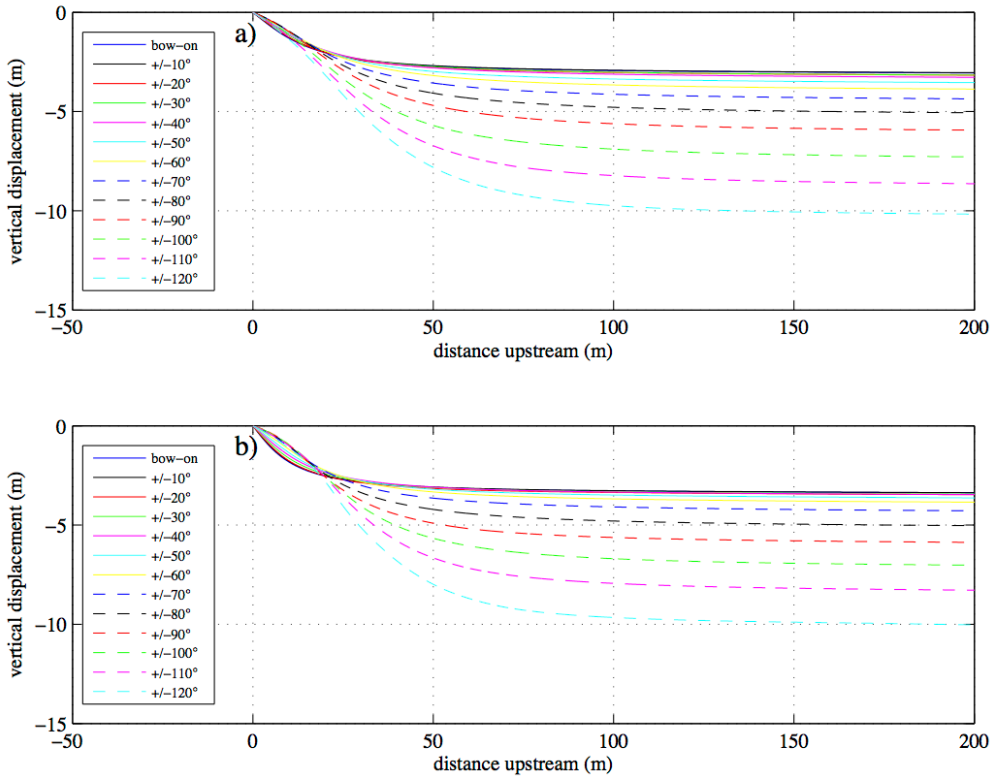

Figure 6. The variation in the vertical displacement of the flow with distance upwind of the a) **METEK** sonic anemometer and b) **CSAT** sonic site.

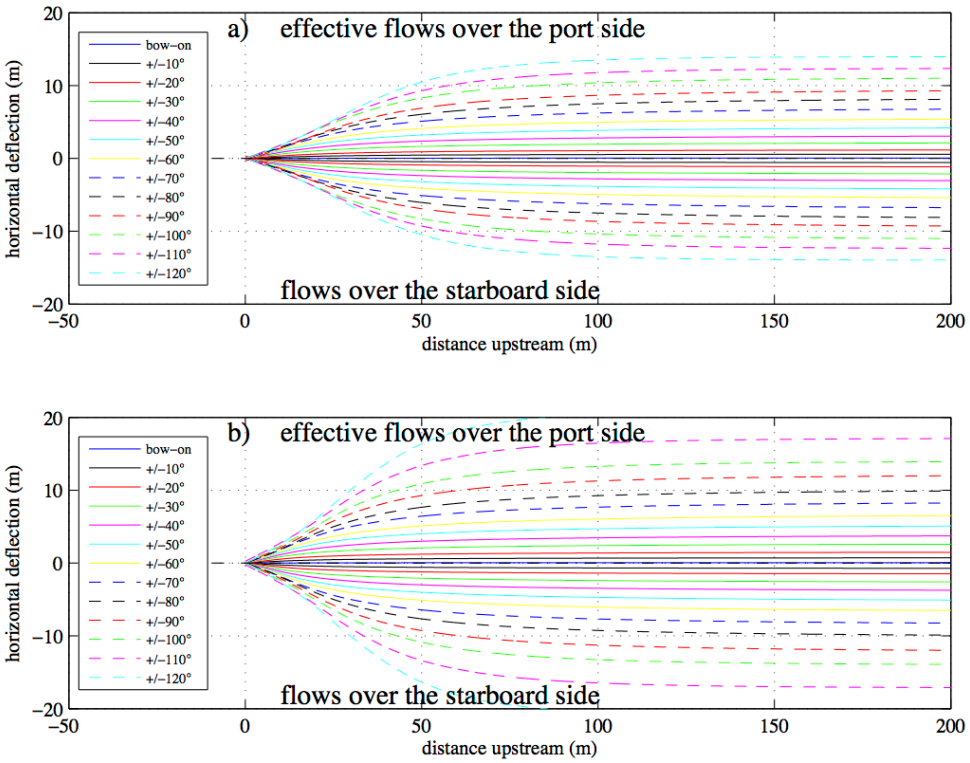

Figure 7. The variation in the horizontal deflection of the flow with distance upwind of the a) METEK and b) CSAT site.

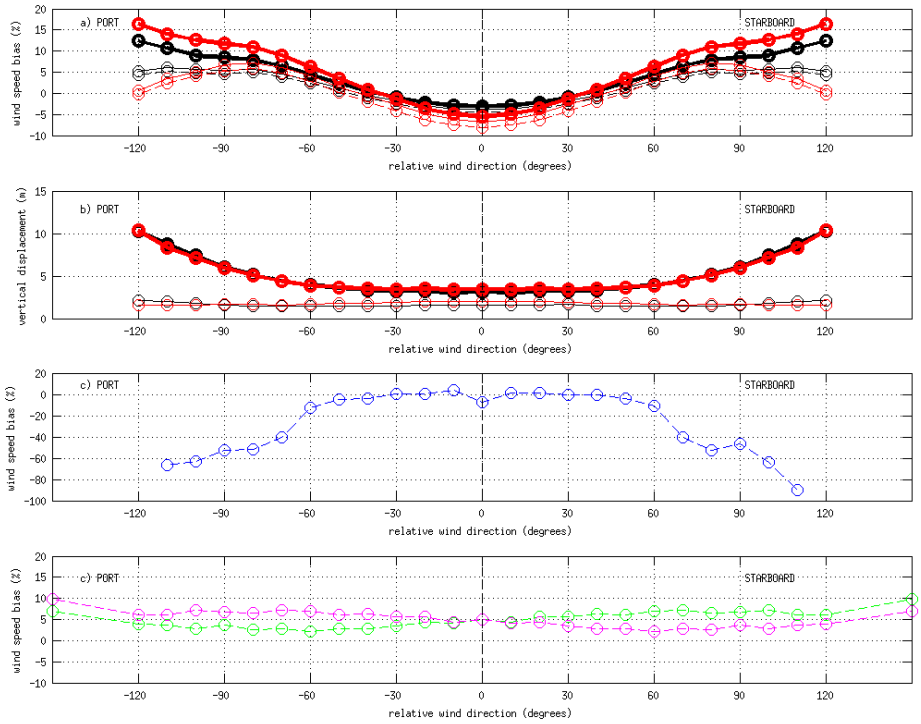

Figure 8. The wind speed bias and vertical displacement at the Leeds METEK anemometer (black), Stockholm CSAT anemometer (red), weather station (blue) and ship's port main mast anemometer (green) and starboard main mast anemometer (magenta). The thick solid lines indicate the wind speed bias using the free stream velocity from the height it originated (i.e. includes the full vertical displacement Δz) and the thin solid lines indicate the wind speed bias using the free stream velocity from the height 2 seconds upstream of the anemometer location. (i.e. includes $\Delta z_{t=2}$). The dashed lines indicate a wind speed bias at the height of the instrument.

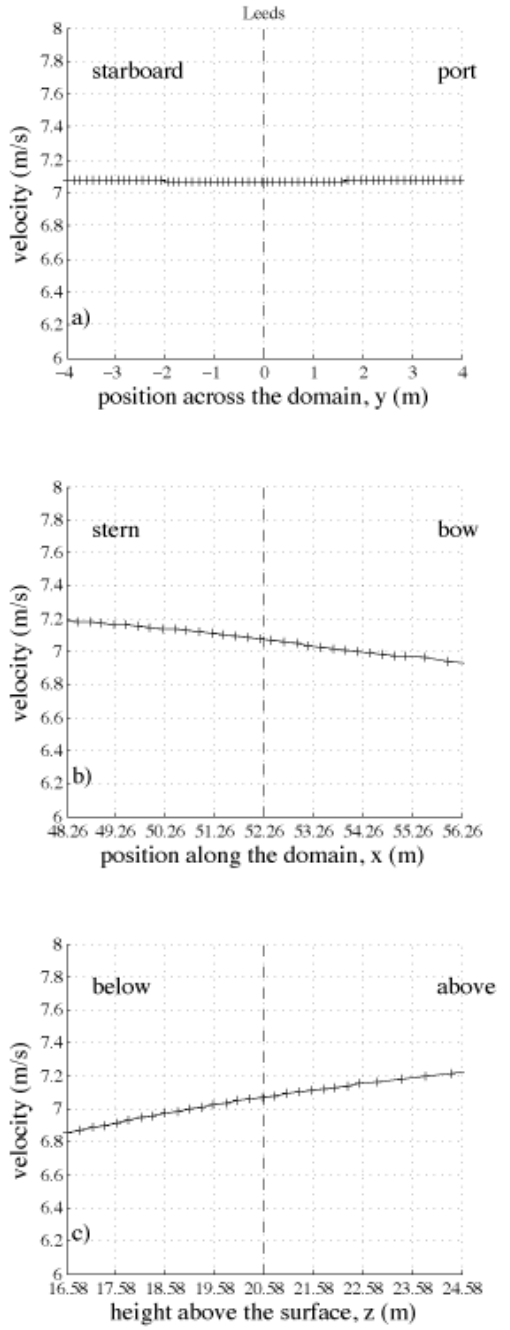

Figure 9. Lines of velocity data through the instrument position (indicated by the dashed line) in all three directions: top – across the domain; middle – along the domain, and bottom – vertically. The results are for a flow to the **METEK sonic at 0 degrees** (bow-on).

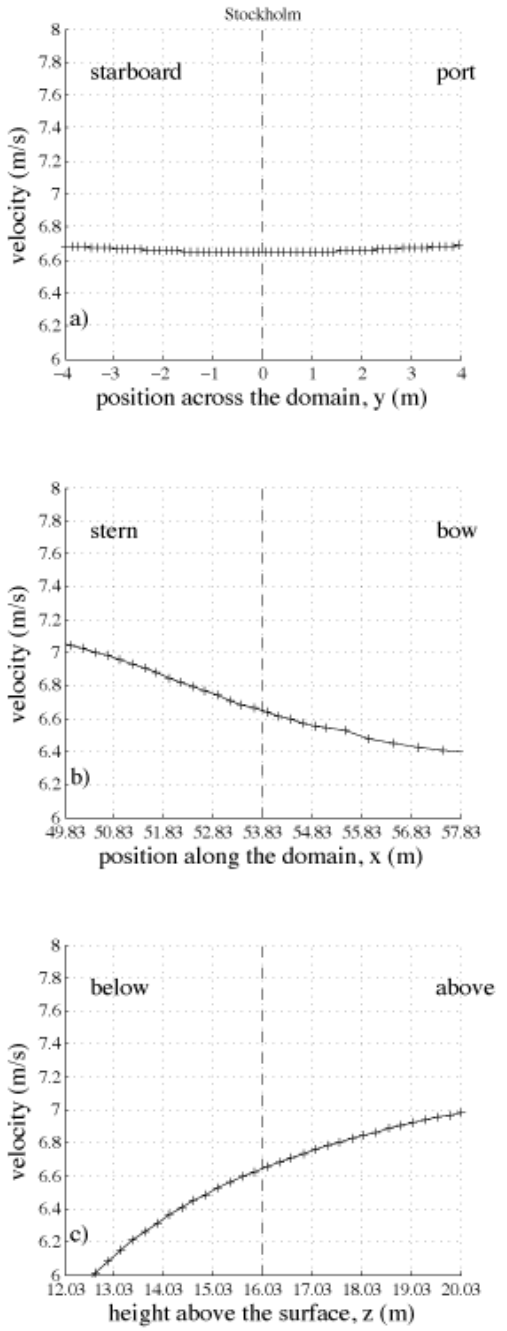

Figure 10. The **CSAT sonic site at 0 degrees** (bow-on).

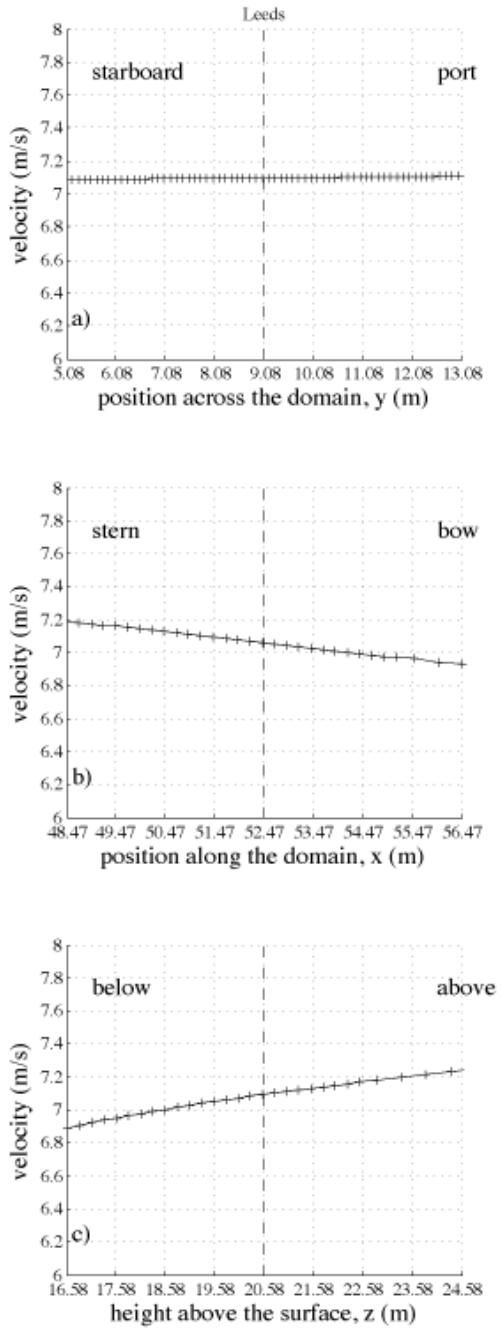

Figure 11. Lines of velocity data through the instrument position (indicated by the dashed line) in all three directions: top – across the domain; middle – along the domain, and bottom – vertically. The results are for a flow to the **METEK sonic at ±10 degrees** off the bow.

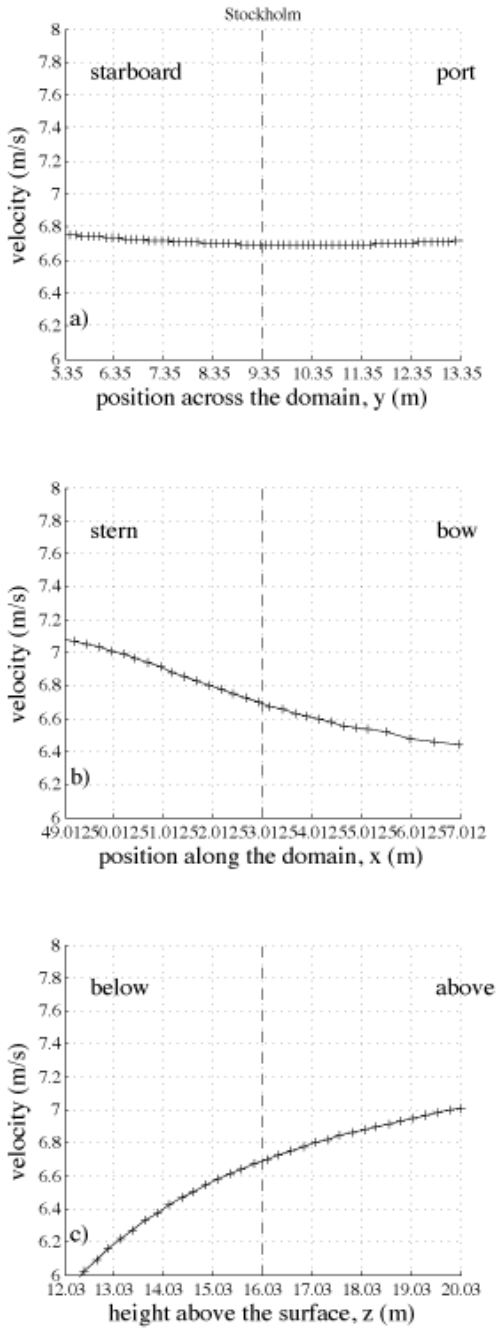

Figure 12. The **CSAT sonic site at ±10 degrees** off the bow.

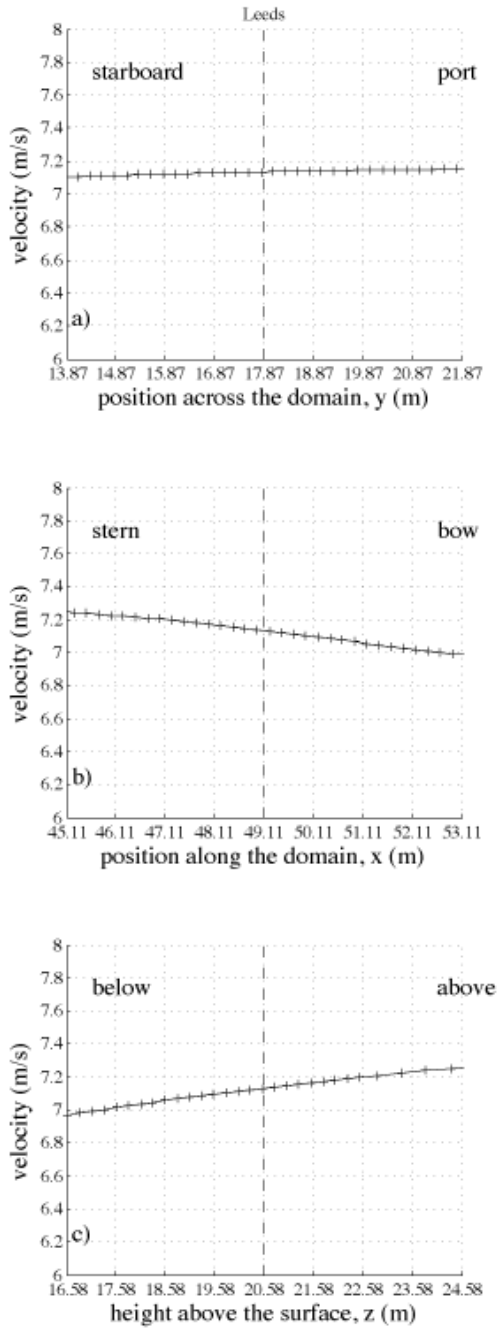

Figure 13. Lines of velocity data through the instrument position (indicated by the dashed line) in all three directions: top – across the domain; middle – along the domain, and bottom – vertically. The results are for a flow to the **METEK sonic at ±20 degrees** off the bow.

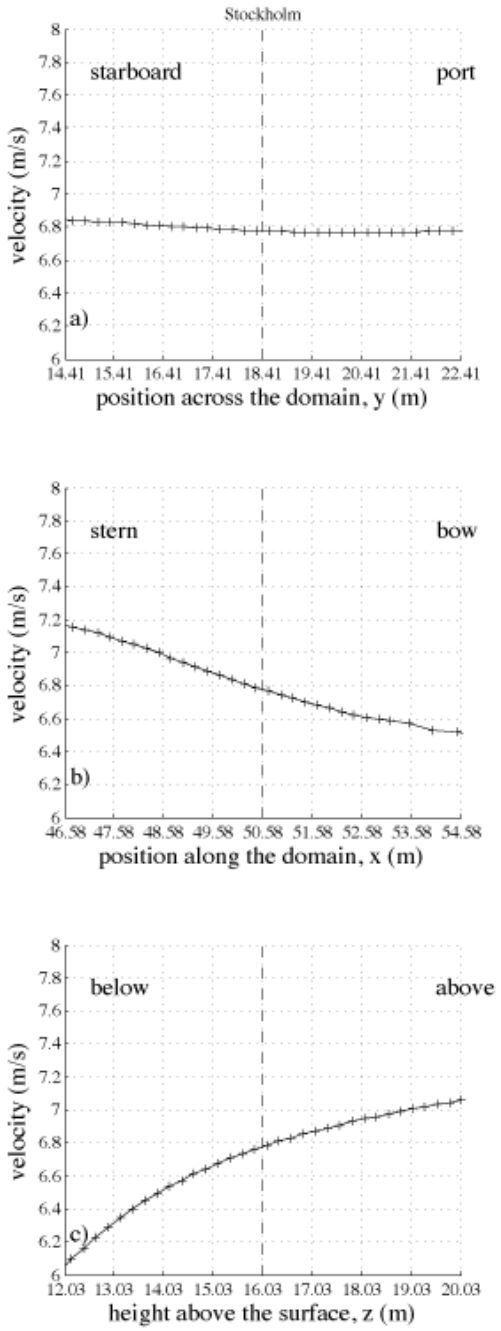

Figure 14. The **CSAT sonic site at ±20 degrees** off the bow.

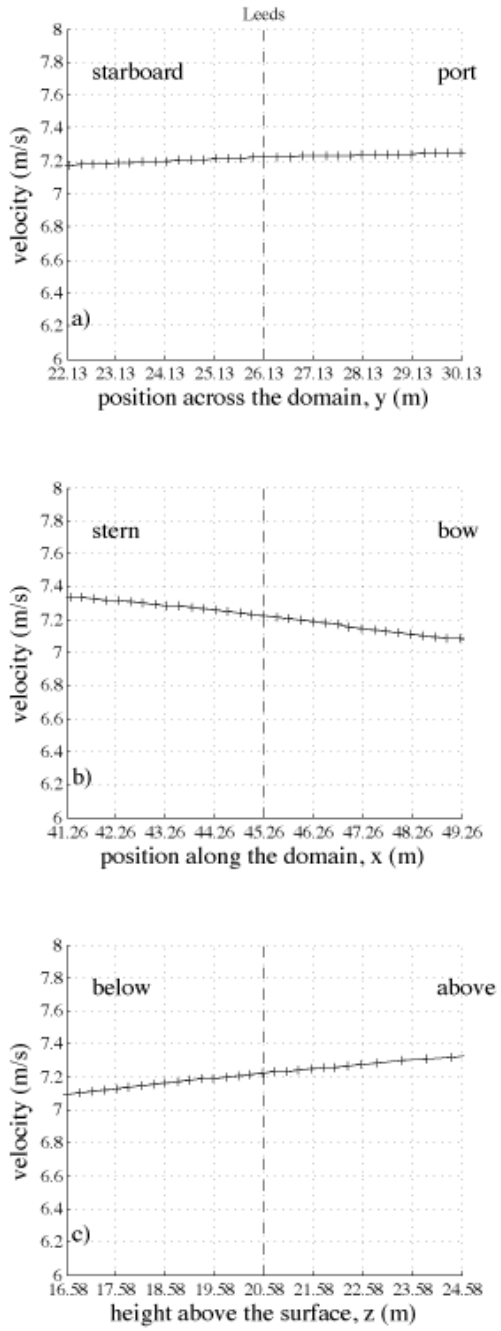

Figure 15. Lines of velocity data through the instrument position (indicated by the dashed line) in all three directions: top – across the domain; middle – along the domain, and bottom – vertically. The results are for a flow to the **METEK sonic at ±30 degrees** off the bow.

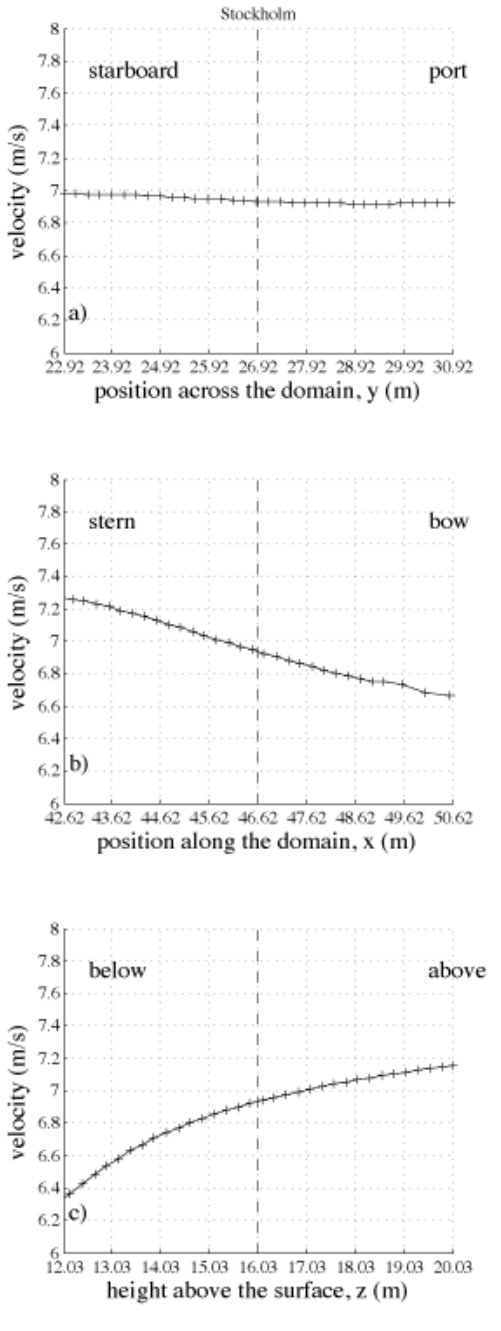

Figure 16. The **CSAT sonic site at ±30 degrees** off the bow.

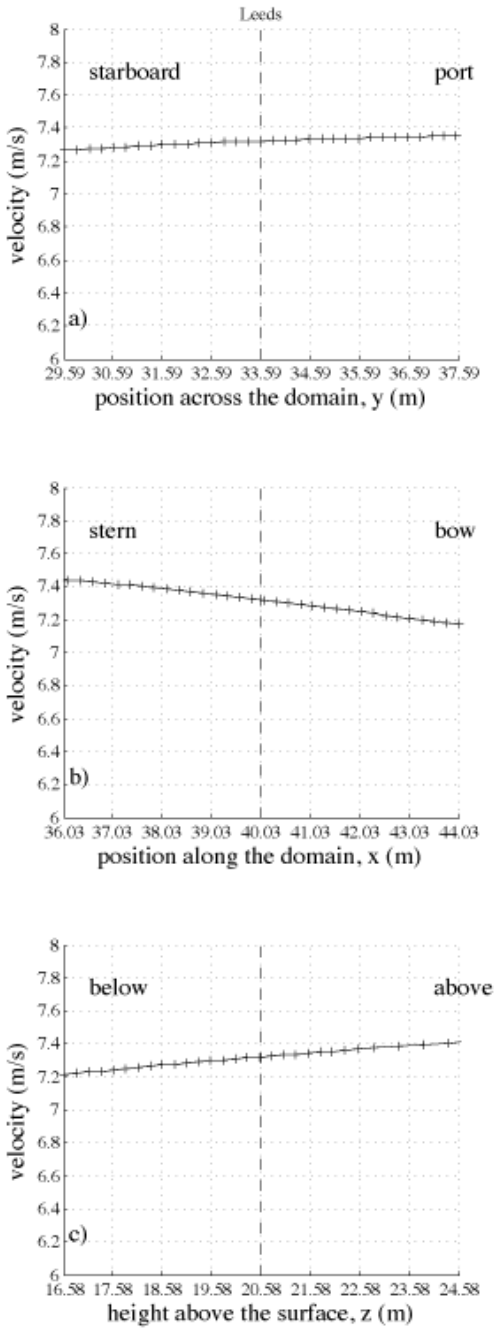

Figure 17. Lines of velocity data through the instrument position (indicated by the dashed line) in all three directions: top – across the domain; middle – along the domain, and bottom – vertically. The results are for a flow to the **METEK sonic at ±40 degrees** off the bow.

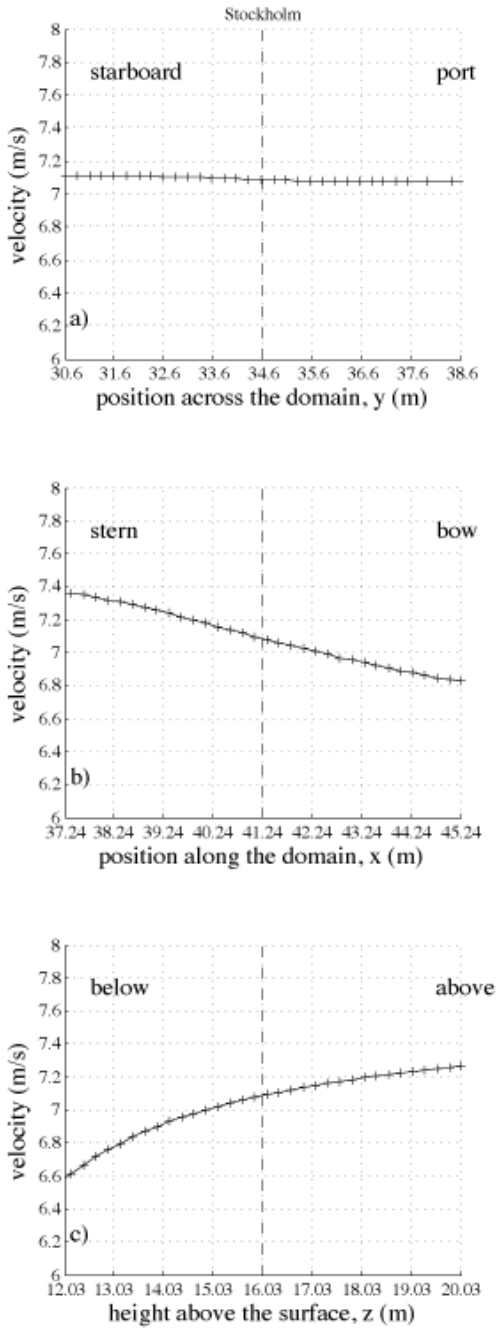

Figure 18. The **CSAT sonic site at ±40 degrees** off the bow.

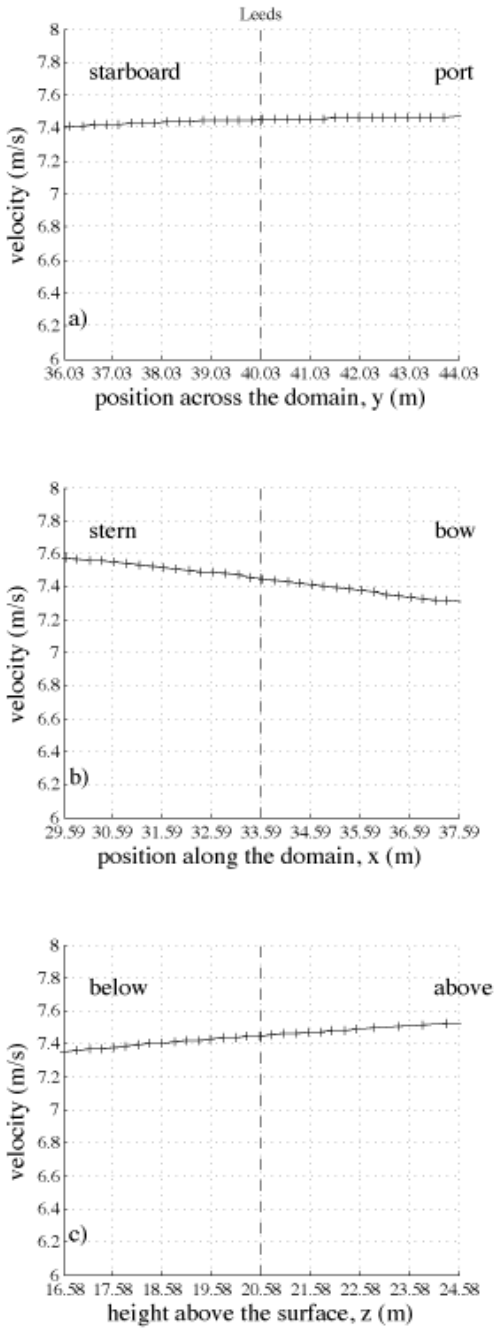

Figure 19. Lines of velocity data through the instrument position (indicated by the dashed line) in all three directions: top – across the domain; middle – along the domain, and bottom – vertically. The results are for a flow to the **METEK sonic at ±50 degrees** off the bow.

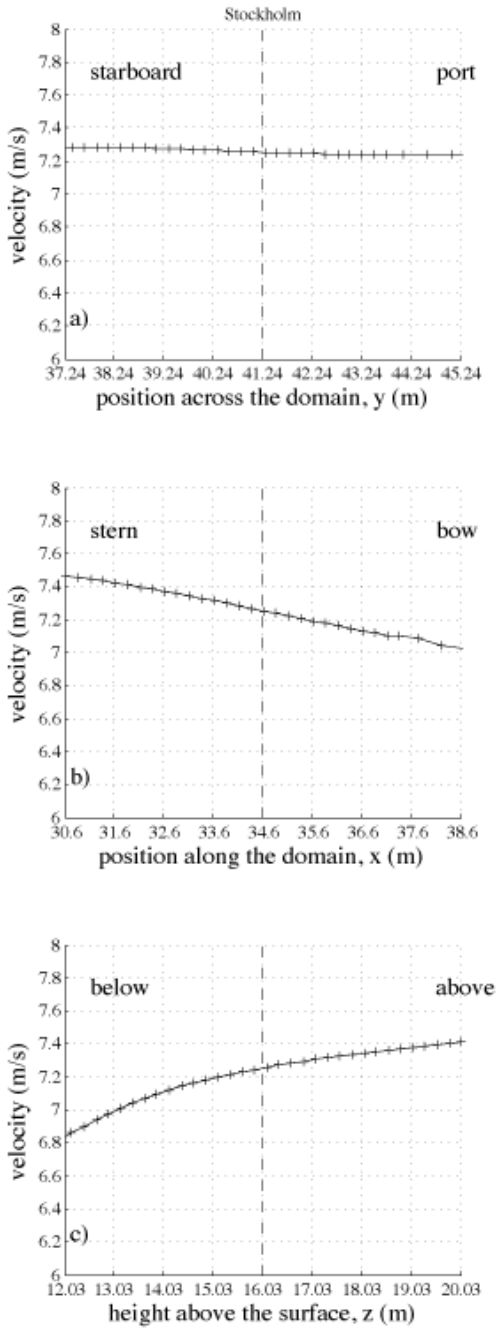

Figure 20. The **CSAT sonic site at ±50 degrees** off the bow.

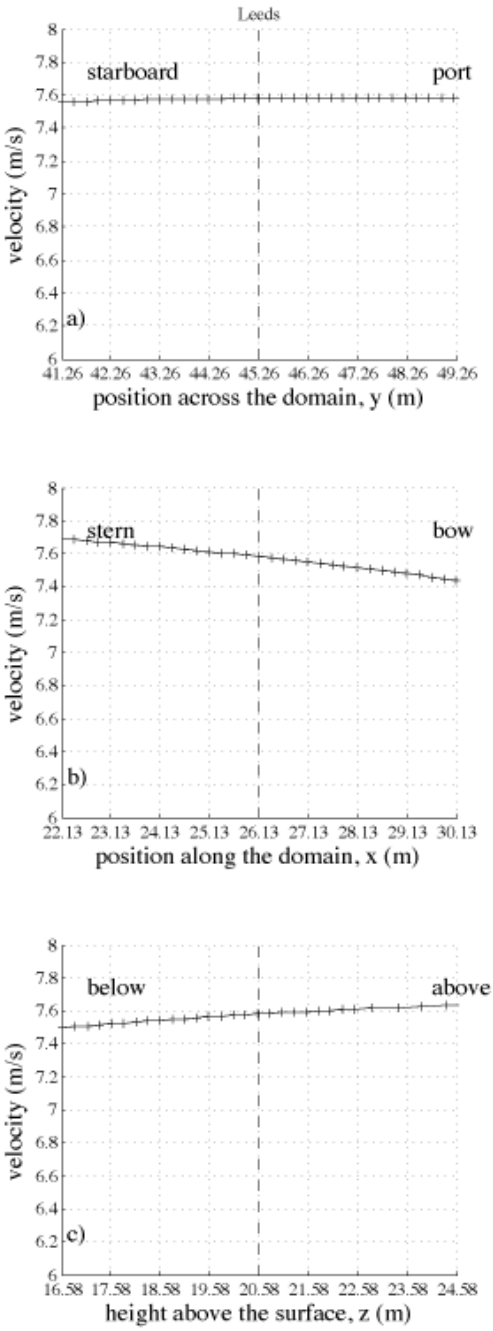

Figure 21. Lines of velocity data through the instrument position (indicated by the dashed line) in all three directions: top – across the domain; middle – along the domain, and bottom – vertically. The results are for a flow to the **METEK sonic at ±60 degrees** off the bow.

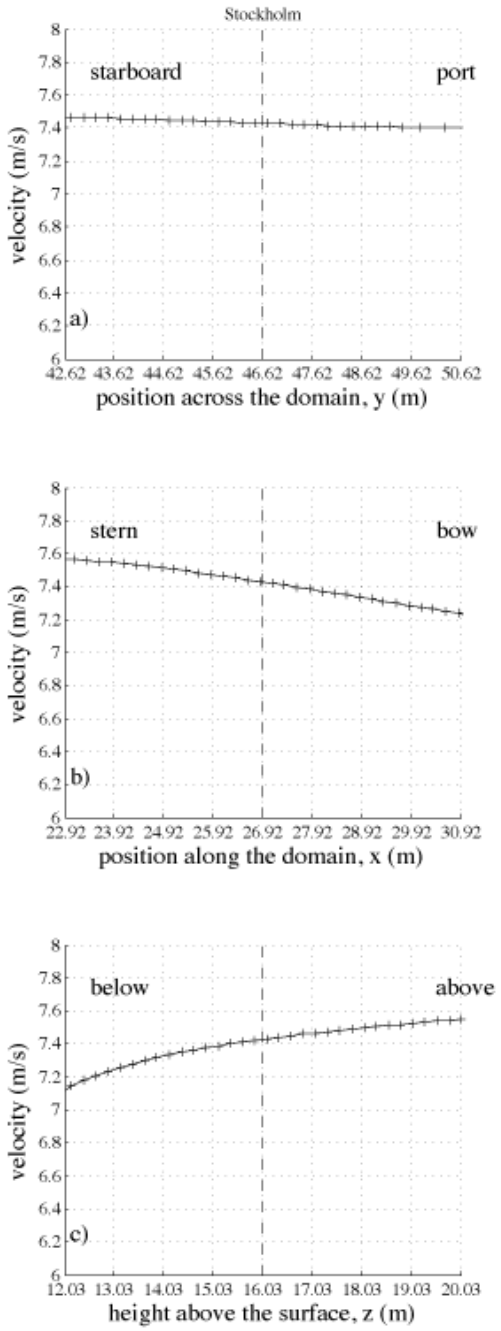

Figure 22. The **CSAT sonic site at ±60 degrees** off the bow.

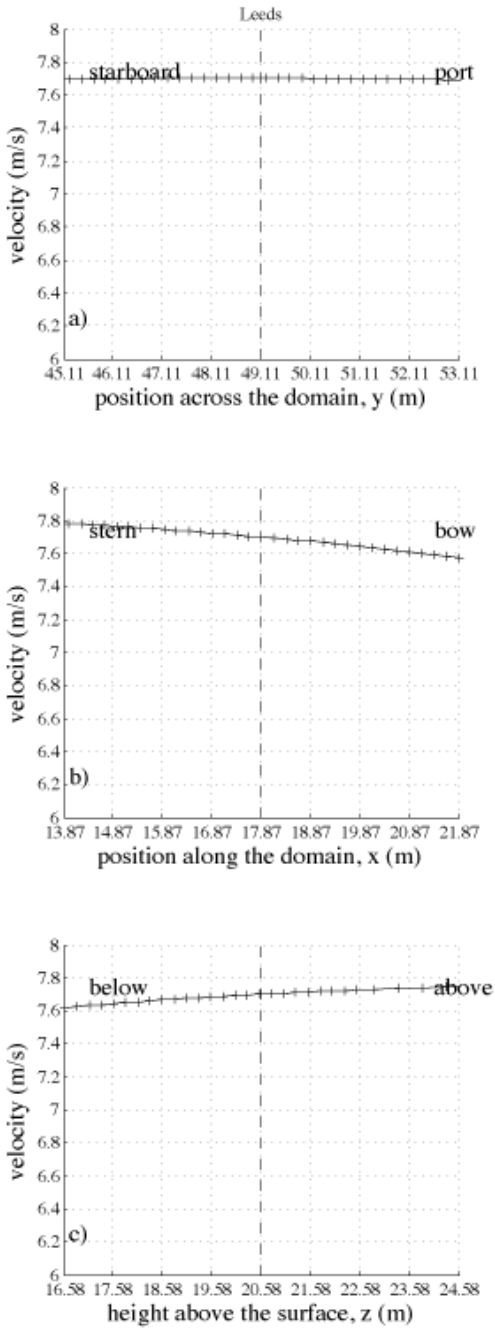

Figure 23. Lines of velocity data through the instrument position (indicated by the dashed line) in all three directions: top – across the domain; middle – along the domain, and bottom – vertically. The results are for a flow to the **METEK sonic at ±70 degrees** off the bow.

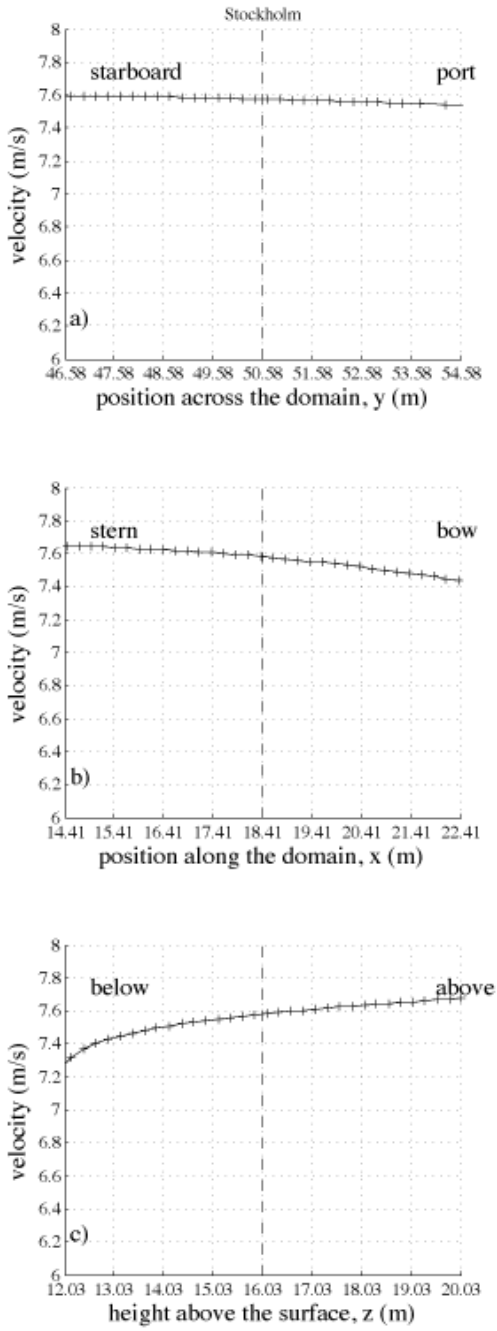

Figure 24. The **CSAT sonic site at ±70 degrees** off the bow.

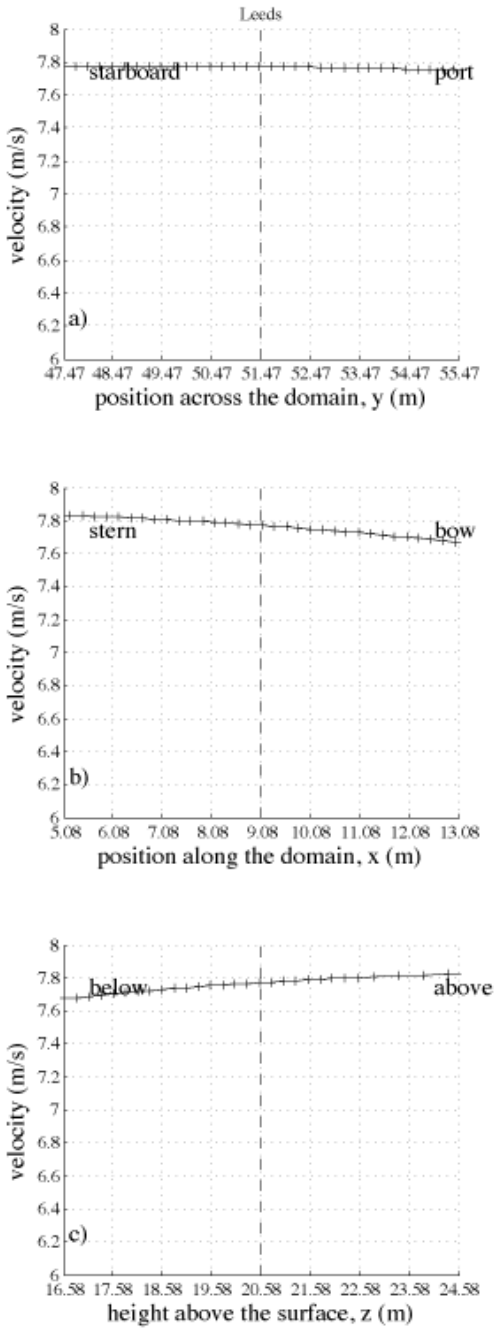

Figure 25. Lines of velocity data through the instrument position (indicated by the dashed line) in all three directions: top – across the domain; middle – along the domain, and bottom – vertically. The results are for a flow to the **METEK sonic at ±80 degrees** off the bow.

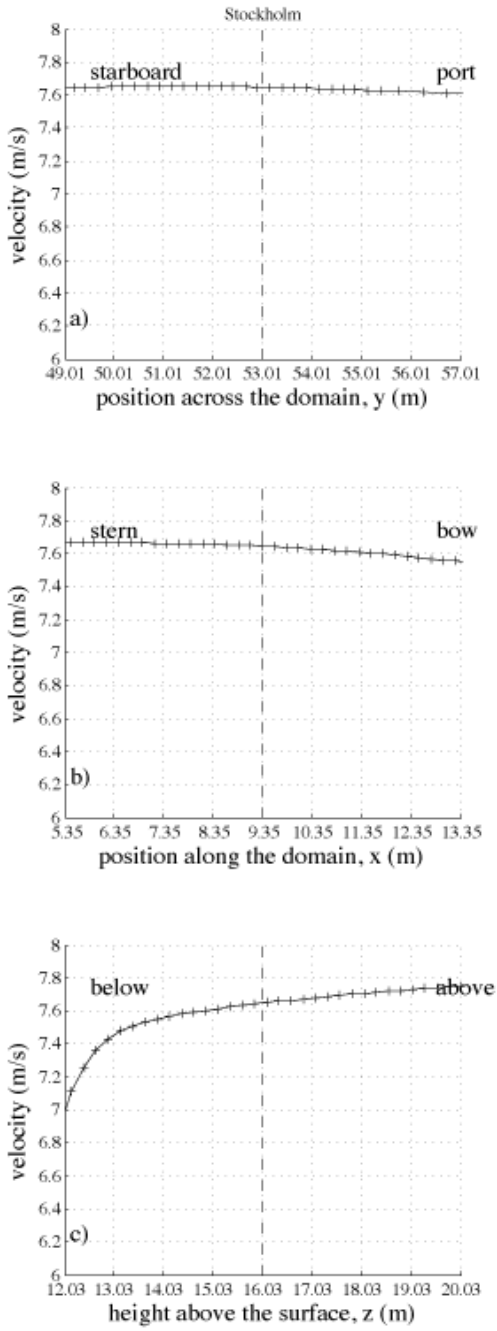

Figure 26. The **CSAT sonic site at ±80 degrees** off the bow.

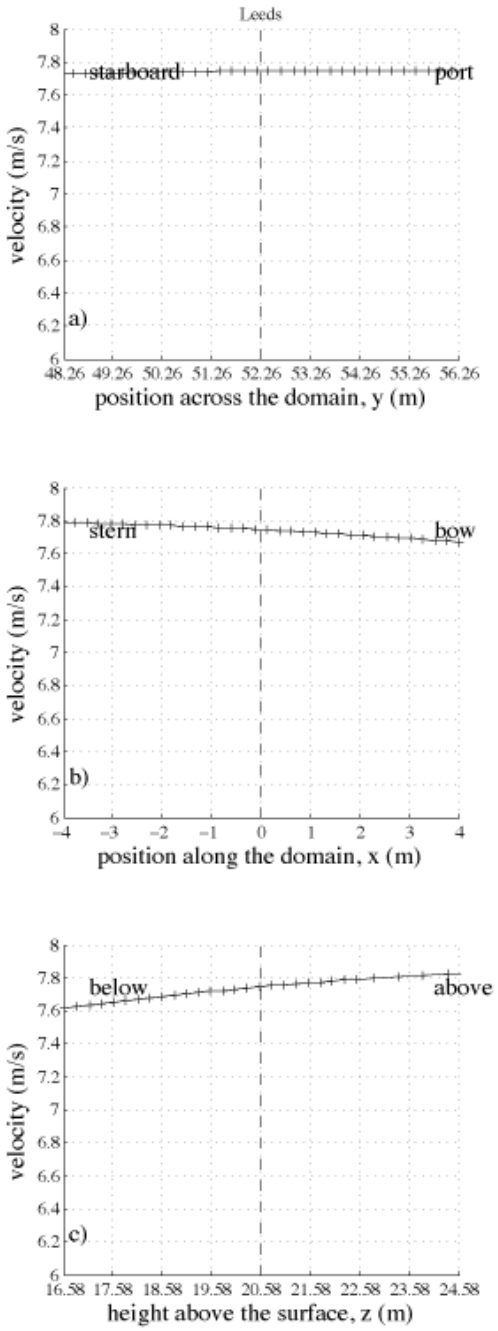

Figure 27. Lines of velocity data through the instrument position (indicated by the dashed line) in all three directions: top – across the domain; middle – along the domain, and bottom – vertically. The results are for a flow to the **METEK sonic at ±90 degrees** off the bow.

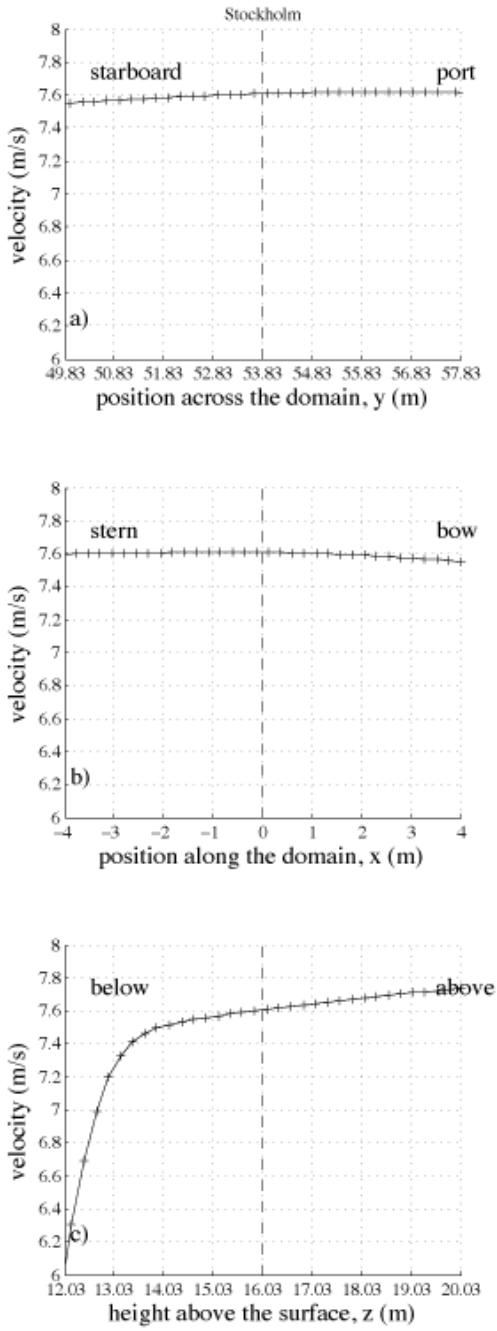

Figure 28. The **CSAT sonic site at ±90 degrees** off the bow.

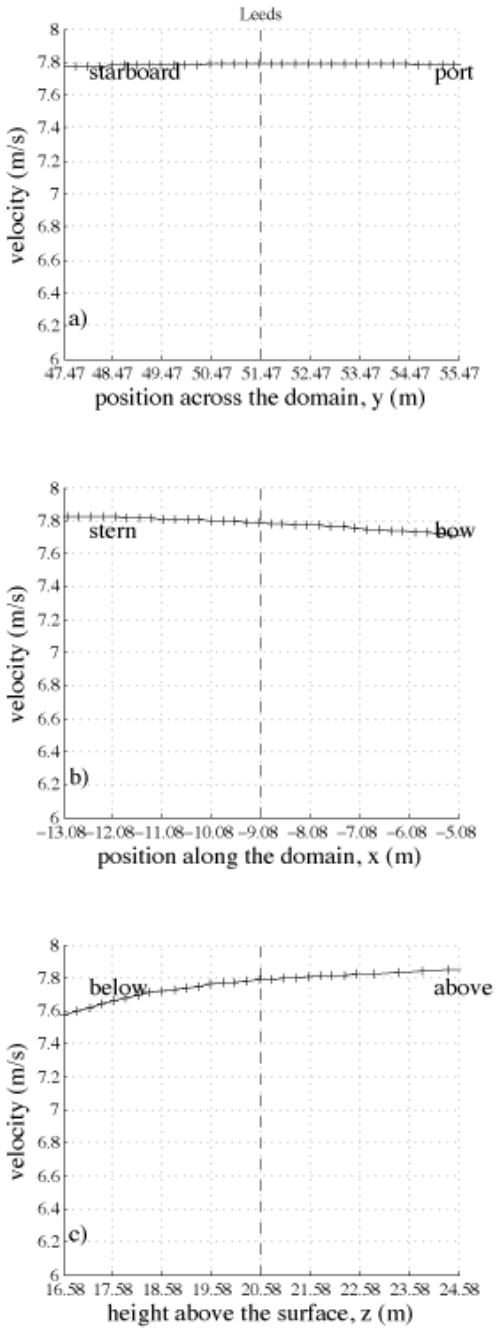

Figure 29. Lines of velocity data through the instrument position (indicated by the dashed line) in all three directions: top – across the domain; middle – along the domain, and bottom – vertically. The results are for a flow to the **METEK sonic at ±100 degrees** off the bow.

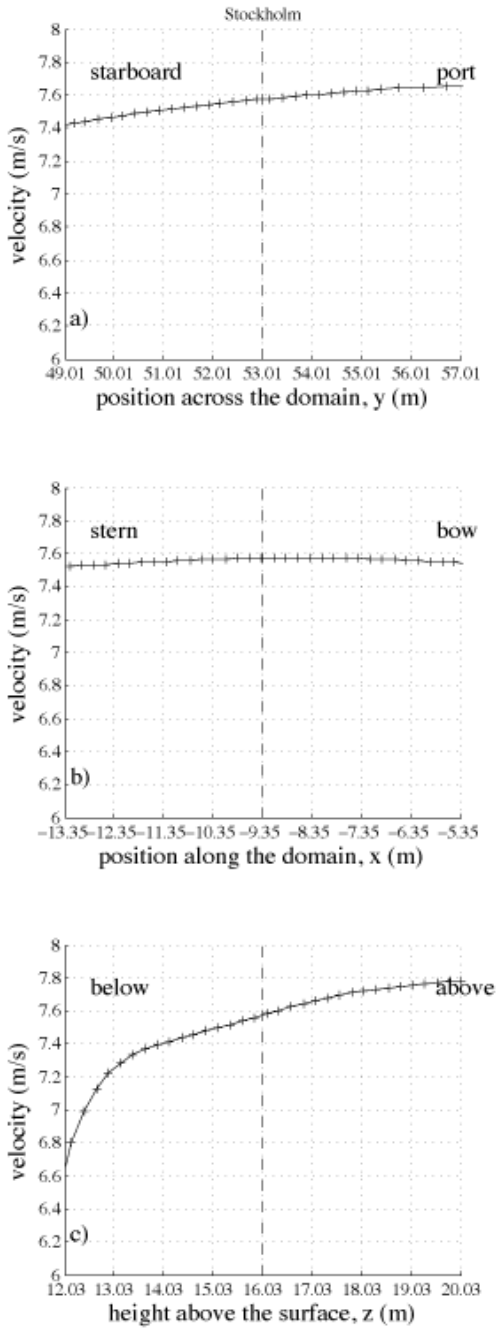

Figure 30. The **CSAT sonic site at ±100 degrees** off the bow.

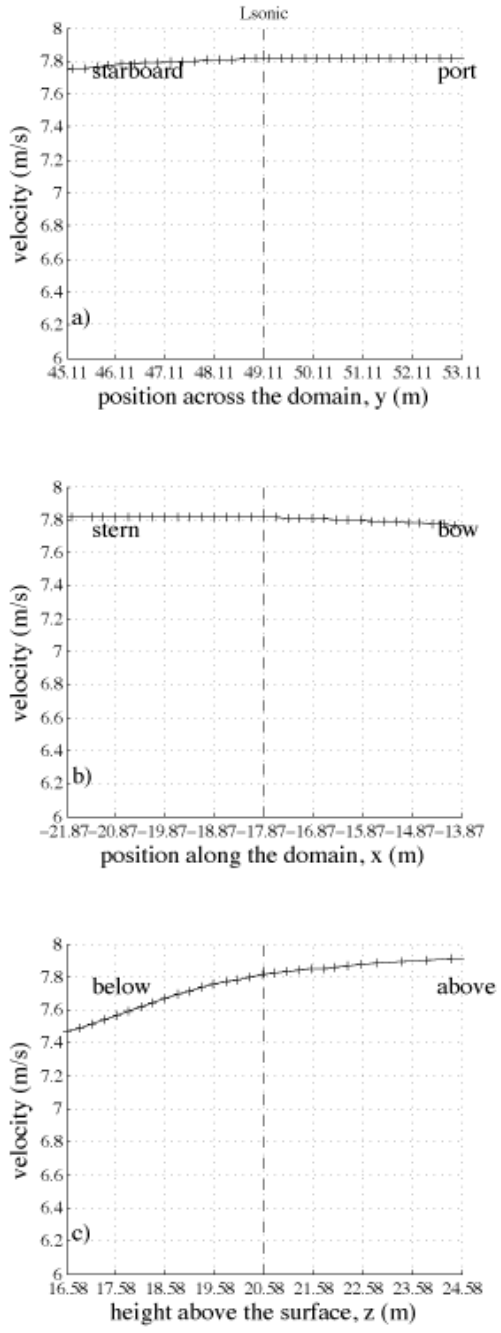

Figure 31. Lines of velocity data through the instrument position (indicated by the dashed line) in all three directions: top – across the domain; middle – along the domain, and bottom – vertically. The results are for a flow to the **METEK sonic at ±110 degrees** off the bow.

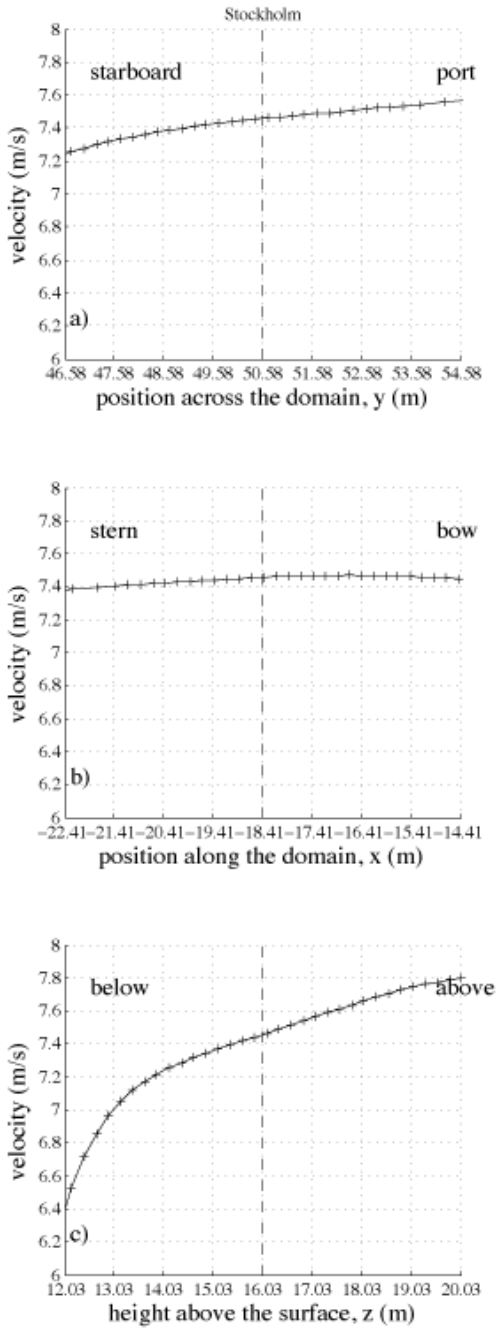

Figure 32. The **CSAT sonic site at ±110 degrees** off the bow.

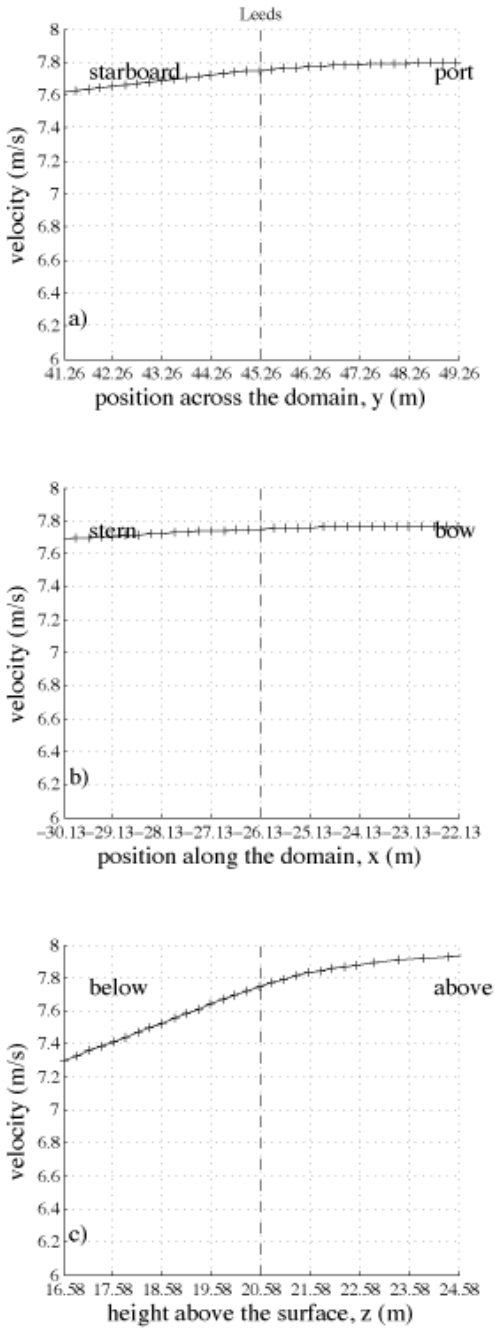

Figure 33. Lines of velocity data through the instrument position (indicated by the dashed line) in all three directions: top – across the domain; middle – along the domain, and bottom – vertically. The results are for a flow to the **METEK sonic at ±120 degrees** off the bow.

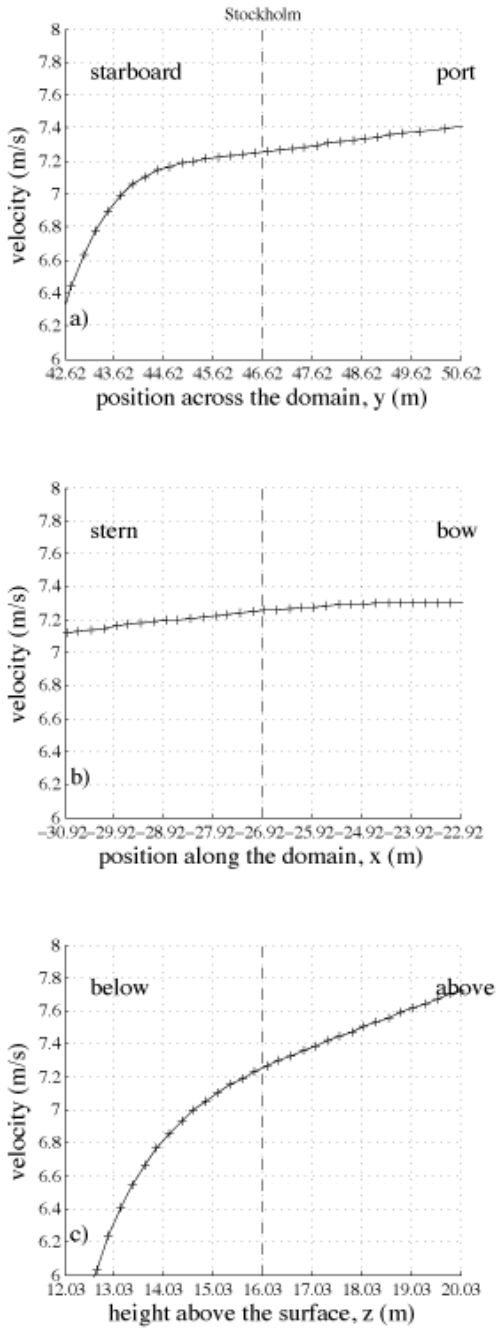

Figure 34. The **CSAT sonic site at ±120 degrees** off the bow.

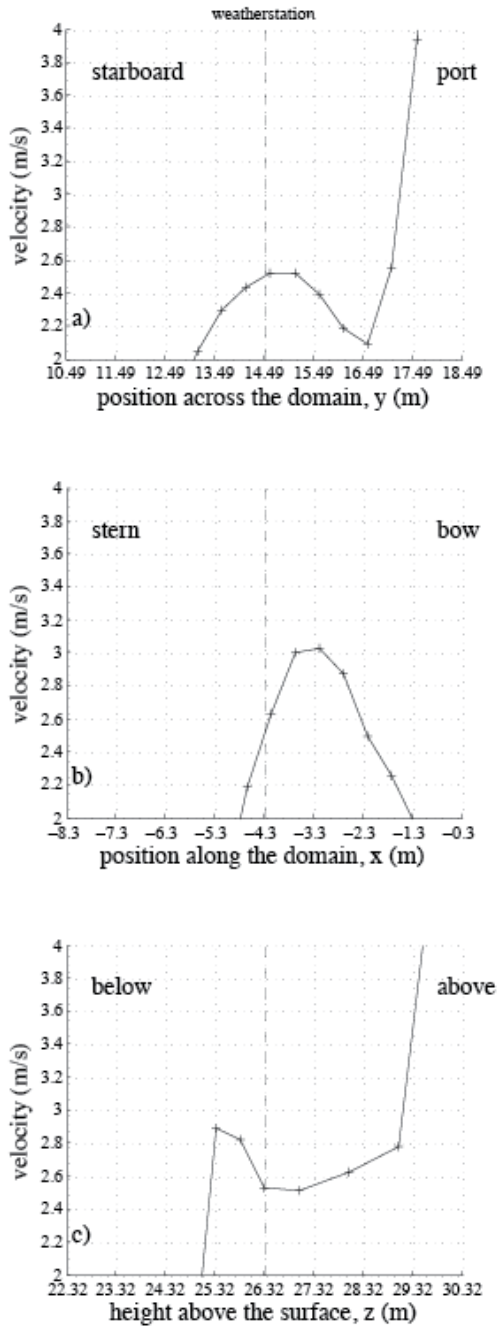

Figure 35. Lines of velocity data through the instrument position (indicated by the dashed line) in all three directions: top – across the domain; middle – along the domain, and bottom – vertically. The results are for a flow to the **weather station anemometer at 110 degrees** over the port side.

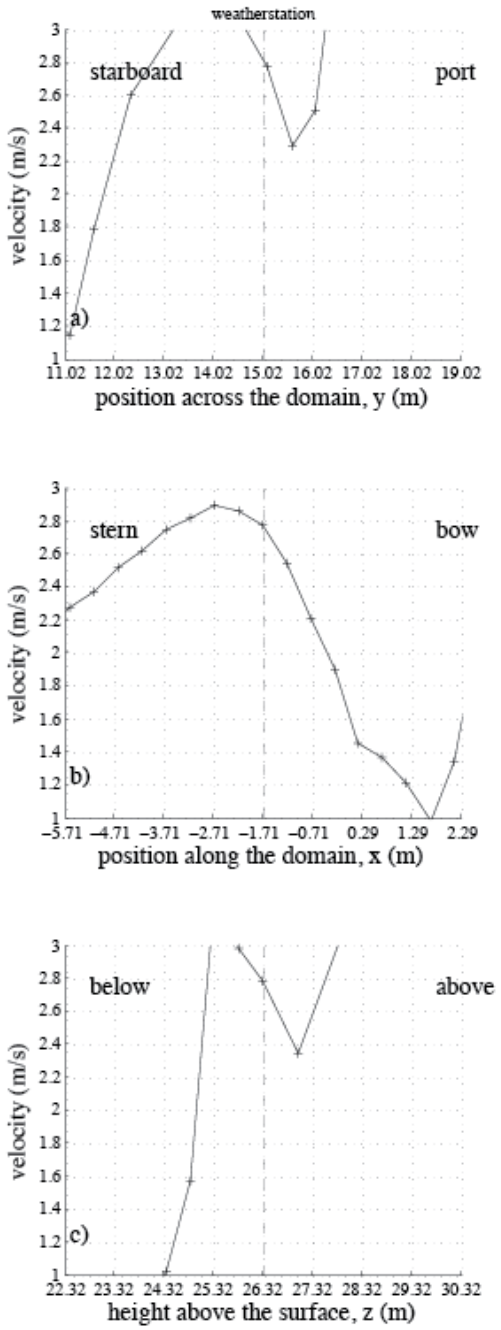

Figure 36. Lines of velocity data through the instrument position (indicated by the dashed line) in all three directions: top – across the domain; middle – along the domain, and bottom – vertically. The results are for a flow to the **weather station anemometer at 100 degrees** over the port side.

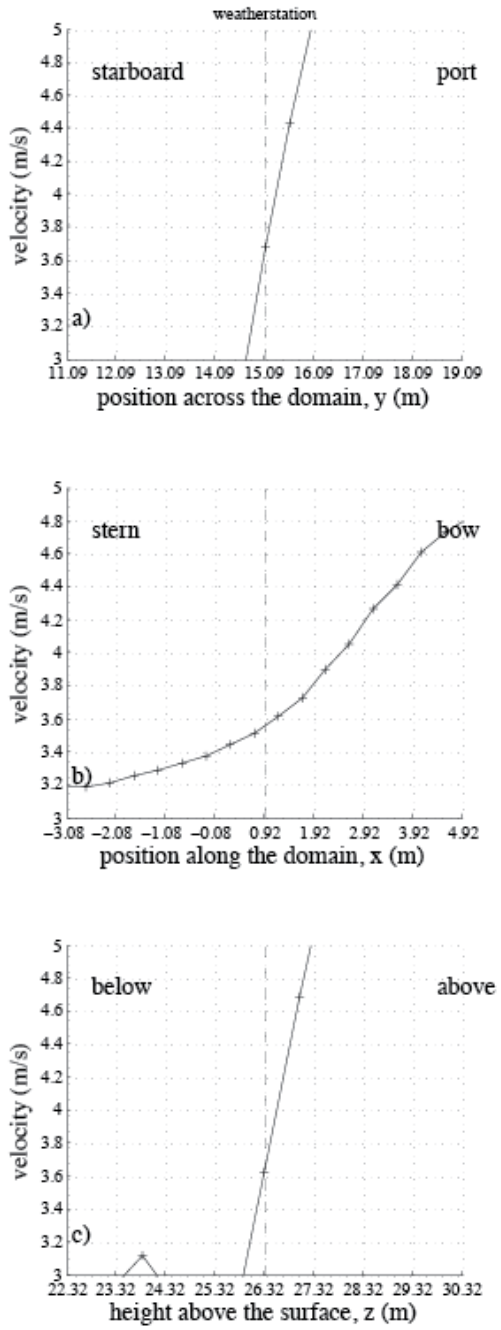

Figure 37. Lines of velocity data through the instrument position (indicated by the dashed line) in all three directions: top – across the domain; middle – along the domain, and bottom – vertically. The results are for a flow to the **weather station anemometer at 90 degrees** over the port side (beam-on).

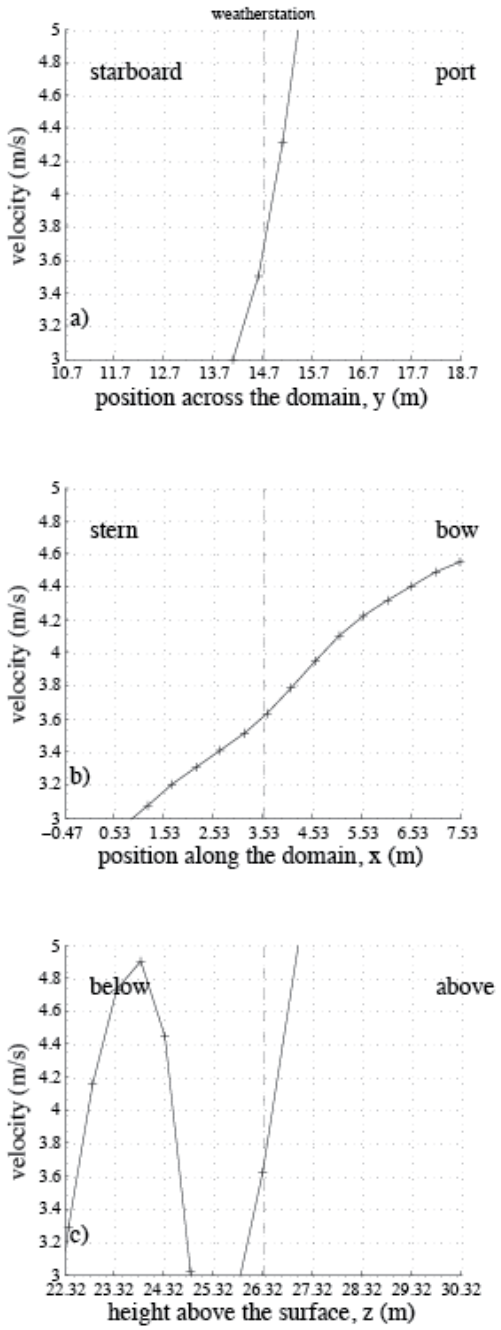

Figure 38. Lines of velocity data through the instrument position (indicated by the dashed line) in all three directions: top – across the domain; middle – along the domain, and bottom – vertically. The results are for a flow to the **weather station anemometer at 80 degrees** over the port side.

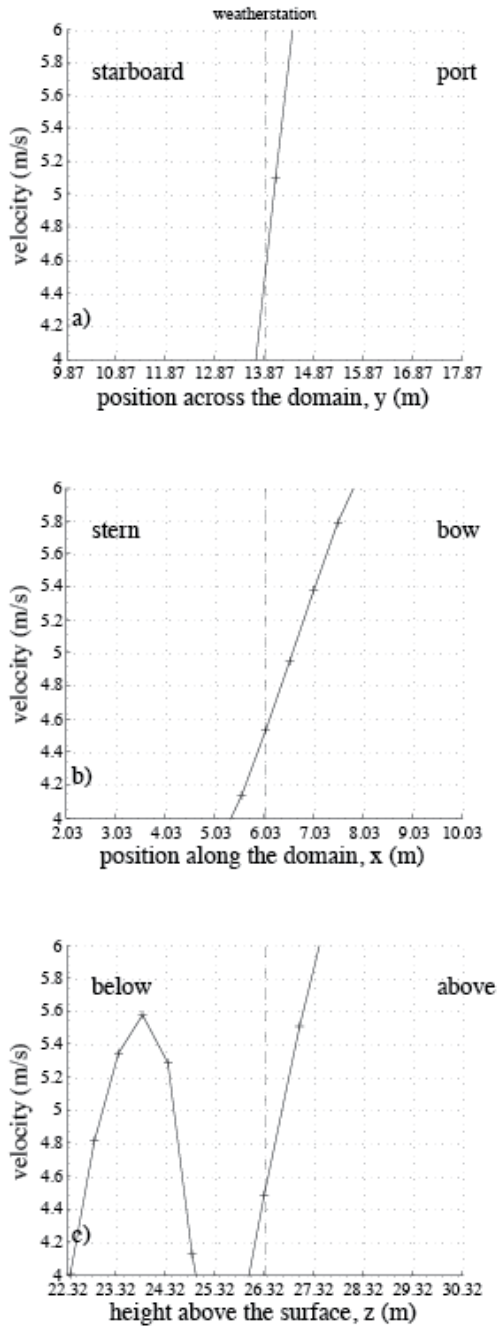

Figure 39. Lines of velocity data through the instrument position (indicated by the dashed line) in all three directions: top – across the domain; middle – along the domain, and bottom – vertically. The results are for a flow to the **weather station anemometer at 70 degrees** over the port side.

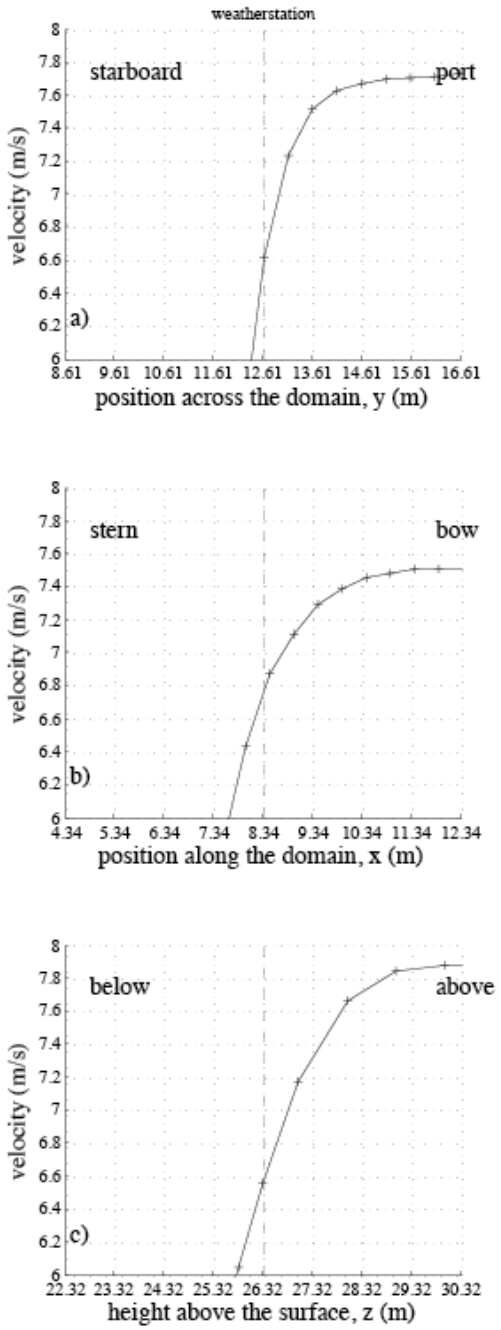

Figure 40. Lines of velocity data through the instrument position (indicated by the dashed line) in all three directions: top – across the domain; middle – along the domain, and bottom – vertically. The results are for a flow to the **weather station anemometer at 60 degrees** over the port side.

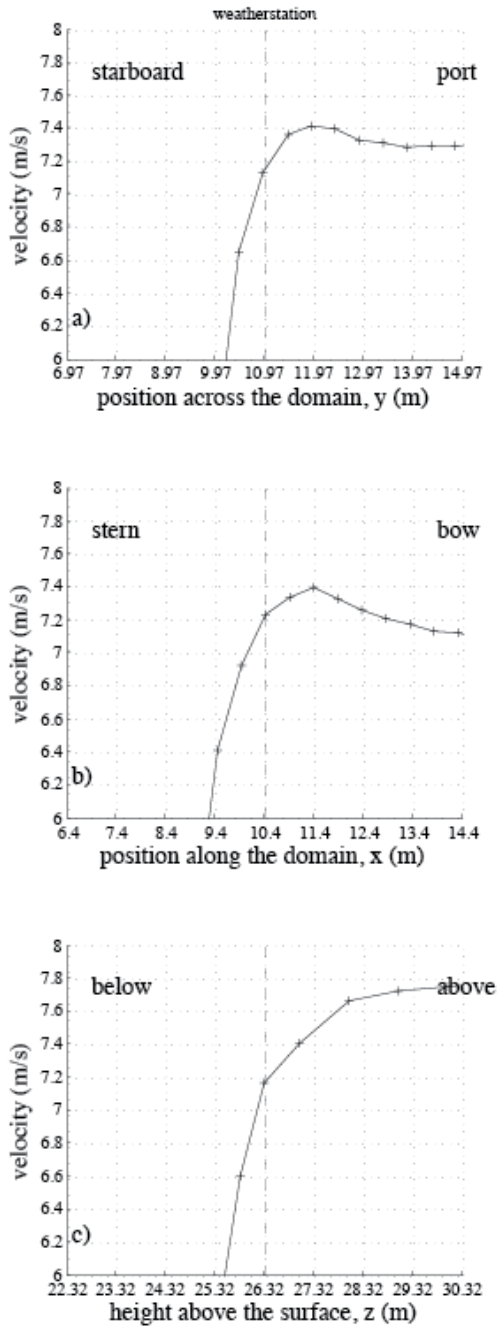

Figure 41. Lines of velocity data through the instrument position (indicated by the dashed line) in all three directions: top – across the domain; middle – along the domain, and bottom – vertically. The results are for a flow to the **weather station anemometer at 50 degrees** over the port side.

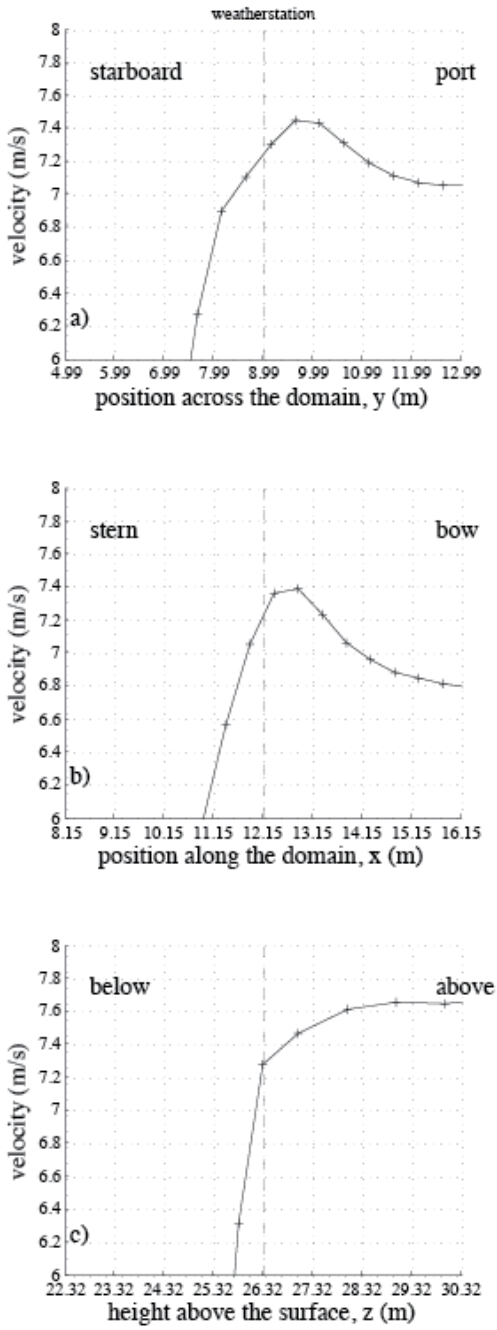

Figure 42. Lines of velocity data through the instrument position (indicated by the dashed line) in all three directions: top – across the domain; middle – along the domain, and bottom – vertically. The results are for a flow to the **weather station anemometer at 40 degrees** over the port side.

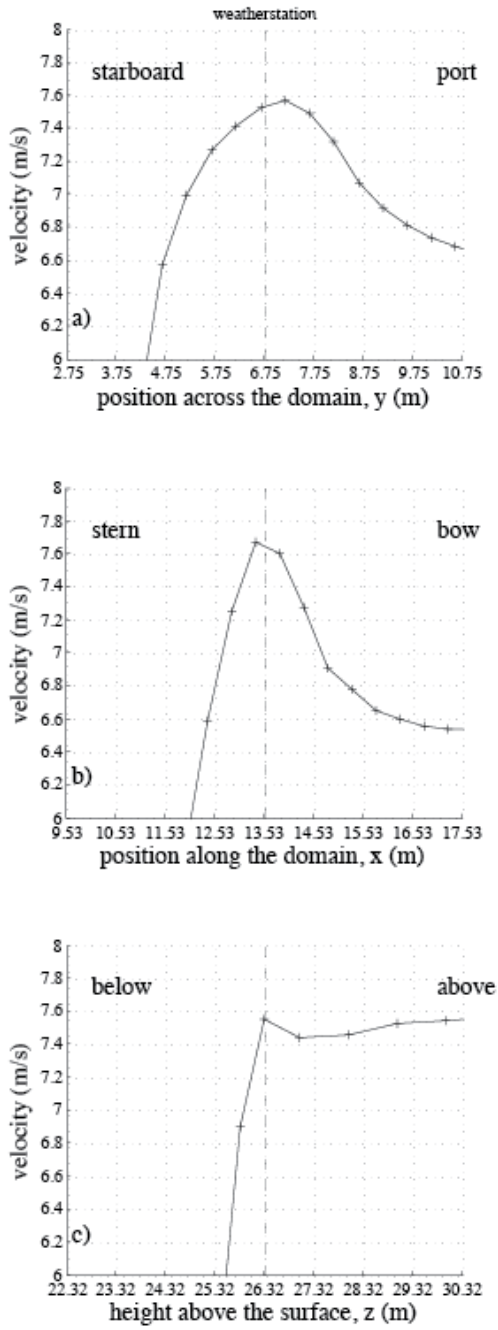

Figure 43. Lines of velocity data through the instrument position (indicated by the dashed line) in all three directions: top – across the domain; middle – along the domain, and bottom – vertically. The results are for a flow to the **weather station anemometer at 30 degrees** over the port side.

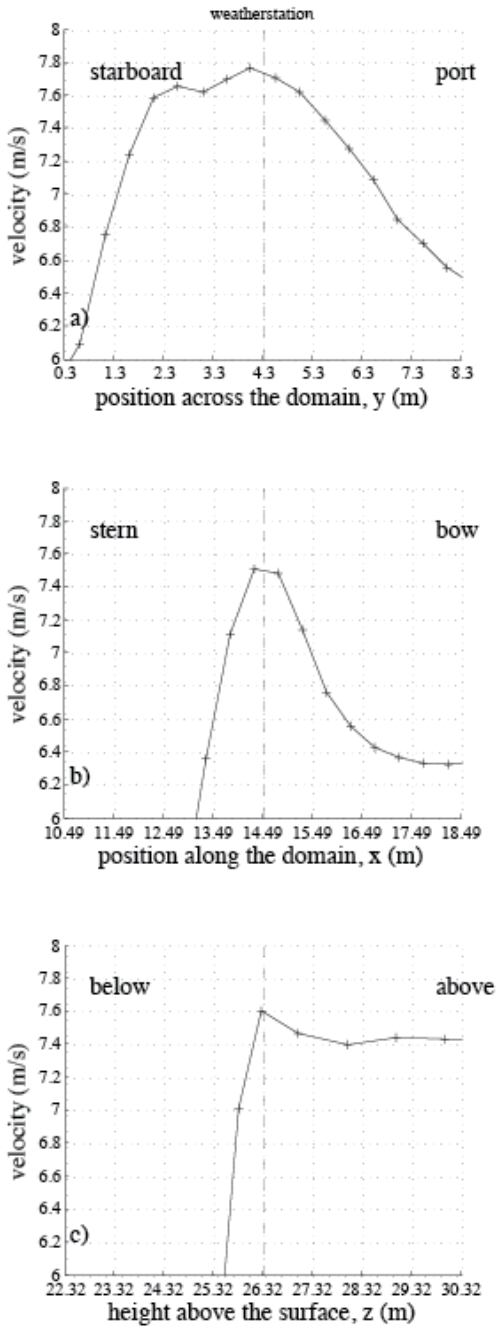

Figure 44. Lines of velocity data through the instrument position (indicated by the dashed line) in all three directions: top – across the domain; middle – along the domain, and bottom – vertically. The results are for a flow to the **weather station anemometer at 20 degrees** over the port side.

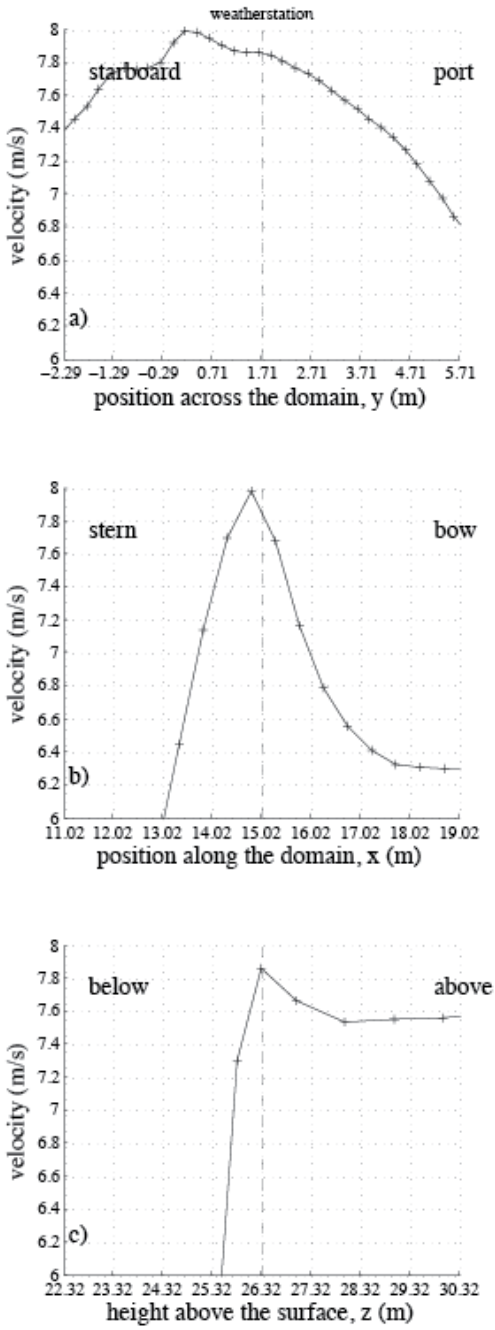

Figure 45. Lines of velocity data through the instrument position (indicated by the dashed line) in all three directions: top – across the domain; middle – along the domain, and bottom – vertically. The results are for a flow to the **weather station anemometer at 10 degrees** over the port side.

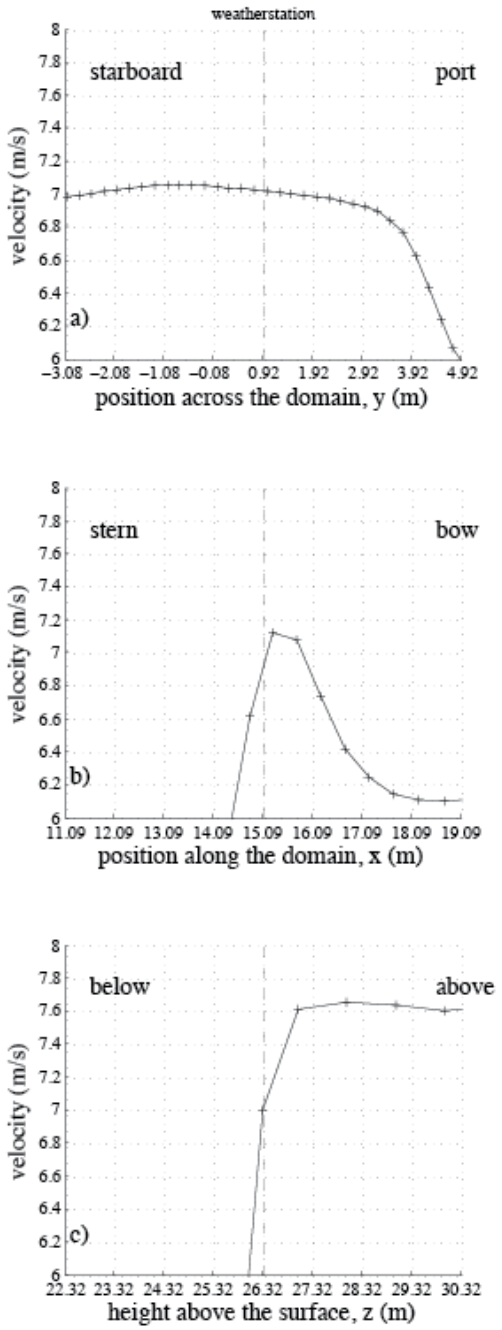

Figure 46. Lines of velocity data through the instrument position (indicated by the dashed line) in all three directions: top – across the domain; middle – along the domain, and bottom – vertically. The results are for a flow to the **weather station anemometer for a flow directly over the bow (bow-on).**

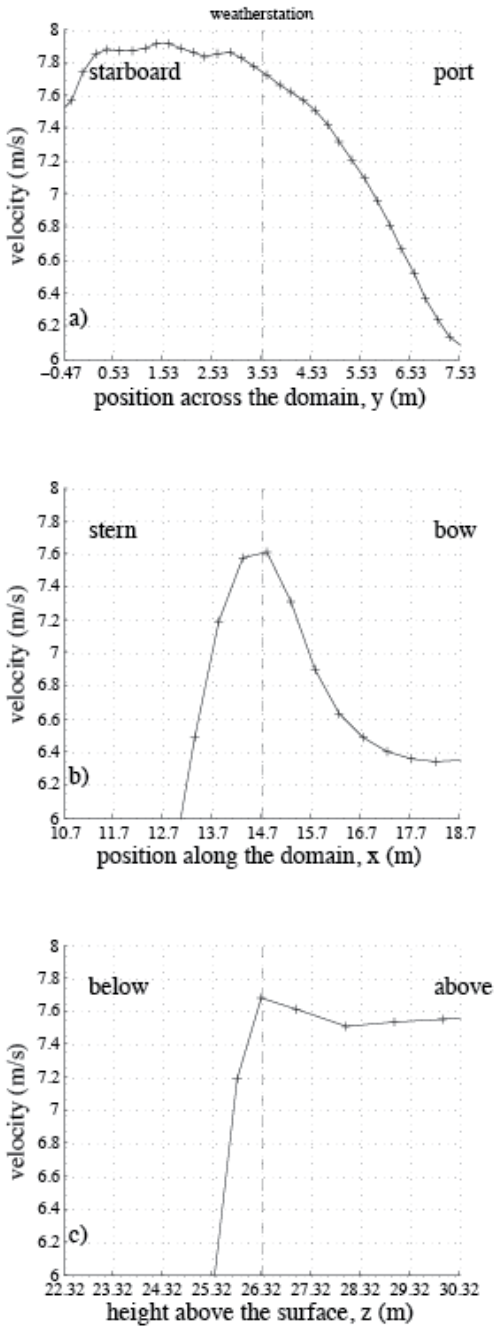

Figure 47. Lines of velocity data through the instrument position (indicated by the dashed line) in all three directions: top – across the domain; middle – along the domain, and bottom – vertically. The results are for a flow to the **weather station anemometer at 10 degrees** over the starboard side.

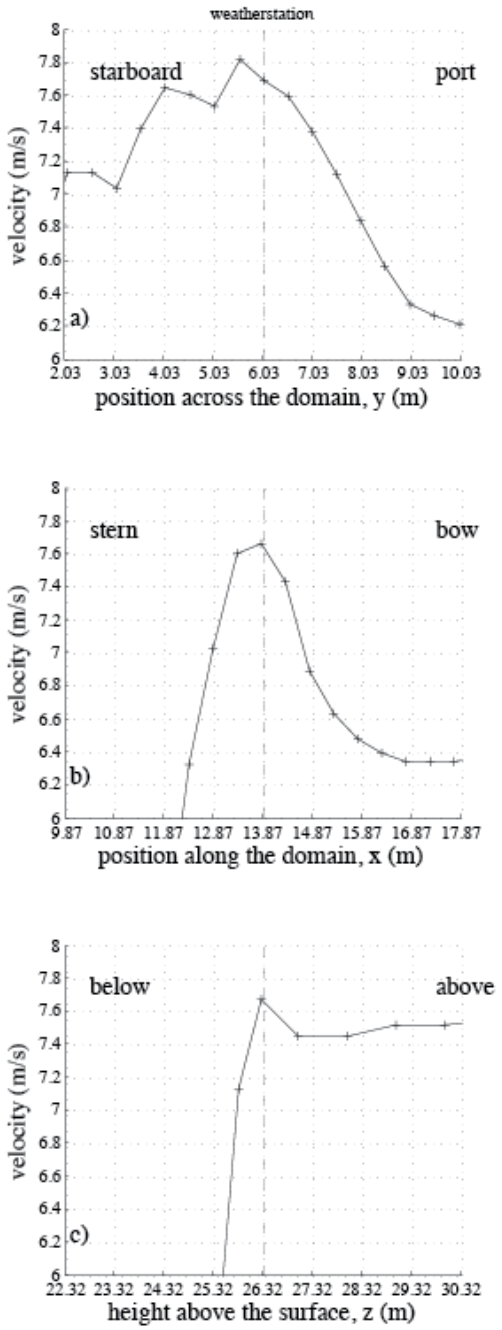

Figure 48. Lines of velocity data through the instrument position (indicated by the dashed line) in all three directions: top – across the domain; middle – along the domain, and bottom – vertically. The results are for a flow to the **weather station anemometer at 20 degrees** over the starboard side.

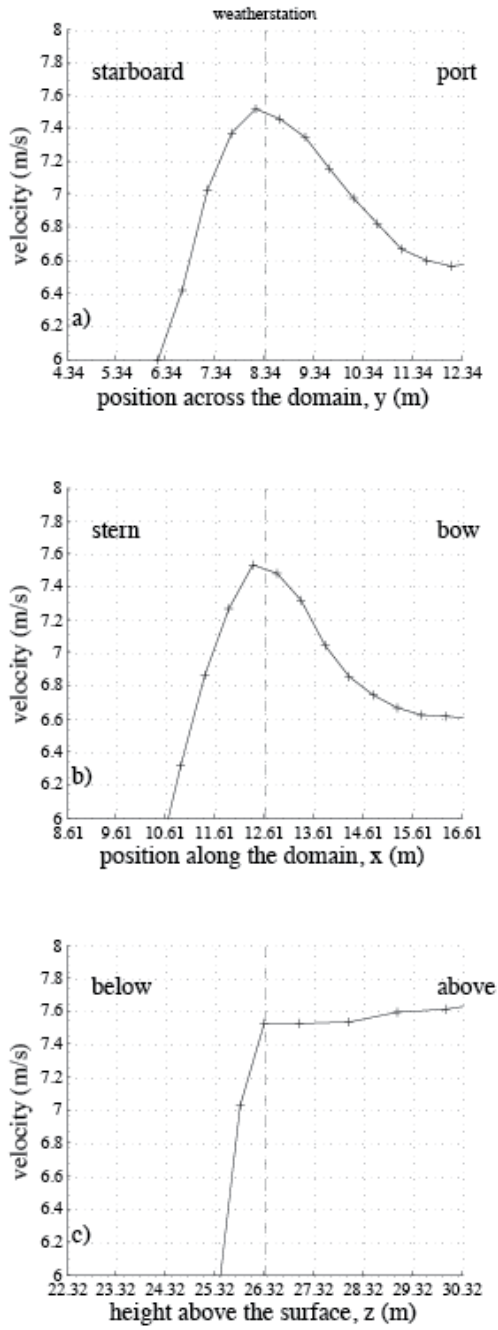

Figure 49. Lines of velocity data through the instrument position (indicated by the dashed line) in all three directions: top – across the domain; middle – along the domain, and bottom – vertically. The results are for a flow to the **weather station anemometer at 30 degrees** over the starboard side.

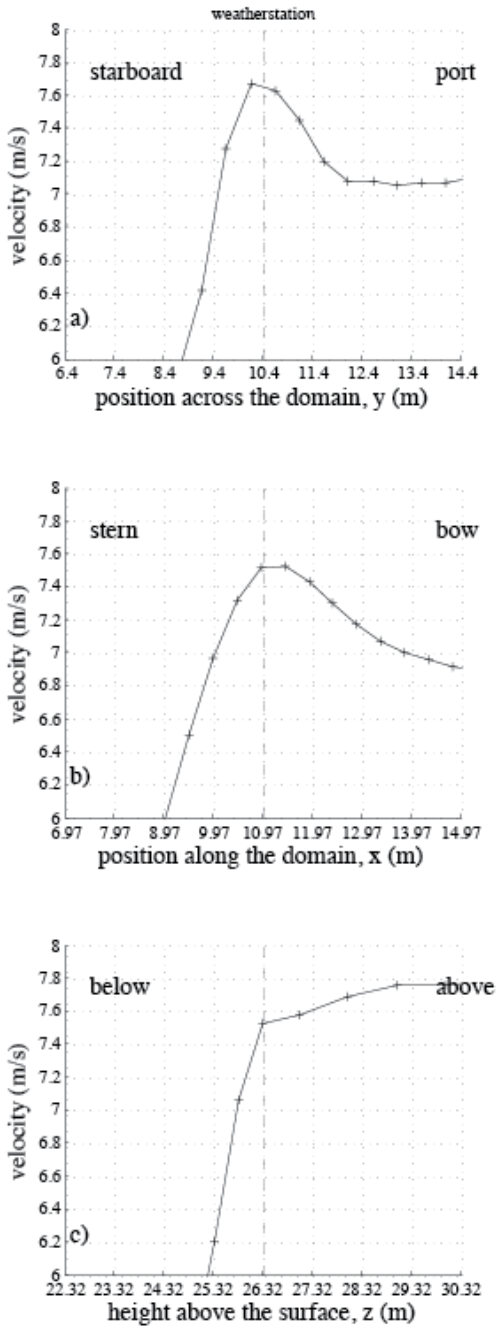

Figure 50. Lines of velocity data through the instrument position (indicated by the dashed line) in all three directions: top – across the domain; middle – along the domain, and bottom – vertically. The results are for a flow to the **weather station anemometer at 40 degrees** over the starboard side.

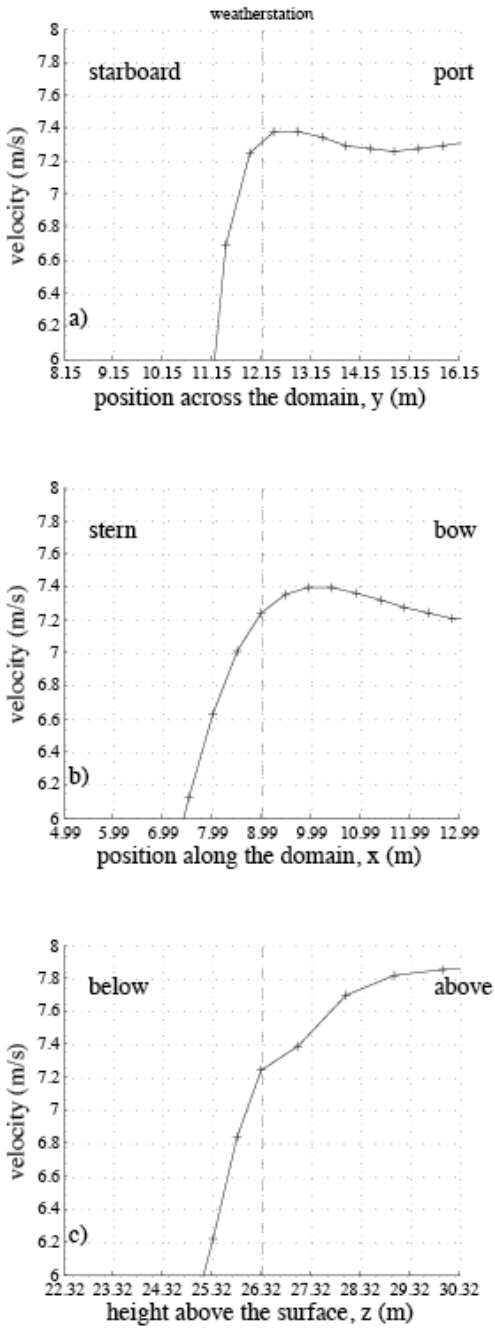

Figure 51. Lines of velocity data through the instrument position (indicated by the dashed line) in all three directions: top – across the domain; middle – along the domain, and bottom – vertically. The results are for a flow to the **weather station anemometer at 50 degrees** over the starboard side.

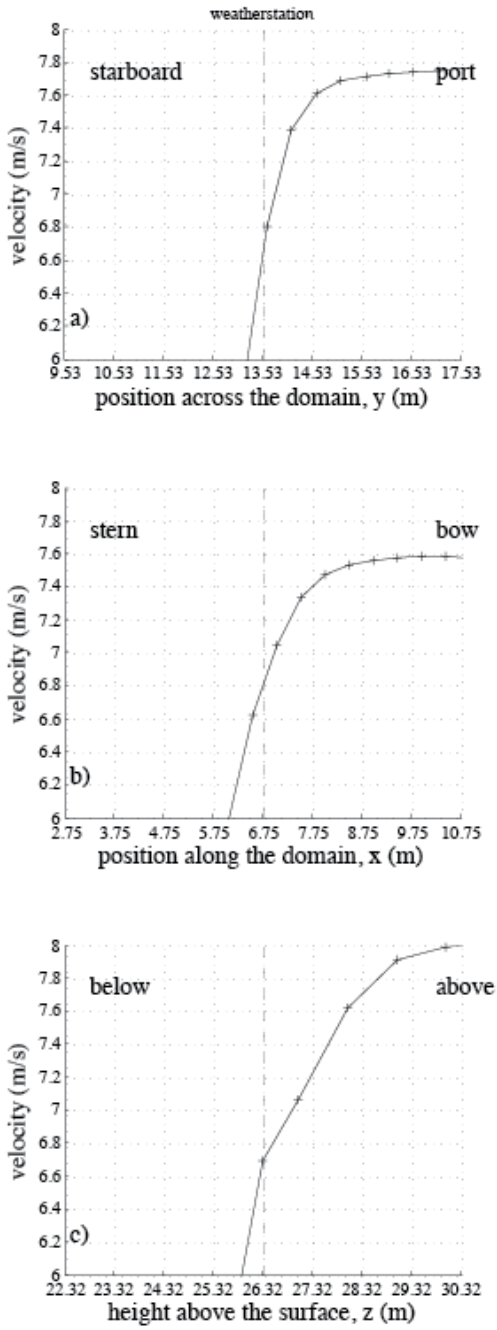

Figure 52. Lines of velocity data through the instrument position (indicated by the dashed line) in all three directions: top – across the domain; middle – along the domain, and bottom – vertically. The results are for a flow to the **weather station anemometer at 60 degrees** over the starboard side.

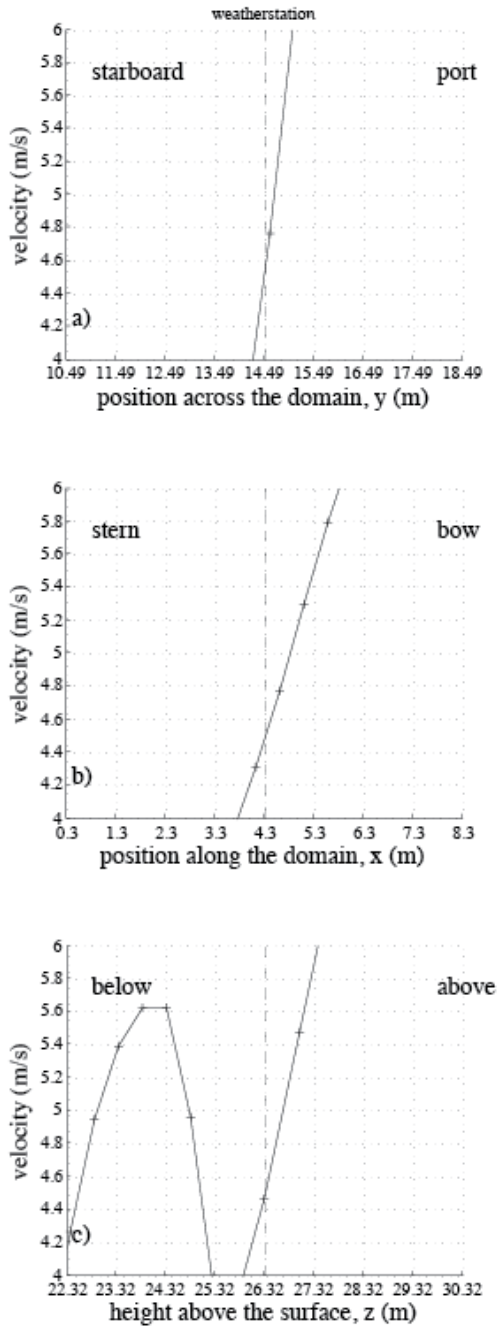

Figure 53. Lines of velocity data through the instrument position (indicated by the dashed line) in all three directions: top – across the domain; middle – along the domain, and bottom – vertically. The results are for a flow to the **weather station anemometer at 70 degrees** over the starboard side.

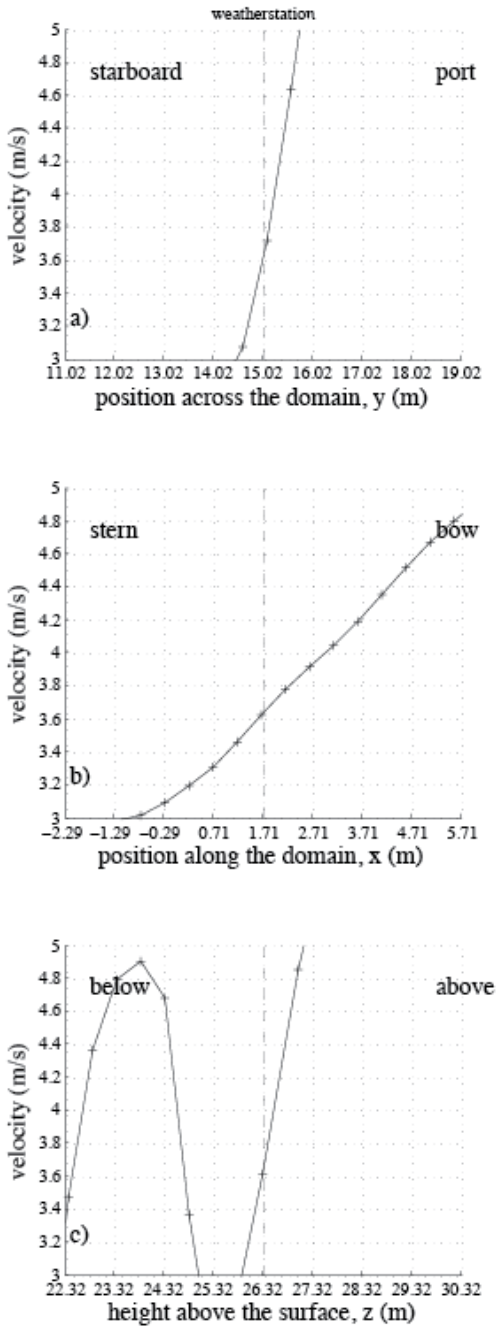

Figure 54. Lines of velocity data through the instrument position (indicated by the dashed line) in all three directions: top – across the domain; middle – along the domain, and bottom – vertically. The results are for a flow to the **weather station anemometer at 80 degrees** over the starboard side.

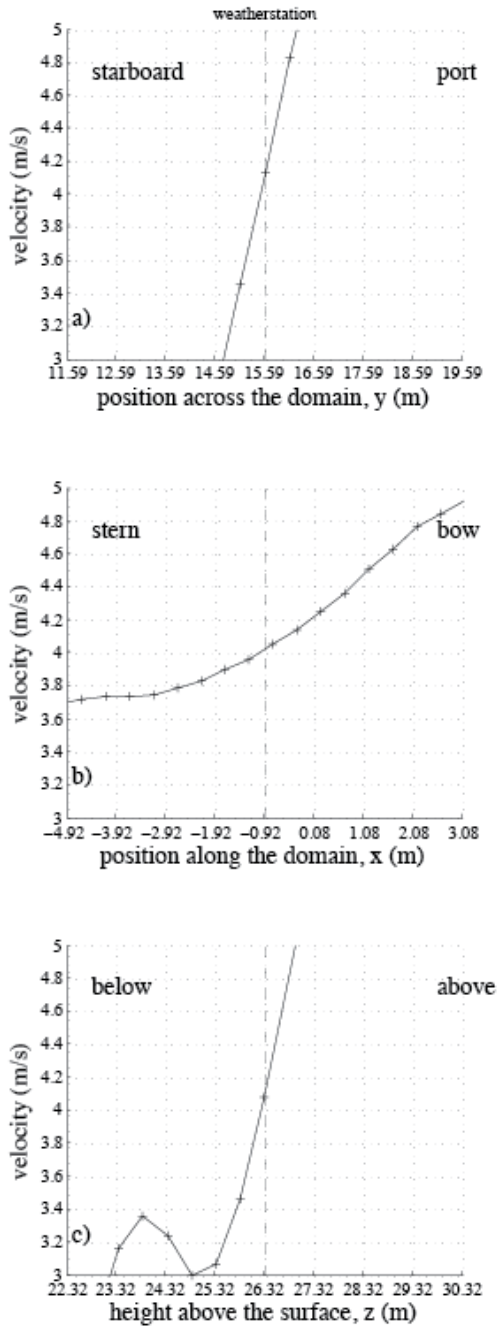

Figure 55. Lines of velocity data through the instrument position (indicated by the dashed line) in all three directions: top – across the domain; middle – along the domain, and bottom – vertically. The results are for a flow to the **weather station anemometer at 90 degrees** over the starboard side (beam-on).

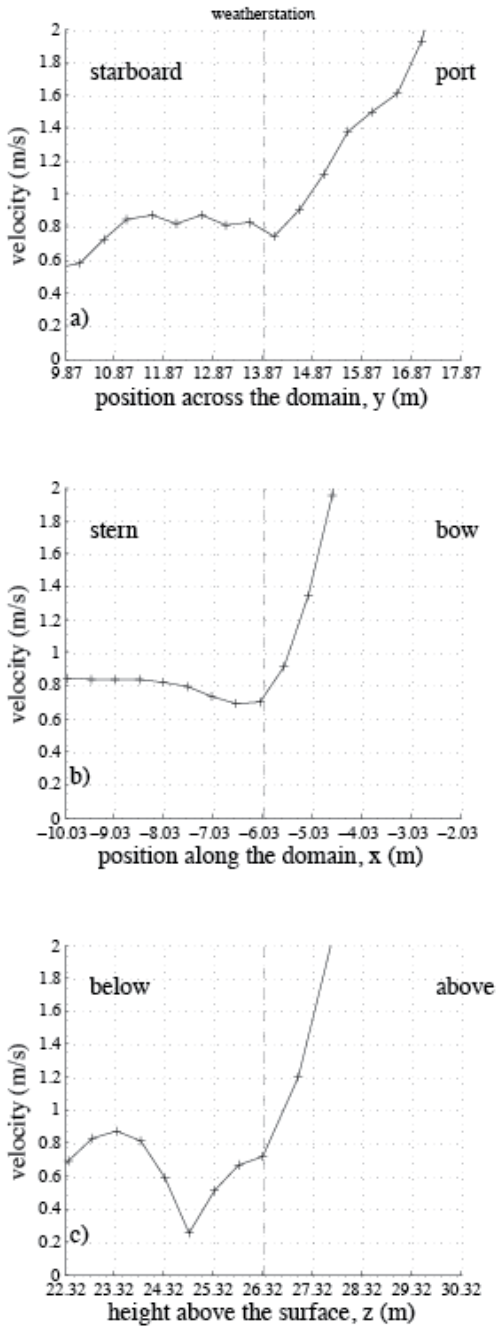

Figure 56. Lines of velocity data through the instrument position (indicated by the dashed line) in all three directions: top – across the domain; middle – along the domain, and bottom – vertically. The results are for a flow to the **weather station anemometer at 110 degrees** over the starboard side.

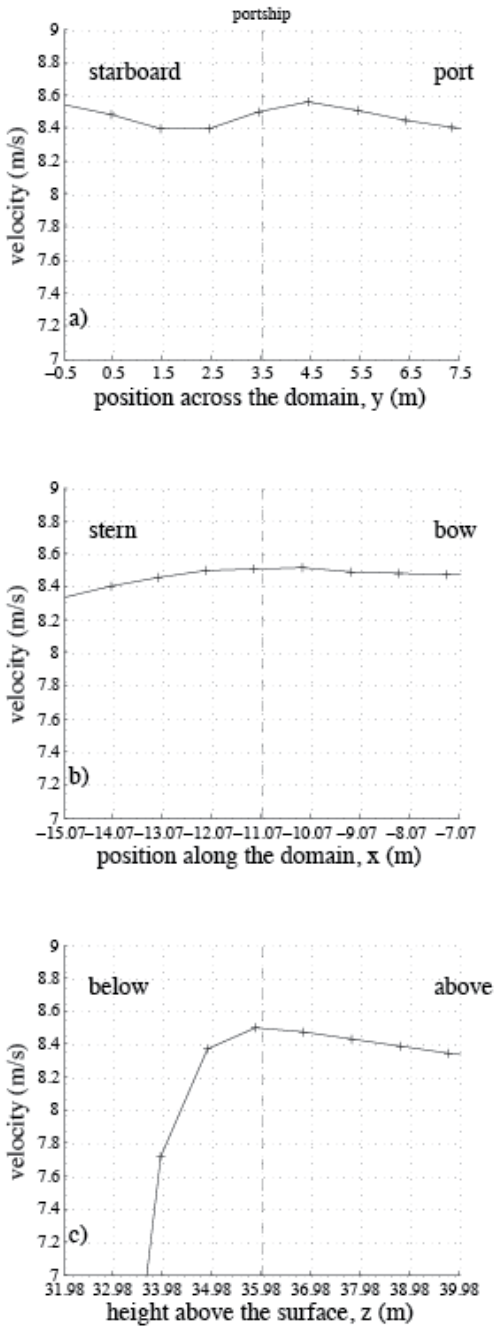

Figure 57. Lines of velocity data through the instrument position (indicated by the dashed line) in all three directions: The results are for a flow to the **port ship's anemometer at 150 degrees** over the starboard side and **starboard ship's anemometer at 150 degrees** over the port side.

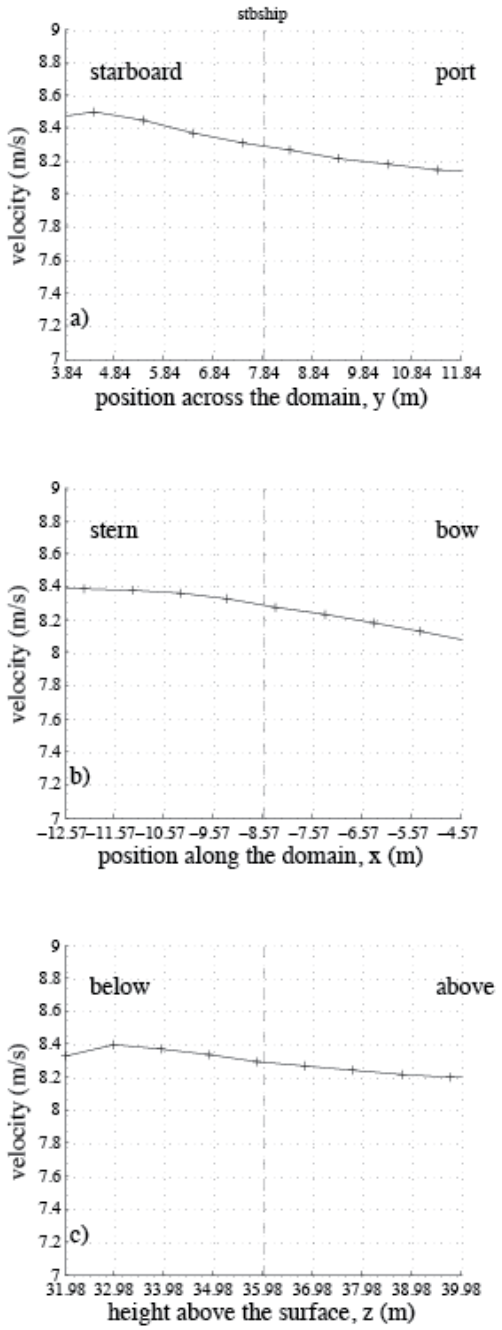

Figure 58. Lines of velocity data through the instrument position (indicated by the dashed line) in all three directions: The results are for a flow to the **starboard ship's anemometer at 150 degrees** over the starboard side and **port ship's anemometer at 150 degrees** over the port side.

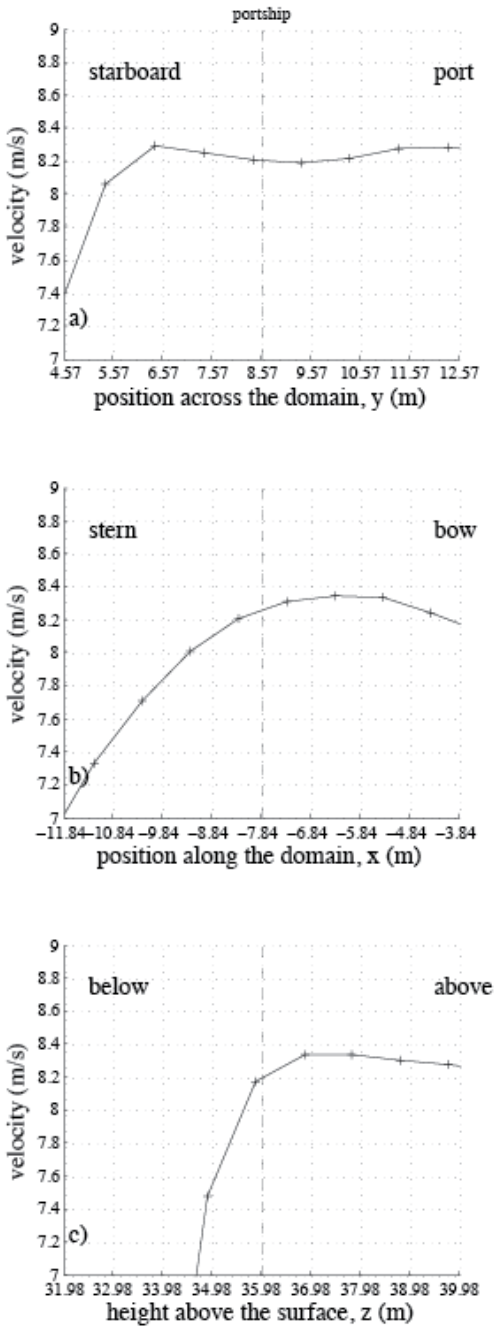

Figure 59. Lines of velocity data through the instrument position (indicated by the dashed line) in all three directions: The results are for a flow to the **port ship's anemometer at 120 degrees** over the starboard side and **starboard ship's anemometer at 120 degrees** over the port side.

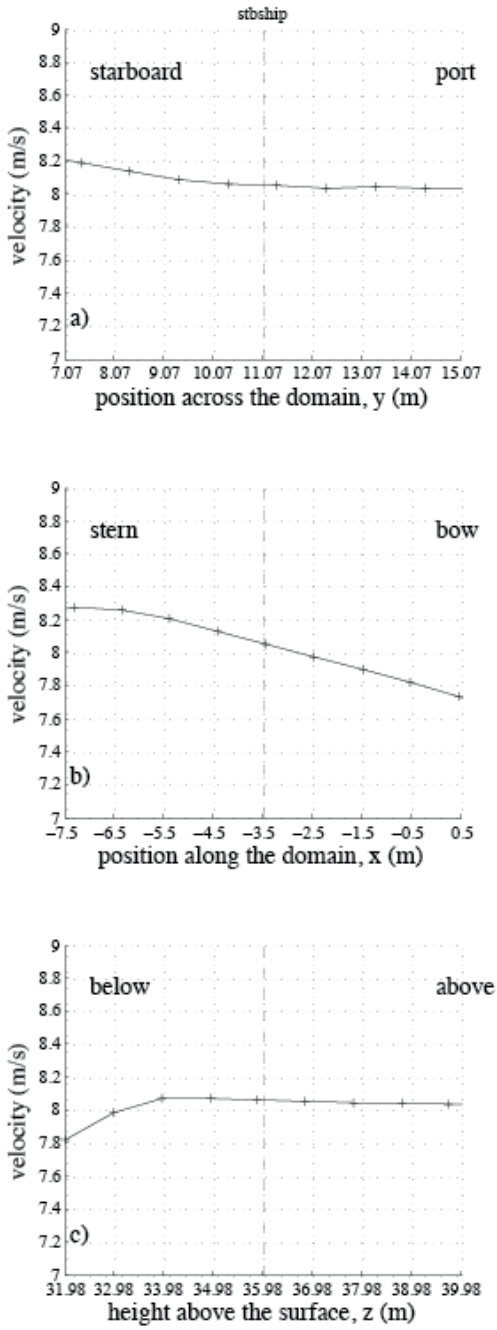

Figure 60. Lines of velocity data through the instrument position (indicated by the dashed line) in all three directions: The results are for a flow to the **starboard ship's anemometer at 120 degrees** over the starboard side and **port ship's anemometer at 120 degrees** over the port side.

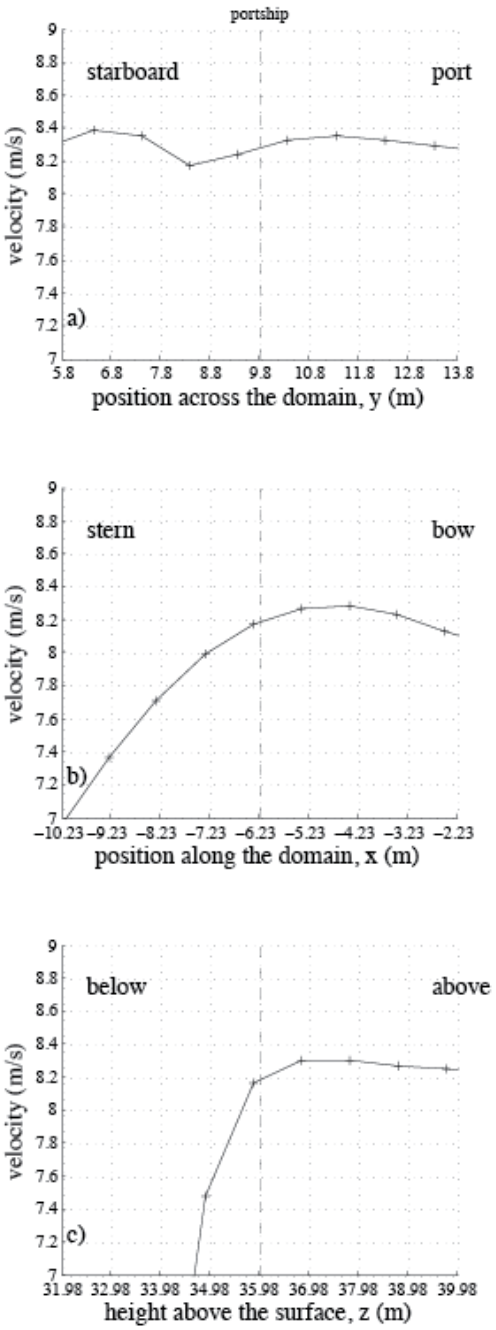

Figure 61. Lines of velocity data through the instrument position (indicated by the dashed line) in all three directions: The results are for a flow to the **port ship's anemometer at 110 degrees** over the starboard side and **starboard ship's anemometer at 110 degrees** over the port side.

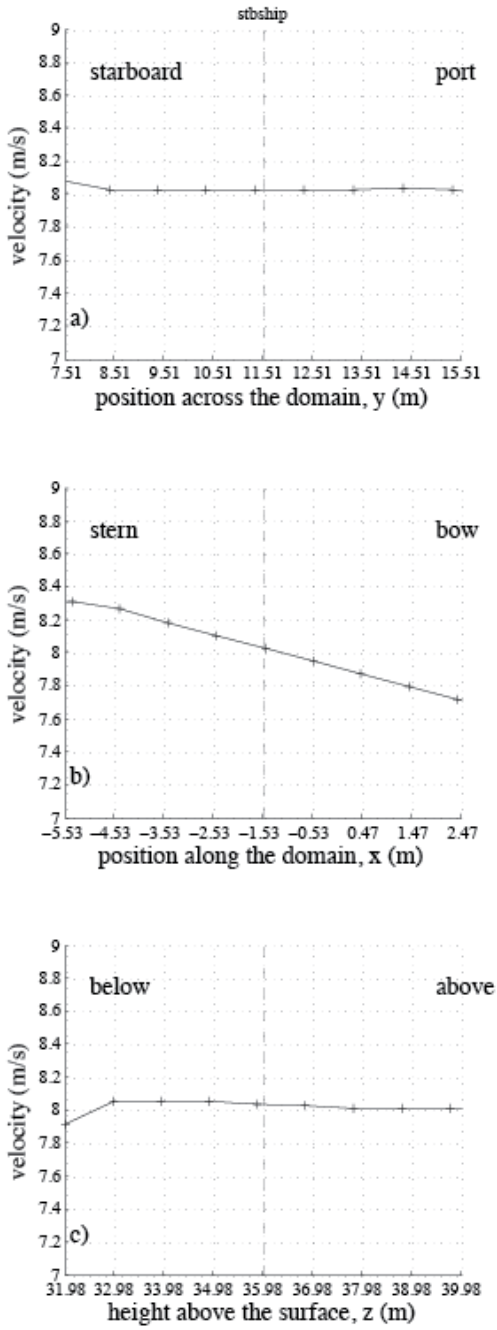

Figure 62. Lines of velocity data through the instrument position (indicated by the dashed line) in all three directions: The results are for a flow to the **starboard ship's anemometer at 110 degrees** over the starboard side and **port ship's anemometer at 110 degrees** over the port side.

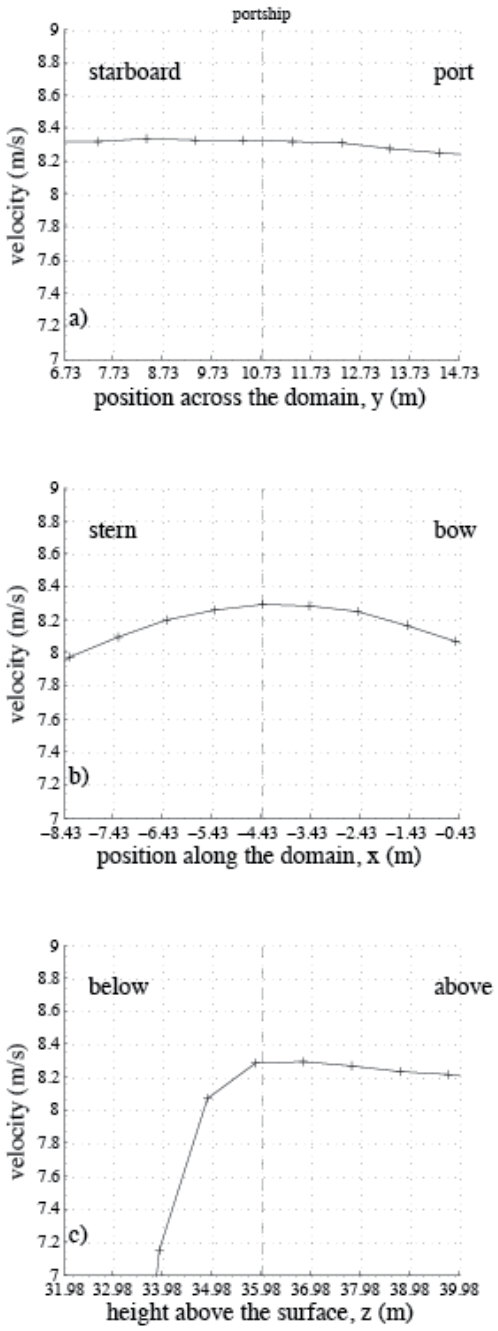

Figure 63. Lines of velocity data through the instrument position (indicated by the dashed line) in all three directions: The results are for a flow to the **port ship's anemometer at 100 degrees** over the starboard side and **starboard ship's anemometer at 100 degrees** over the port side.

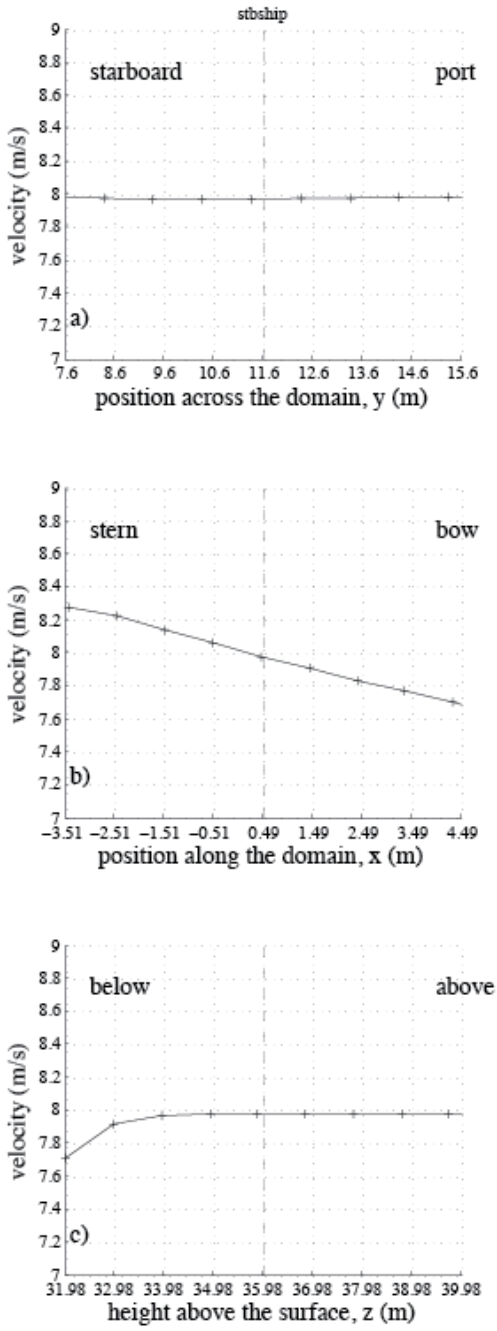

Figure 64. Lines of velocity data through the instrument position (indicated by the dashed line) in all three directions: The results are for a flow to the **starboard ship's anemometer at 100 degrees** over the starboard side and **port ship's anemometer at 100 degrees** over the port side.

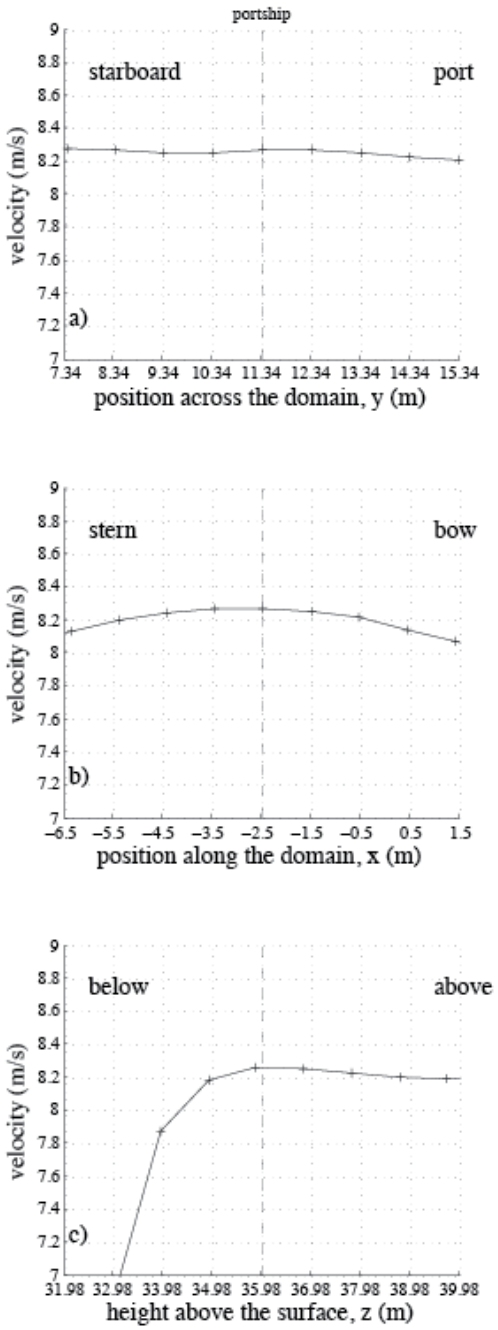

Figure 65. Lines of velocity data through the instrument position (indicated by the dashed line) in all three directions: The results are for a flow to the **port ship's anemometer at 90 degrees** over the starboard side and **starboard ship's anemometer at 90 degrees** over the port side.

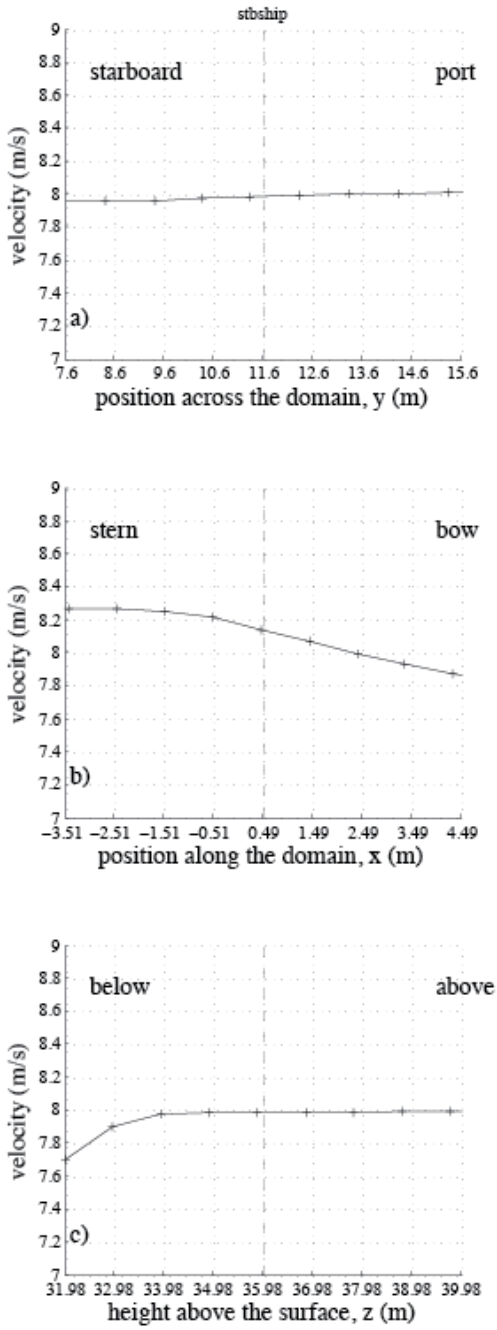

Figure 66. Lines of velocity data through the instrument position (indicated by the dashed line) in all three directions: The results are for a flow to the **starboard ship's anemometer at 90 degrees** over the starboard side and **port ship's anemometer at 90 degrees** over the port side.

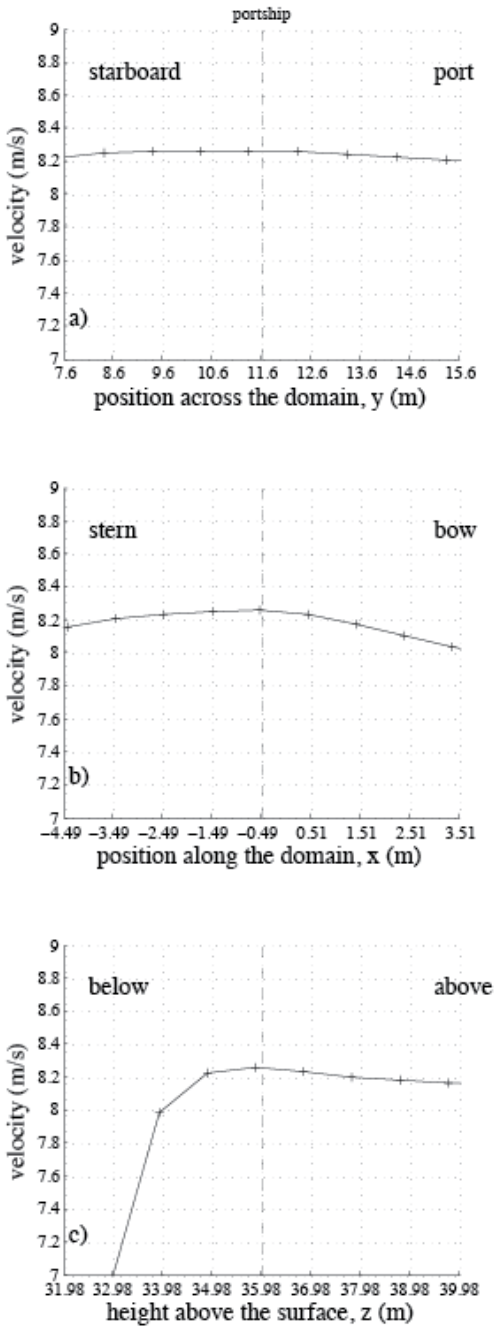

Figure 67. Lines of velocity data through the instrument position (indicated by the dashed line) in all three directions: The results are for a flow to the **port ship's anemometer at 80 degrees** over the starboard side and **starboard ship's anemometer at 80 degrees** over the port side.

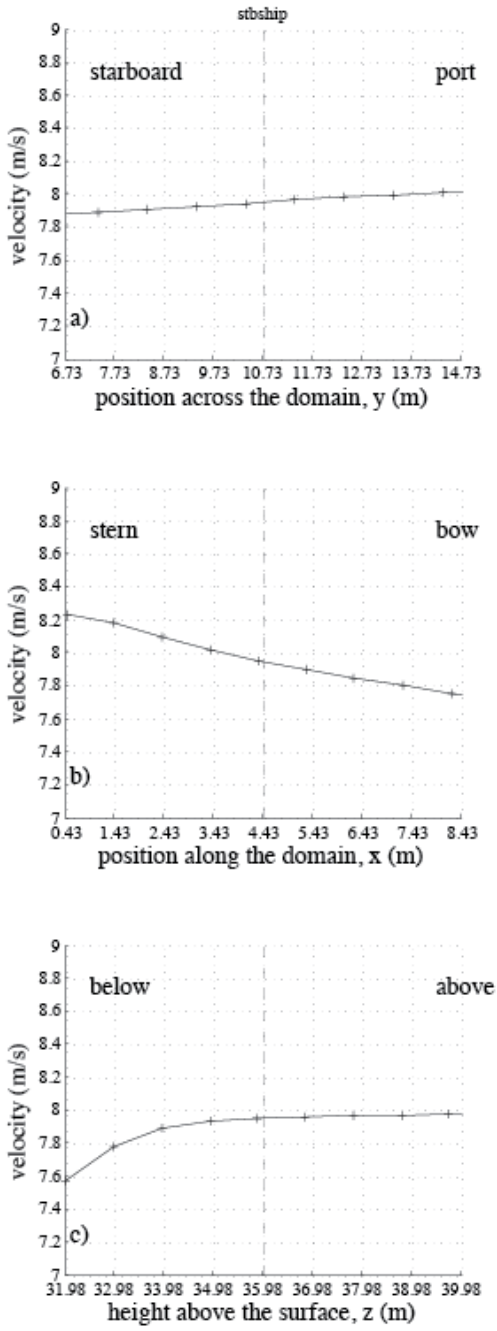

Figure 68. Lines of velocity data through the instrument position (indicated by the dashed line) in all three directions: The results are for a flow to the **starboard ship's anemometer at 80 degrees** over the starboard side and **port ship's anemometer at 80 degrees** over the port side.

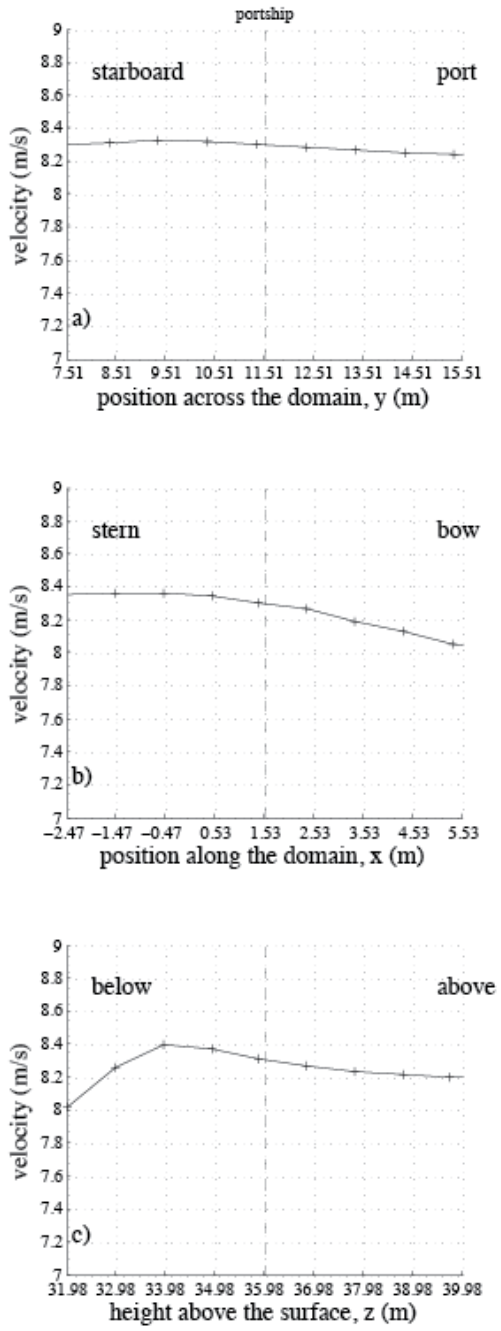

Figure 69. Lines of velocity data through the instrument position (indicated by the dashed line) in all three directions: The results are for a flow to the **port ship's anemometer at 70 degrees** over the starboard side and **starboard ship's anemometer at 70 degrees** over the port side.

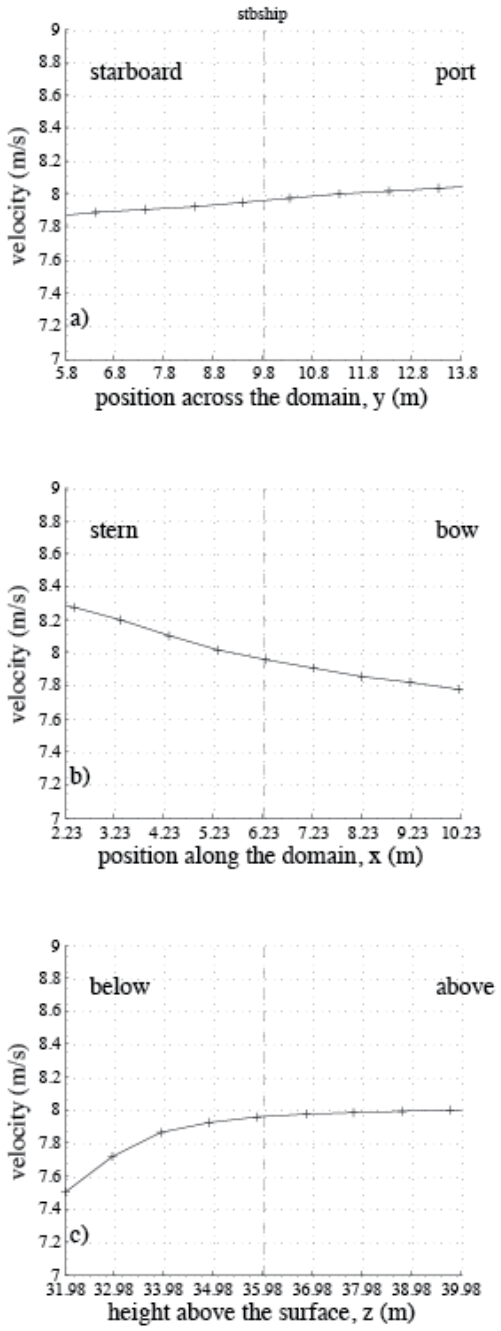

Figure 70. Lines of velocity data through the instrument position (indicated by the dashed line) in all three directions: The results are for a flow to the **starboard ship's anemometer at 70 degrees** over the starboard side and **port ship's anemometer at 70 degrees** over the port side.

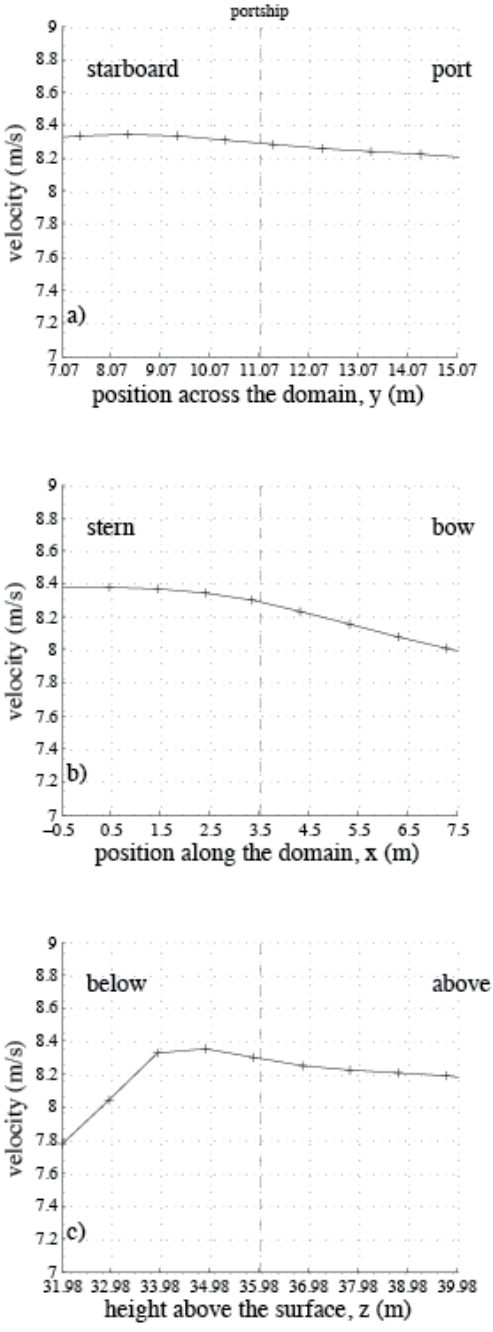

Figure 71. Lines of velocity data through the instrument position (indicated by the dashed line) in all three directions: The results are for a flow to the **port ship's anemometer at 60 degrees** over the starboard side and **starboard ship's anemometer at 60 degrees** over the port side.

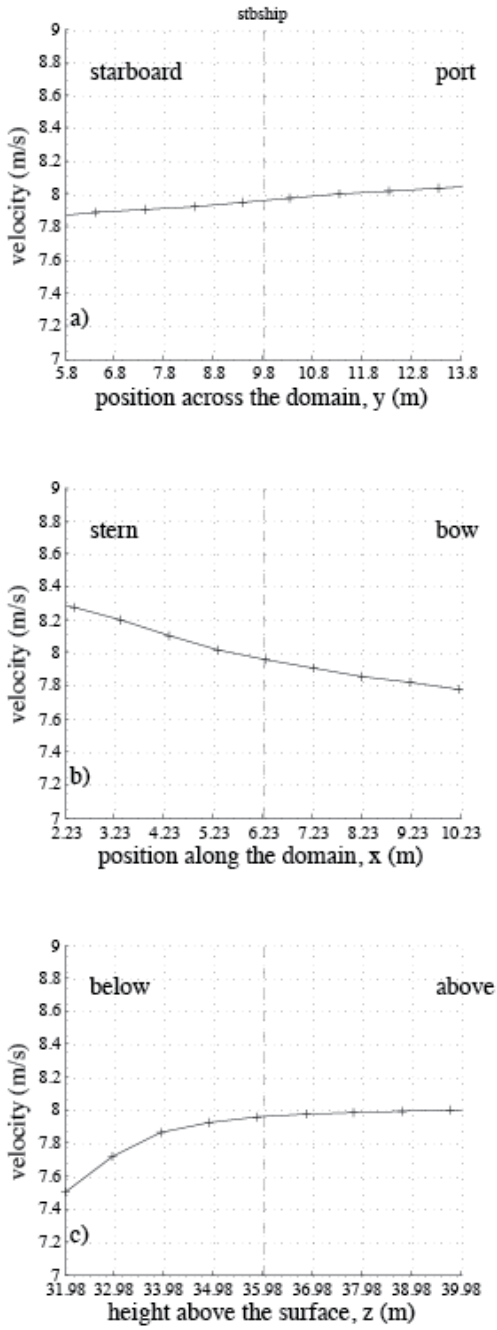

Figure 72. Lines of velocity data through the instrument position (indicated by the dashed line) in all three directions: The results are for a flow to the **starboard ship's anemometer at 60 degrees** over the starboard side and **port ship's anemometer at 60 degrees** over the port side.

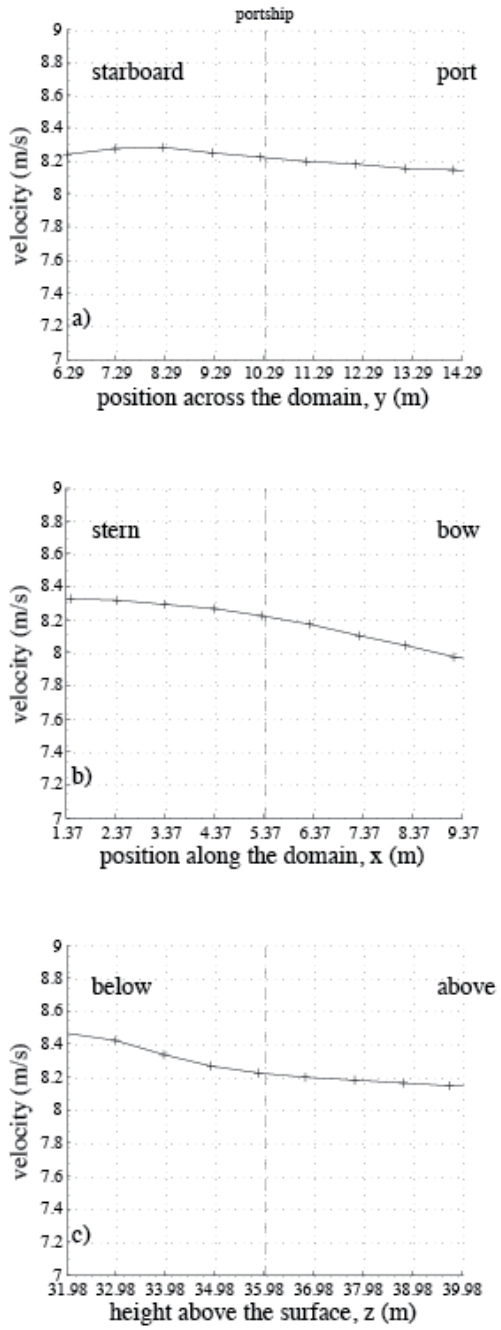

Figure 73. Lines of velocity data through the instrument position (indicated by the dashed line) in all three directions: The results are for a flow to the **port ship's anemometer at 50 degrees** over the starboard side and **starboard ship's anemometer at 50 degrees** over the port side.

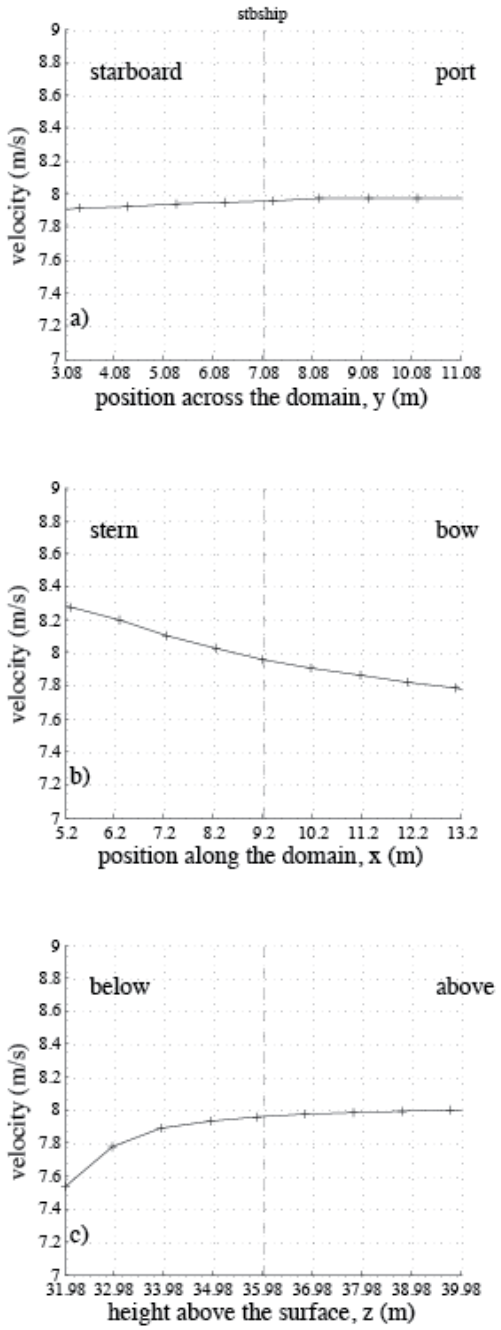

Figure 74. Lines of velocity data through the instrument position (indicated by the dashed line) in all three directions: The results are for a flow to the **starboard ship's anemometer at 50 degrees** over the starboard side and **port ship's anemometer at 50 degrees** over the port side.

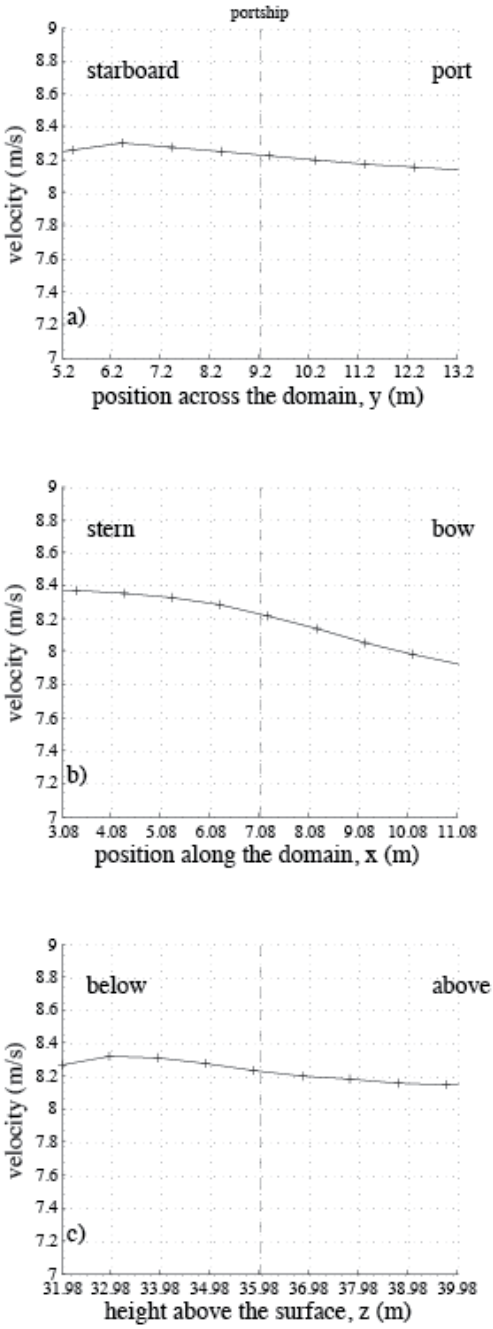

Figure 75. Lines of velocity data through the instrument position (indicated by the dashed line) in all three directions: The results are for a flow to the **port ship's anemometer at 40 degrees** over the starboard side and **starboard ship's anemometer at 40 degrees** over the port side.

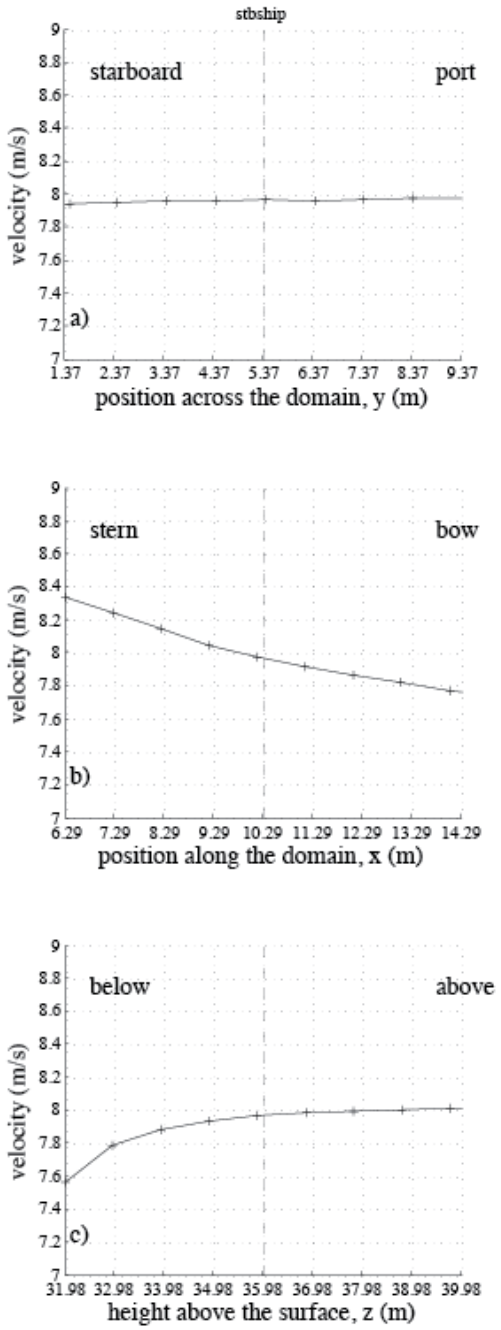

Figure 76. Lines of velocity data through the instrument position (indicated by the dashed line) in all three directions: The results are for a flow to the **starboard ship's anemometer at 40 degrees** over the starboard side and **port ship's anemometer at 40 degrees** over the port side.

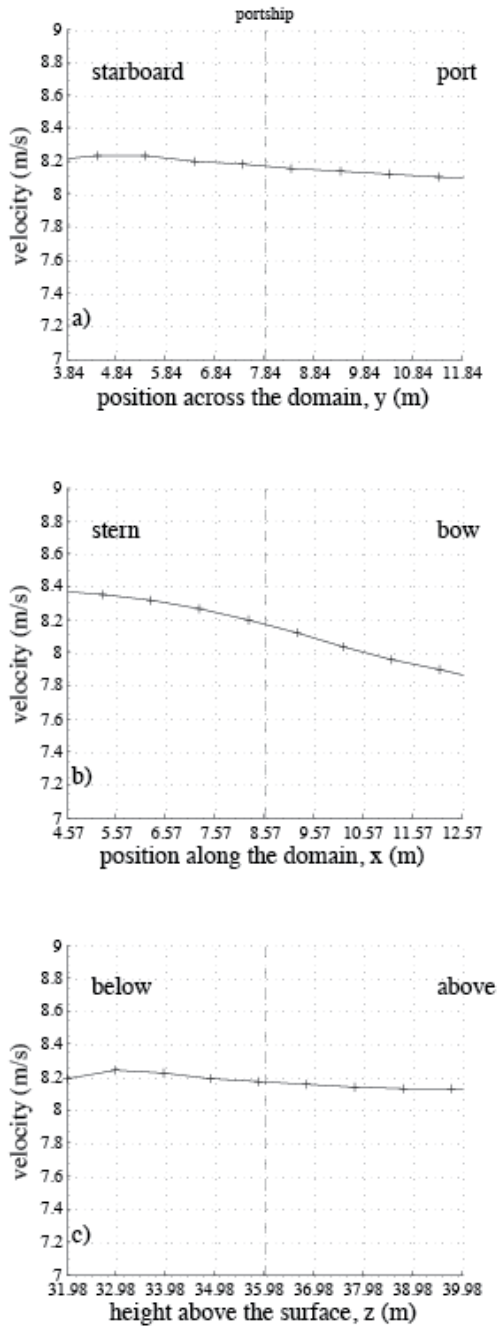

Figure 77. Lines of velocity data through the instrument position (indicated by the dashed line) in all three directions: The results are for a flow to the **port ship's anemometer at 30 degrees** over the starboard side and **starboard ship's anemometer at 30 degrees** over the port side.

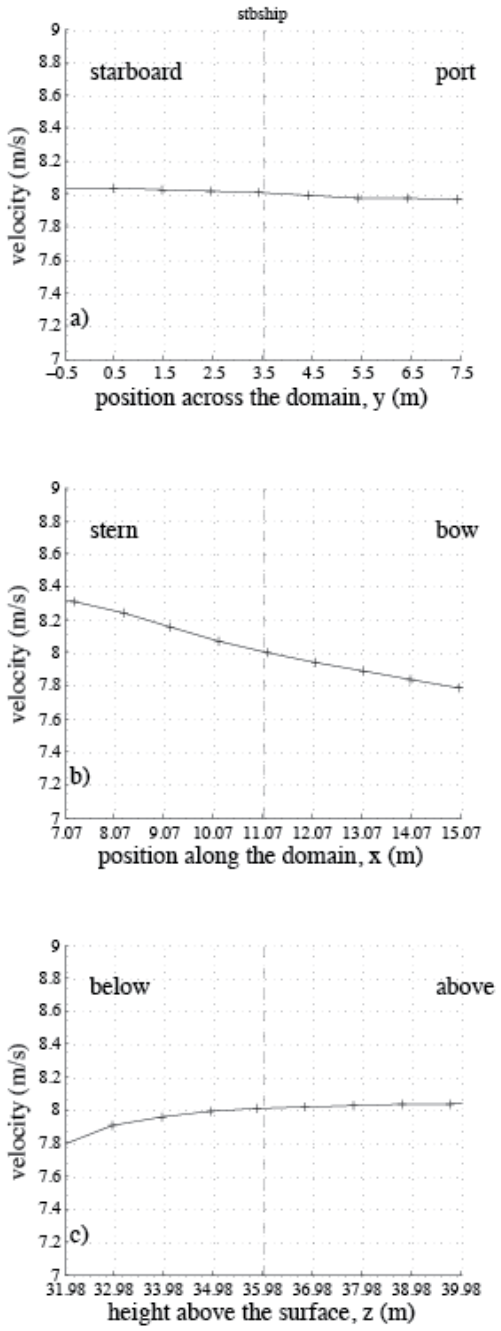

Figure 78. Lines of velocity data through the instrument position (indicated by the dashed line) in all three directions: The results are for a flow to the **starboard ship's anemometer at 30 degrees** over the starboard side and **port ship's anemometer at 30 degrees** over the port side.

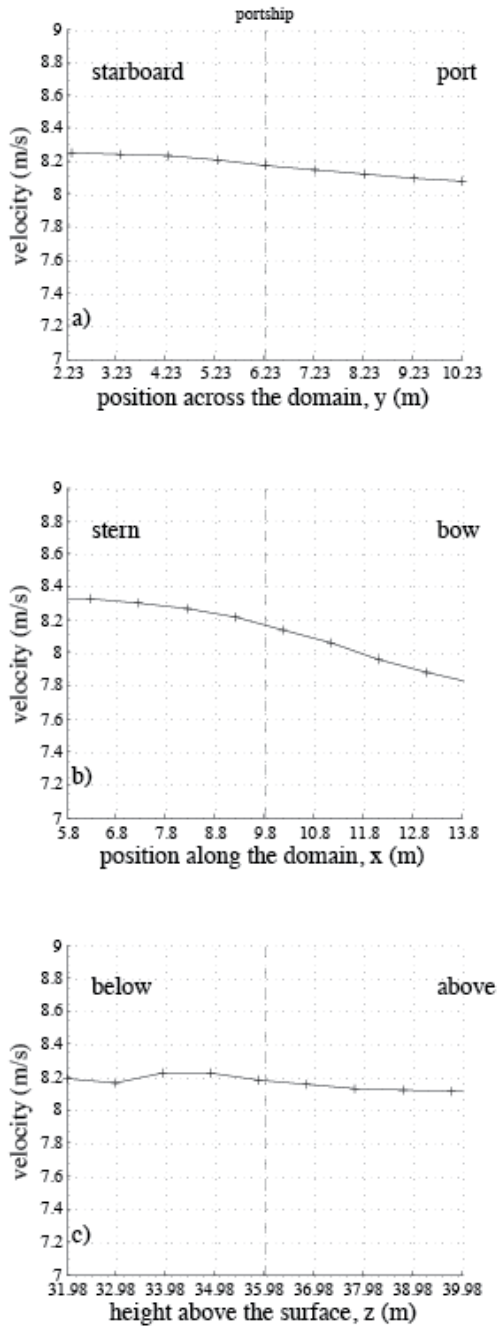

Figure 79. Lines of velocity data through the instrument position (indicated by the dashed line) in all three directions: The results are for a flow to the **port ship's anemometer at 20 degrees** over the starboard side and **starboard ship's anemometer at 20 degrees** over the port side.

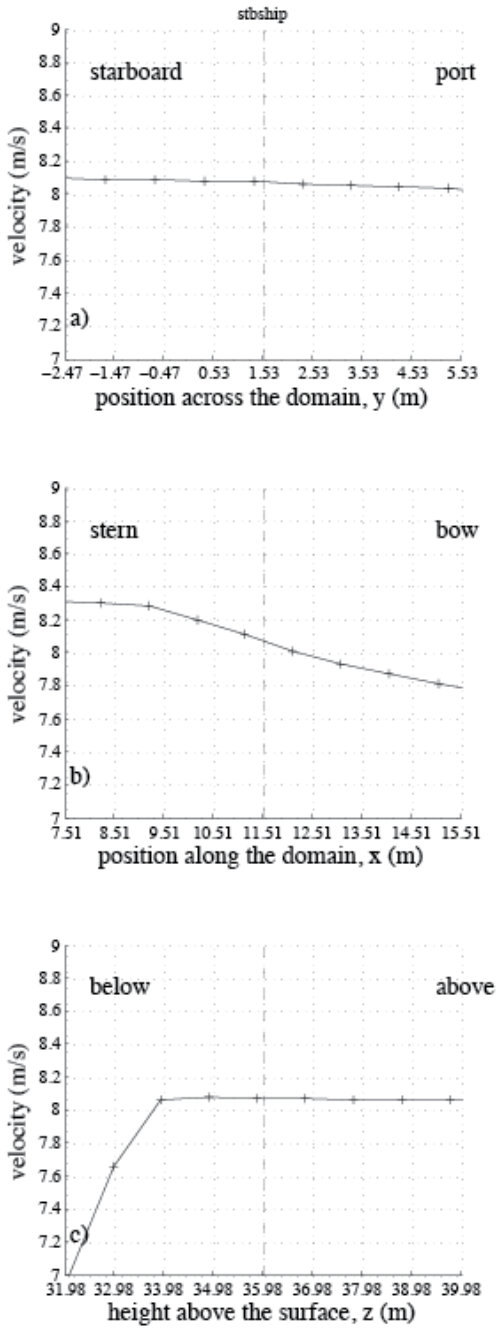

Figure 80. Lines of velocity data through the instrument position (indicated by the dashed line) in all three directions: The results are for a flow to the **starboard ship's anemometer at 20 degrees** over the starboard side and **port ship's anemometer at 20 degrees** over the port side.

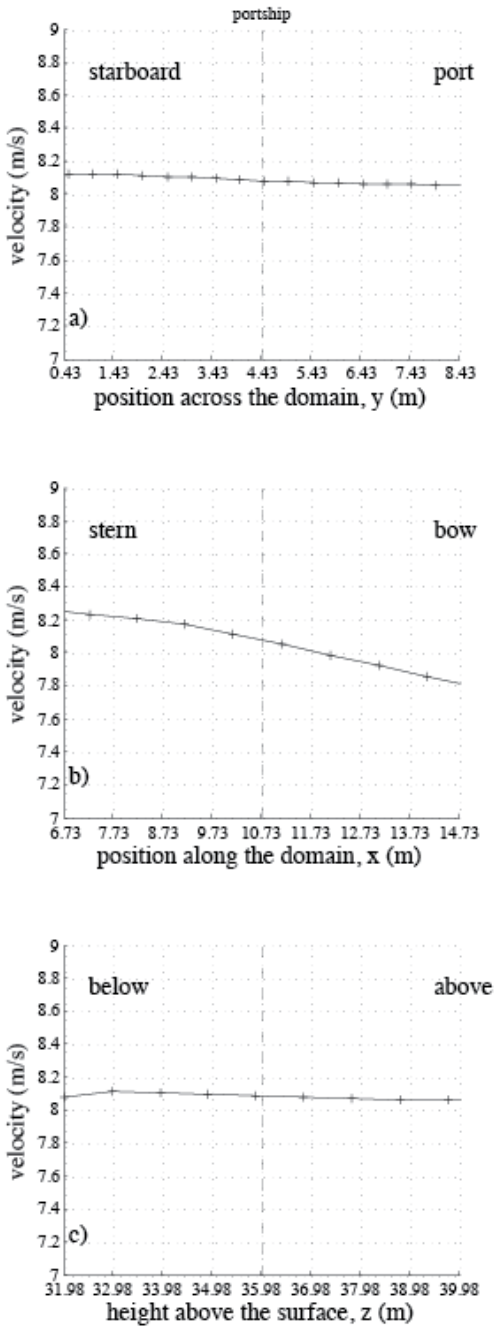

Figure 81. Lines of velocity data through the instrument position (indicated by the dashed line) in all three directions: The results are for a flow to the **port ship's anemometer at 10 degrees** over the starboard side and **starboard ship's anemometer at 10 degrees** over the port side.

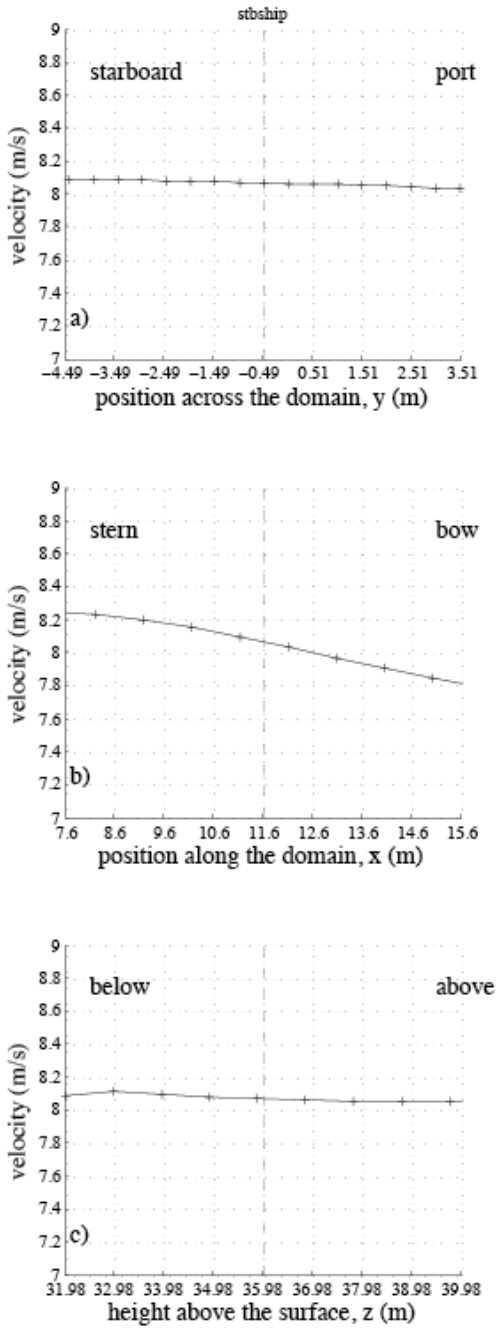

Figure 82. Lines of velocity data through the instrument position (indicated by the dashed line) in all three directions: The results are for a flow to the **starboard ship's anemometer at 10 degrees** over the starboard side and **port ship's anemometer at 10 degrees** over the port side.

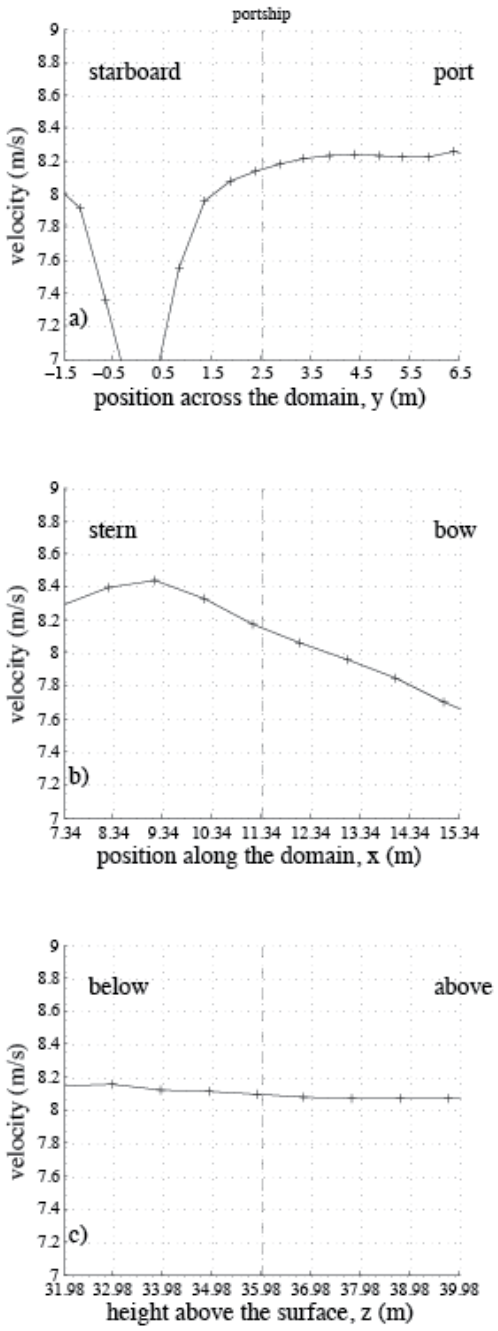

Figure 83. Lines of velocity data through the instrument position (indicated by the dashed line) in all three directions: The results are for a flow to the **port ship's anemometer at for a flow directly over the bow (0 degrees)**.

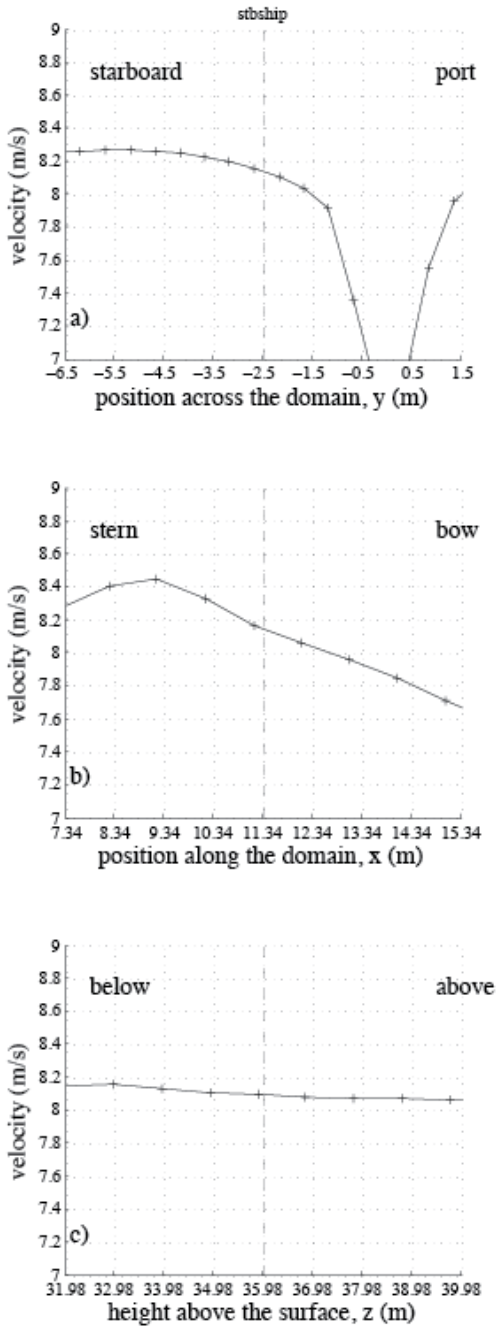

Figure 84. Lines of velocity data through the instrument position (indicated by the dashed line) in all three directions: The results are for a flow to the **starboard ship's anemometer at for a flow directly over the bow (0 degrees)**.

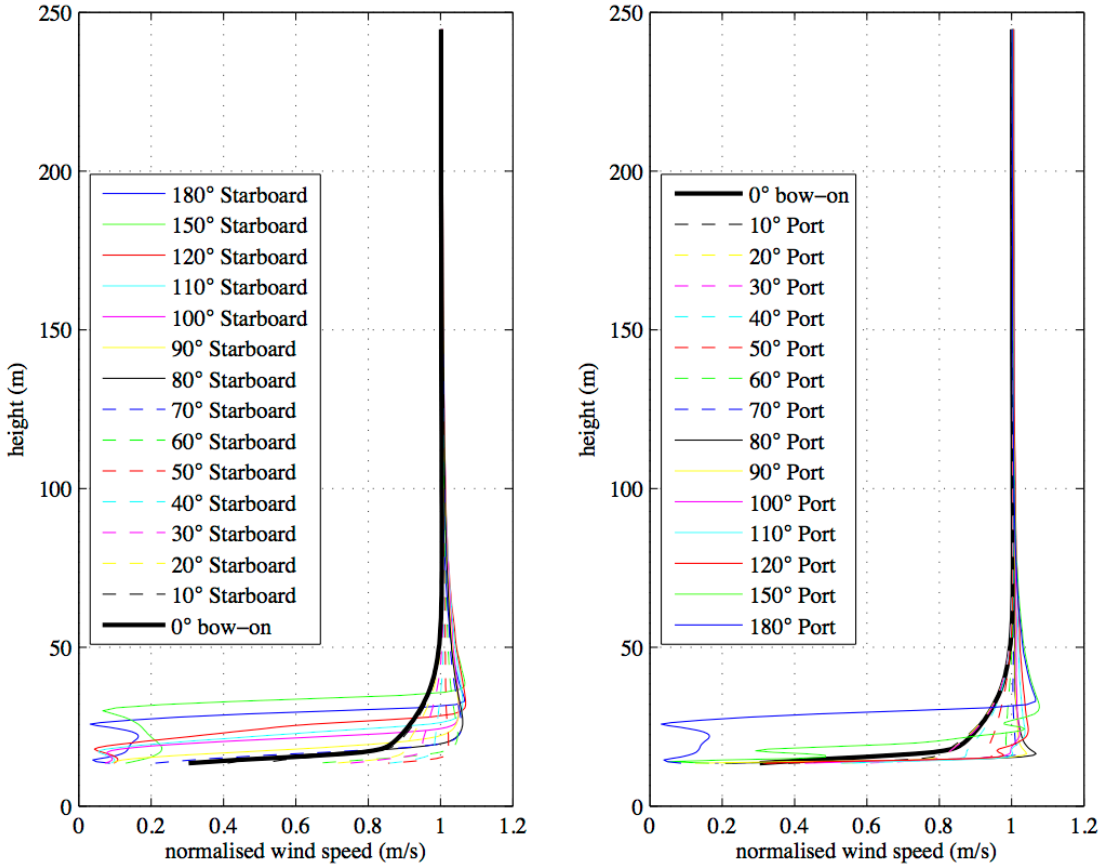

Figure 85 Lidar wind speed profiles normalised by the free stream profile directly abeam of the Lidar site for flows over the starboard beam (left panel) and port beam (right panel).

9. APPENDIX A: Figures showing sections of data on 2-D planes.

The Figures in this Appendix were generated using the VECTIS post-processing software.

FIGURE A1. Velocity vectors on a vertical plane through the **METEK** and **CSAT** anemometer sites for a flow directly over the bow. The magnitude of the velocity is indicated by the colour of the arrows. The length and direction of the arrows represent the magnitude and component of the velocity in the plane of view. Each arrow represents the results from one computational cell. The position of the anemometer is indicated by a cross and the velocity scale corresponds to 6 ms^{-1} to 8 ms^{-1}.

FIGURE A2. Velocity vectors on a vertical plane through the **METEK** anemometer sites for a flow 10 degrees to starboard. The magnitude of the velocity is indicated by the colour of the arrows. The length and direction of the arrows represent the magnitude and component of the velocity in the plane of view. Each arrow represents the results from one computational cell. The position of the anemometer is indicated by a cross and the velocity scale corresponds to 6 ms^{-1} to 8 ms^{-1}.

FIGURE A3. Velocity vectors on a vertical plane through the **CSAT** anemometer sites for a flow 10 degrees to starboard. The magnitude of the velocity is indicated by the colour of the arrows. The length and direction of the arrows represent the magnitude and component of the velocity in the plane of view. Each arrow represents the results from one computational cell. The position of the anemometer is indicated by a cross and the velocity scale corresponds to 6 ms^{-1} to 8 ms^{-1}.

FIGURE A4. As Figure A1 for a flow 20 degrees to starboard.

FIGURE A5. As Figure A1 for a flow 30 degrees to starboard.

FIGURE A6. As Figure A2 for a flow 40 degrees to starboard.

FIGURE A7. As Figure A3 for a flow 40 degrees to starboard.

FIGURE A8. As Figure A1 for a flow 50 degrees to starboard.

FIGURE A9. As Figure A2 for a flow 60 degrees to starboard.

FIGURE A10. As Figure A3 for a flow 60 degrees to starboard.

FIGURE A11. As Figure A2 for a flow 70 degrees to starboard.

FIGURE A12. As Figure A3 for a flow 70 degrees to starboard.

FIGURE A13. As Figure A2 for a flow 80 degrees to starboard.

FIGURE A14. As Figure A3 for a flow 80 degrees to starboard.

FIGURE A15. As Figure A2 for a flow 90 degrees to starboard (beam on).

FIGURE A16. As Figure A3 for a flow 90 degrees to starboard (beam on).

FIGURE A17. As Figure A2 for a flow 100 degrees to starboard

FIGURE A18. As Figure A3 for a flow 100 degrees to starboard.

FIGURE A19. As Figure A2 for a flow 110 degrees to starboard.

FIGURE A20. As Figure A3 for a flow 110 degrees to starboard.

FIGURE A21. As Figure A2 for a flow 120 degrees to starboard.

FIGURE A22. As Figure A3 for a flow 120 degrees to starboard.

FIGURE A23. As Figure A1 for a flow 150 degrees to starboard.

FIGURE A24. Velocity vectors on a horizontal plane through the **METEK** anemometer site for a flow directly over the bow. The magnitude of the velocity is indicated by the colour of the arrows. The length and direction of the arrows represent the magnitude and component of the velocity in the plane of view. Each arrow represents the results from one computational cell. The position of the anemometer is indicated by a cross and the velocity scale corresponds to 6 ms^{-1} to 8 ms^{-1}.

FIGURE A25. Velocity vectors on a horizontal plane through the **CSAT** anemometer site for a flow directly over the bow. The magnitude of the velocity is indicated by the colour of the arrows. The length and direction of the arrows represent the magnitude and component of the velocity in the plane of view. Each arrow represents the results from one computational cell. The position of the anemometer is indicated by a cross and the velocity scale corresponds to 6 ms^{-1} to 8 ms^{-1}.

FIGURE A26. As Figure A24 for a flow 10 degrees to starboard.

FIGURE A27. As Figure A25 for a flow 10 degrees to starboard.

FIGURE A28. As Figure A24 for a flow 20 degrees to starboard.

FIGURE A29. As Figure A25 for a flow 20 degrees to starboard.

FIGURE A30. As Figure A24 for a flow 30 degrees to starboard.

FIGURE A31. As Figure A25 for a flow 30 degrees to starboard.

FIGURE A32. As Figure A24 for a flow 40 degrees to starboard.

FIGURE A33. As Figure A25 for a flow 40 degrees to starboard.

FIGURE A34. As Figure A24 for a flow 50 degrees to starboard.

FIGURE A35. As Figure A25 for a flow 50 degrees to starboard.

FIGURE A36. As Figure A24 for a flow 60 degrees to starboard.

FIGURE A37. As Figure A25 for a flow 60 degrees to starboard.

FIGURE A38. As Figure A24 for a flow 70 degrees to starboard.

FIGURE A39. As Figure A25 for a flow 70 degrees to starboard.

FIGURE A40. As Figure A24 for a flow 80 degrees to starboard.

FIGURE A41. As Figure A25 for a flow 80 degrees to starboard.

FIGURE A42. As Figure A24 for a flow 90 degrees to starboard.

FIGURE A43. As Figure A25 for a flow 90 degrees to starboard.

FIGURE A44. As Figure A24 for a flow 100 degrees to starboard.

FIGURE A45. As Figure A25 for a flow 100 degrees to starboard.

FIGURE A46. As Figure A24 for a flow 110 degrees to starboard.

FIGURE A47. As Figure A25 for a flow 110 degrees to starboard.

FIGURE A48. As Figure A24 for a flow 120 degrees to starboard.

FIGURE A49. As Figure A25 for a flow 120 degrees to starboard.

FIGURE A50. As Figure A24 for a flow 150 degrees to starboard.

FIGURE A51. As Figure A25 for a flow 150 degrees to starboard.

Velocity vectors on a horizontal plane through the R3 sonic anemometer site for a flow directly over the bow. The magnitude of the velocity is indicated by the colour of the arrows. The length and direction of the arrows represent the magnitude and component of the velocity in the plane of view. Each arrow represents the results from one computational cell. The position of the anemometer is indicated by a cross and the velocity scale corresponds to 8 ms^{-1} to 12 ms^{-1}.

Figure A1 – METEK and CSAT for a 0 degree bow-on flow

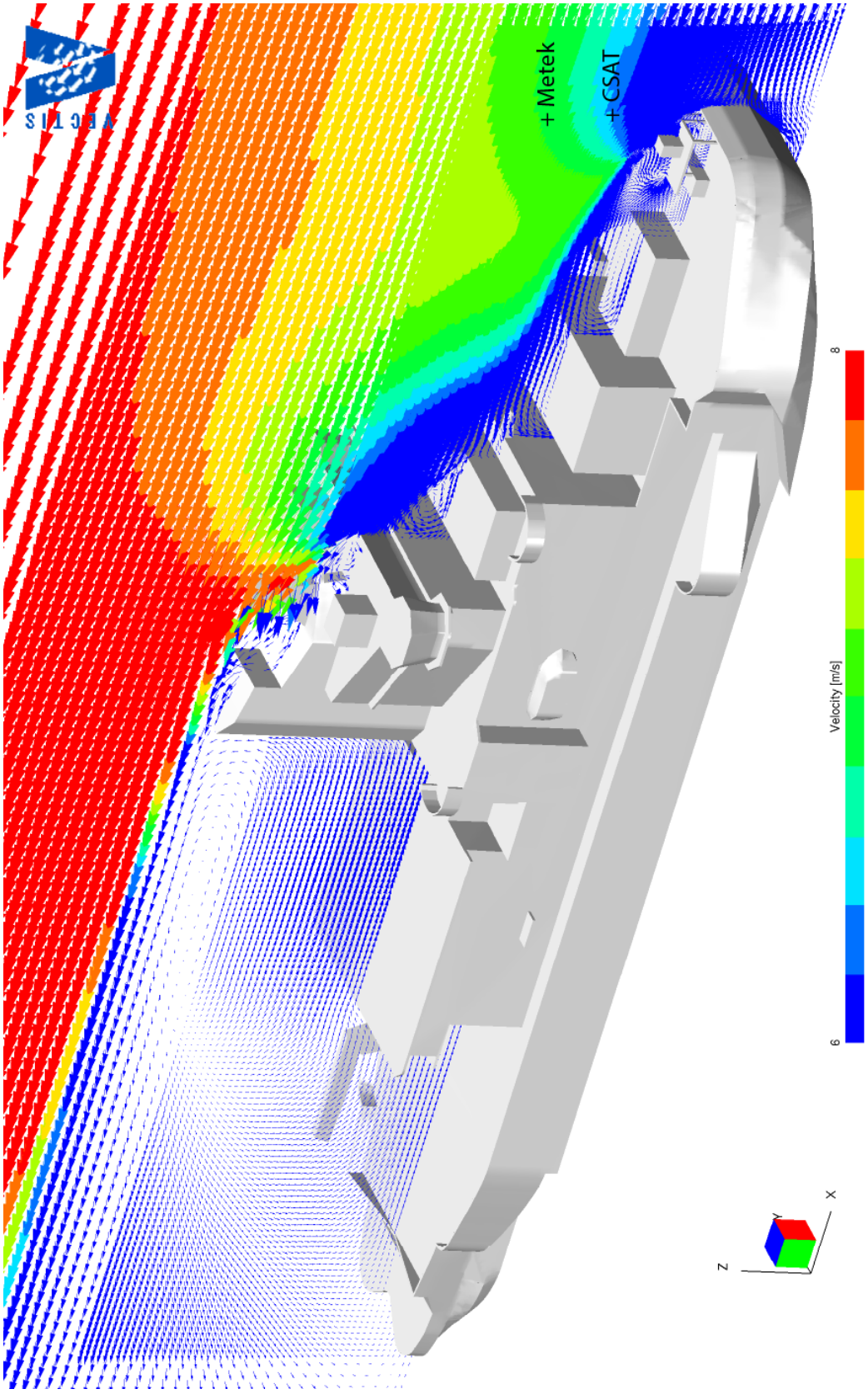

Figure A2 – METEK 10 degree starboard flow

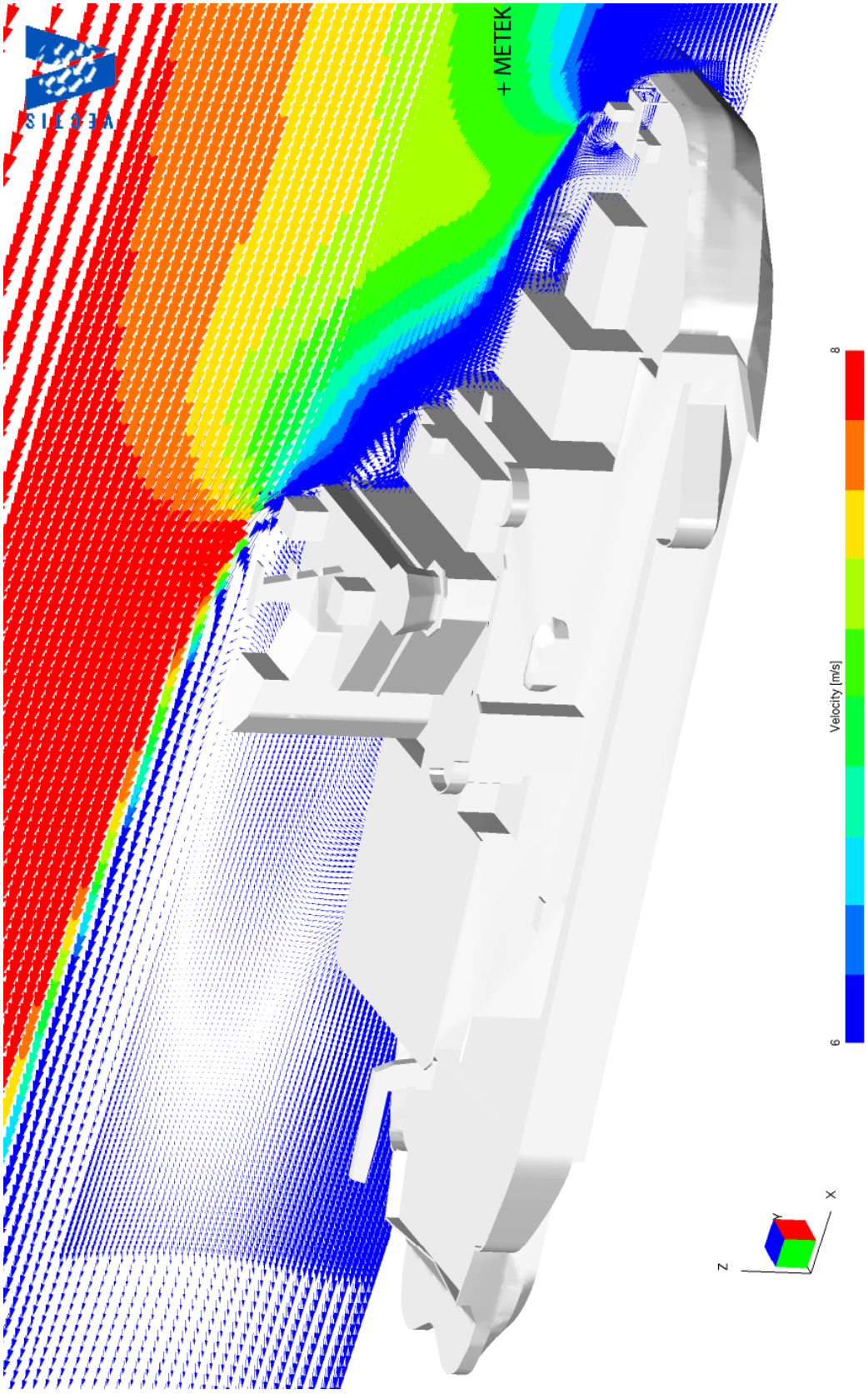

Figure A3 – CSAT 10 degree starboard flow

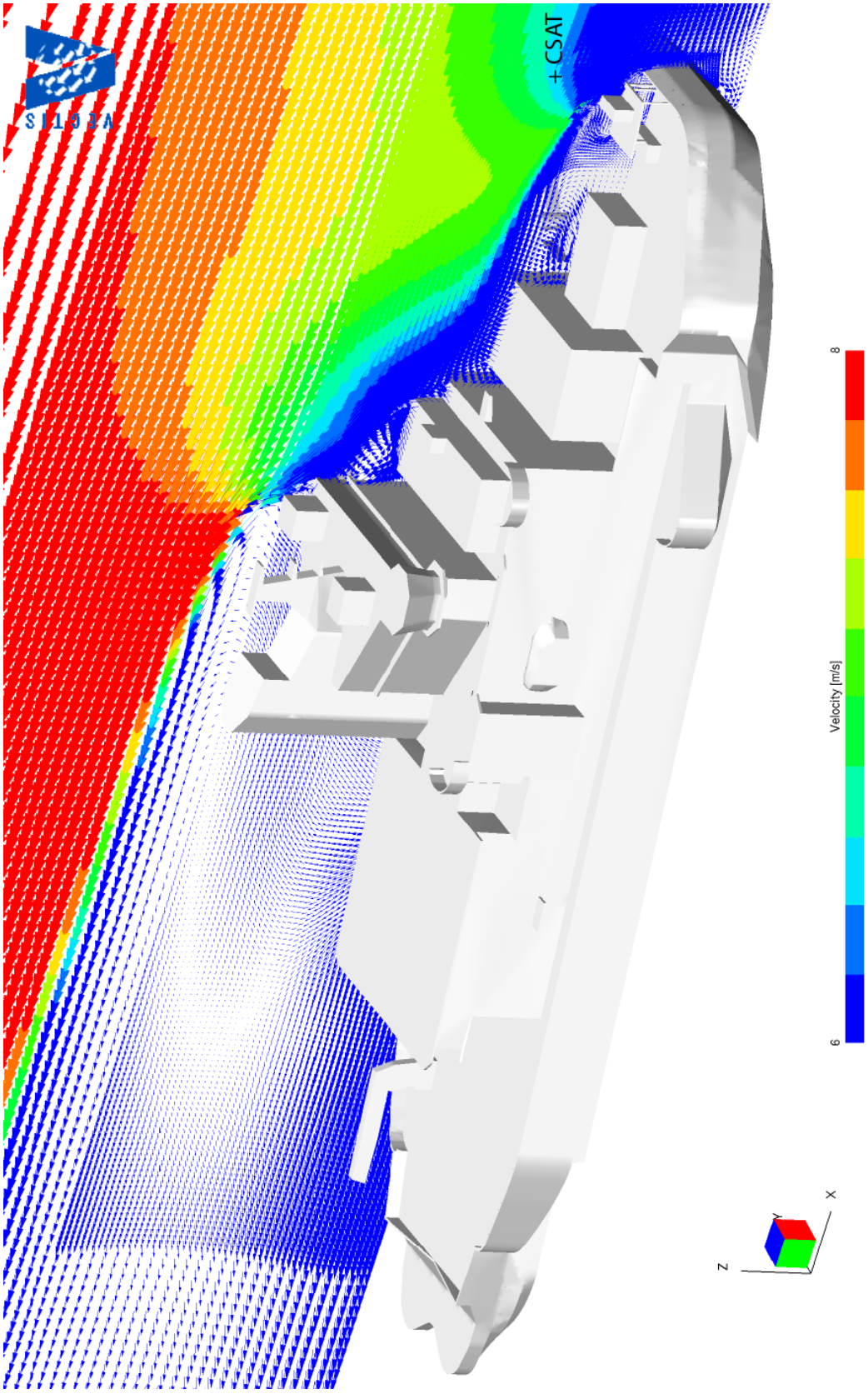

Figure A4 – METEK and CSAT at 20 degree starboard flow

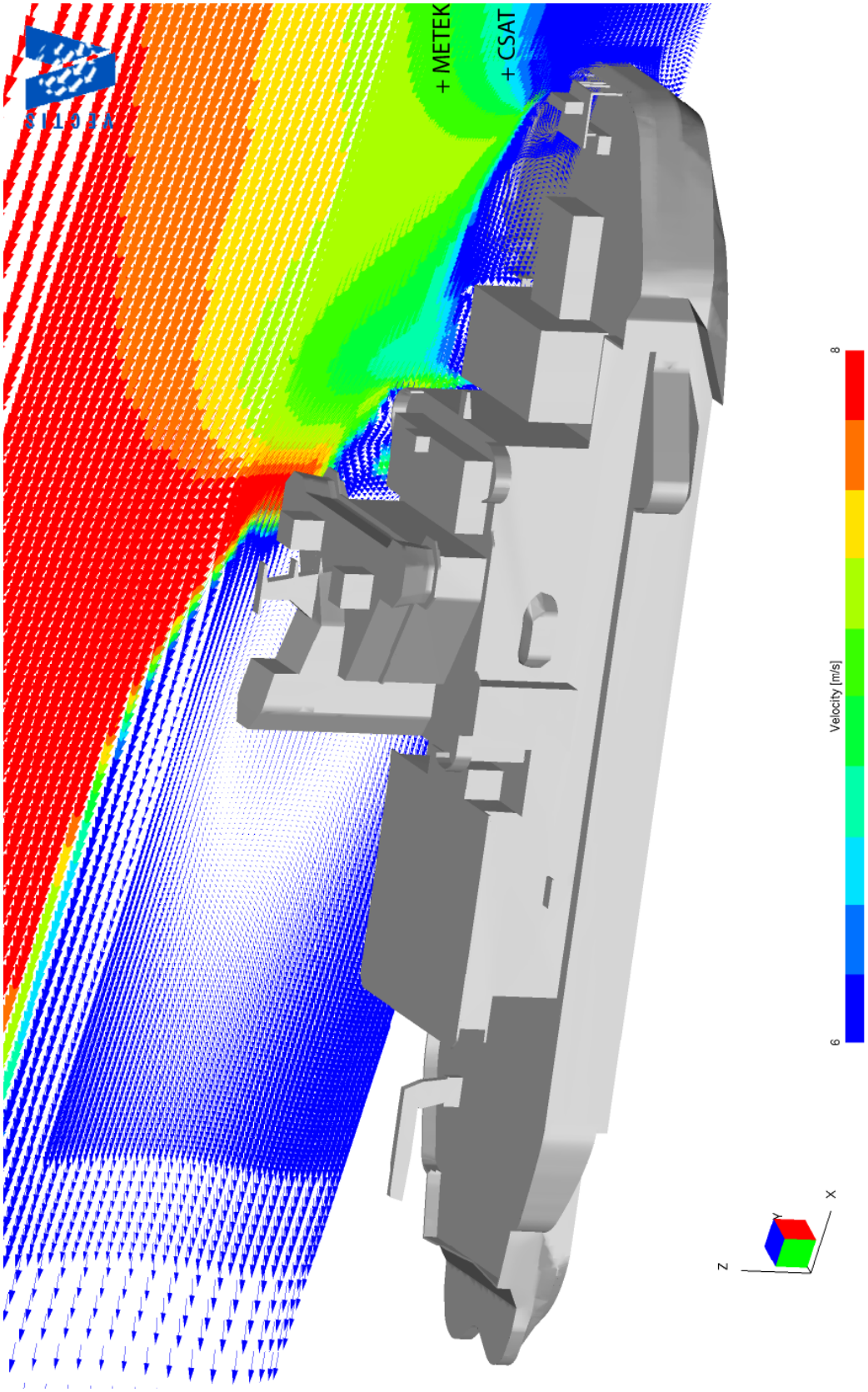

Figure A5 - METEK and CSAT at 30 degree starboard flow

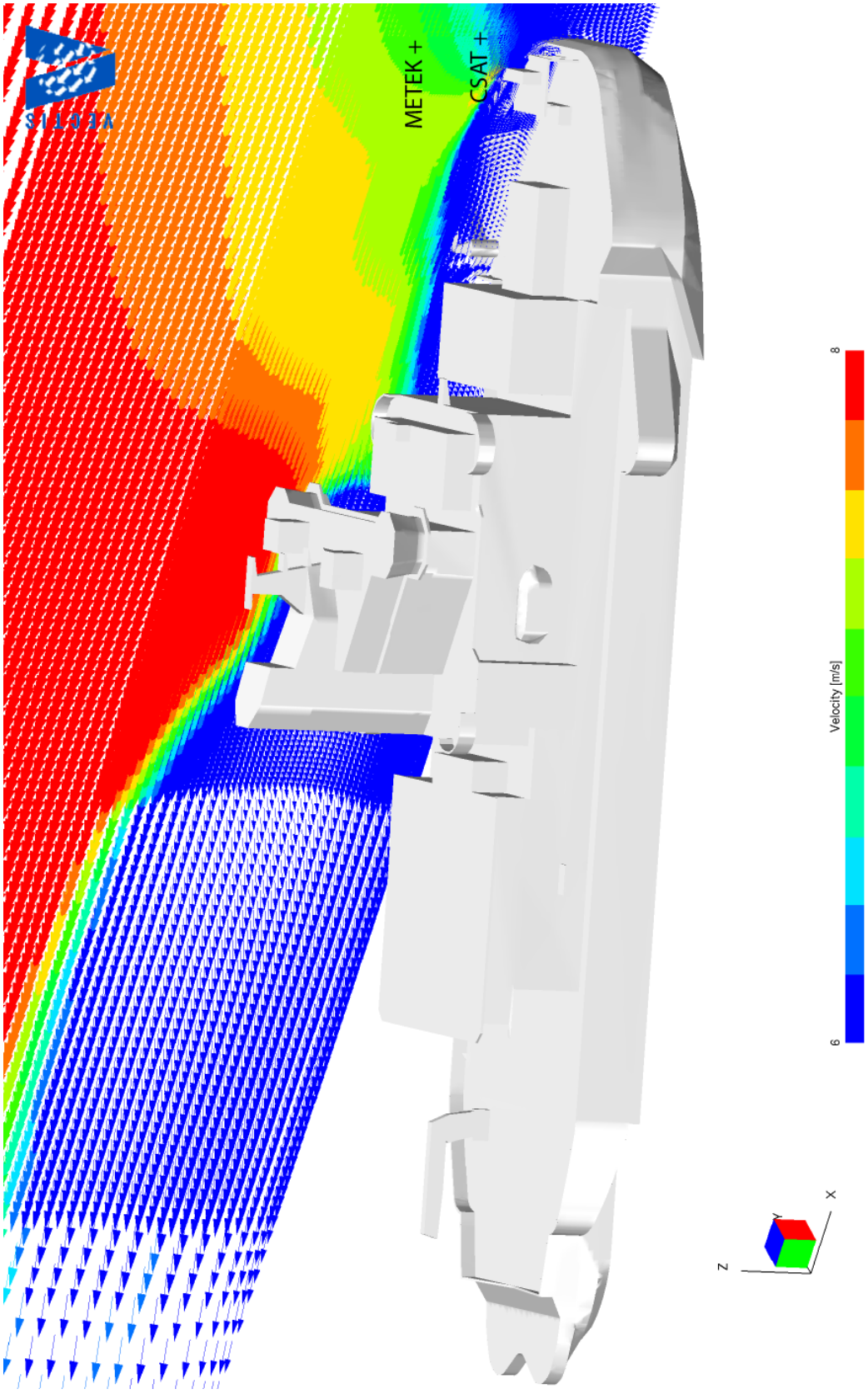

Figure A6 - METEK 40 degree starboard flow

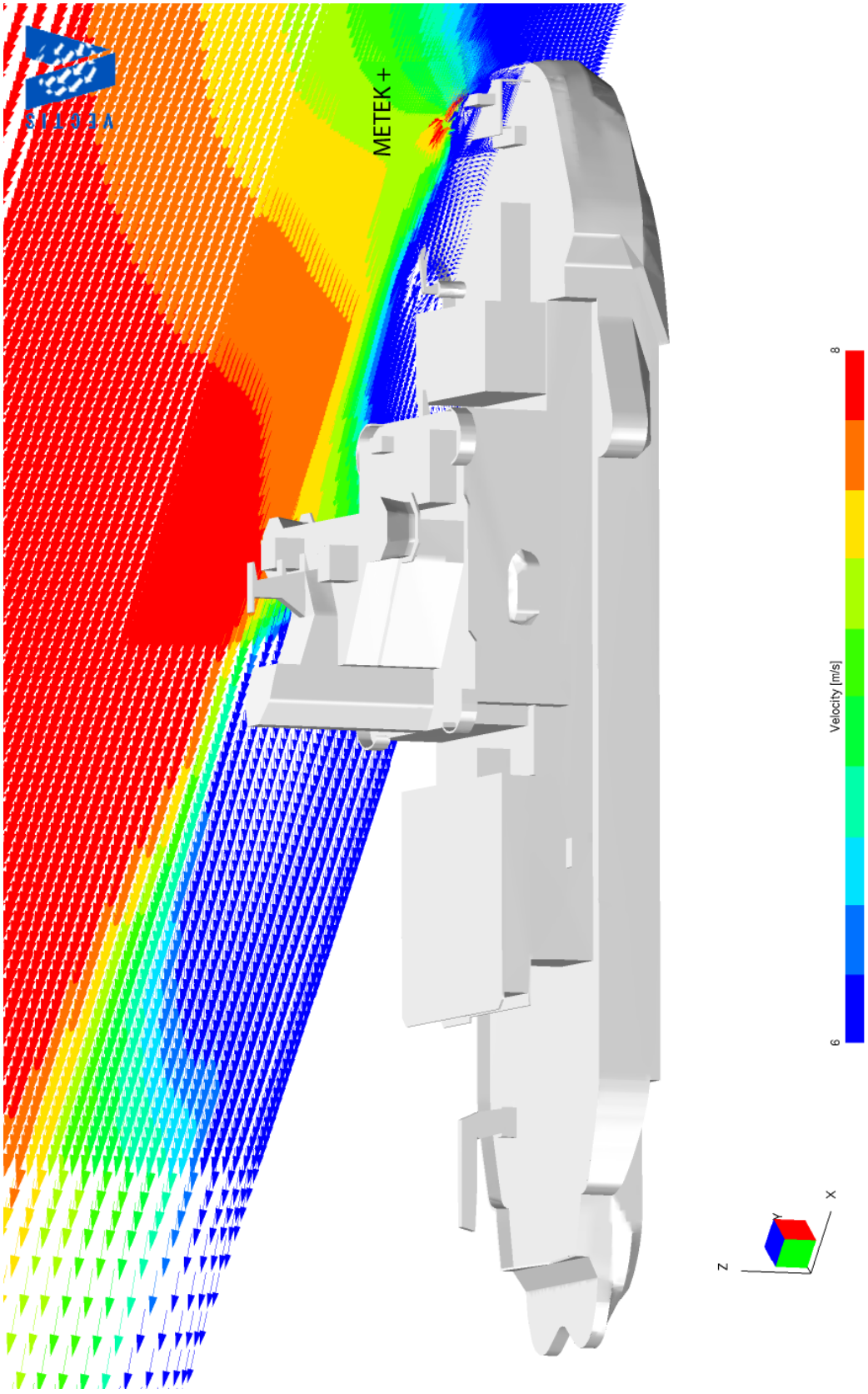

Figure A7 – CSAT 40 degree starboard flow

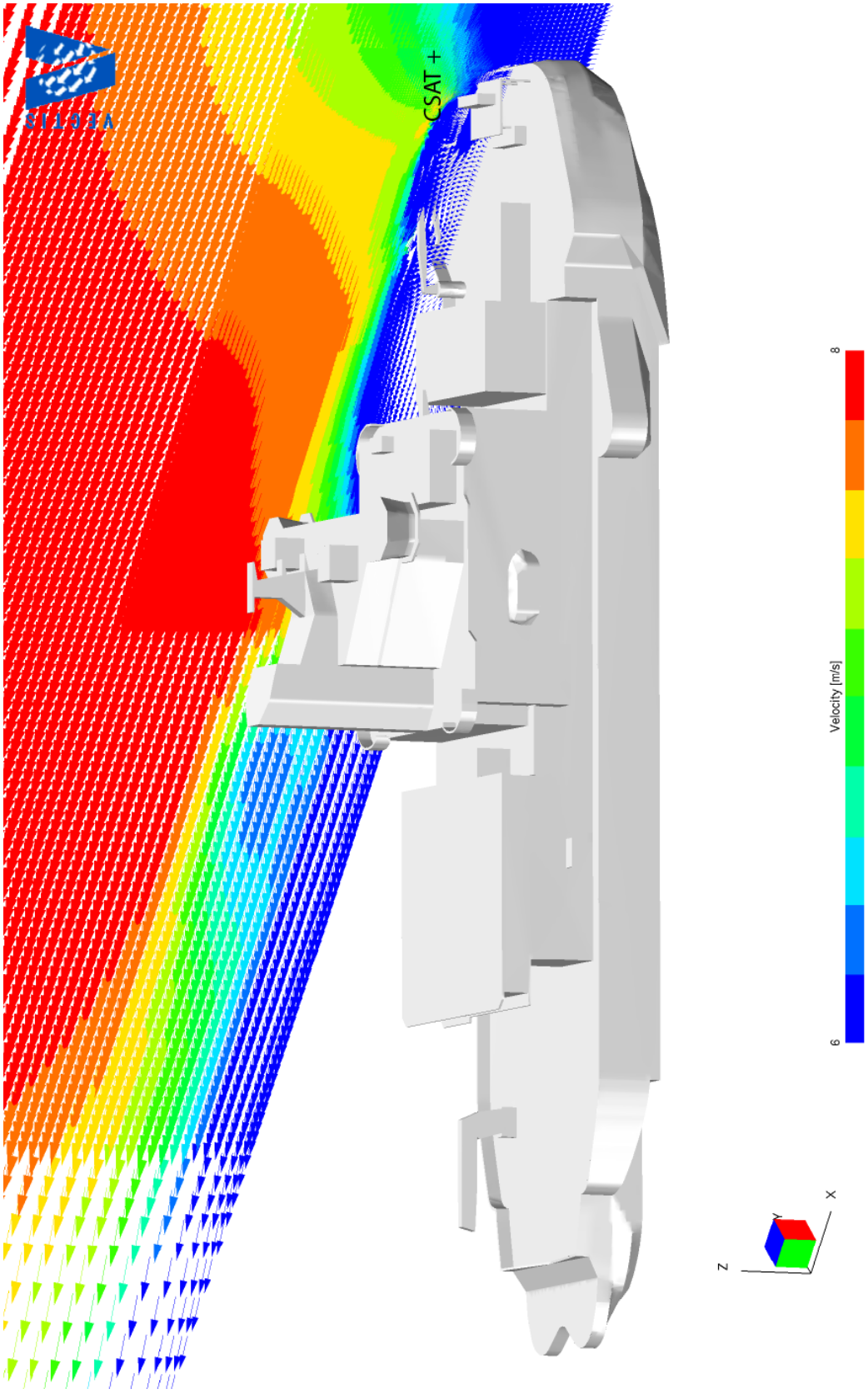

Figure A8 – METEK and CSAT at 50 degree starboard flow

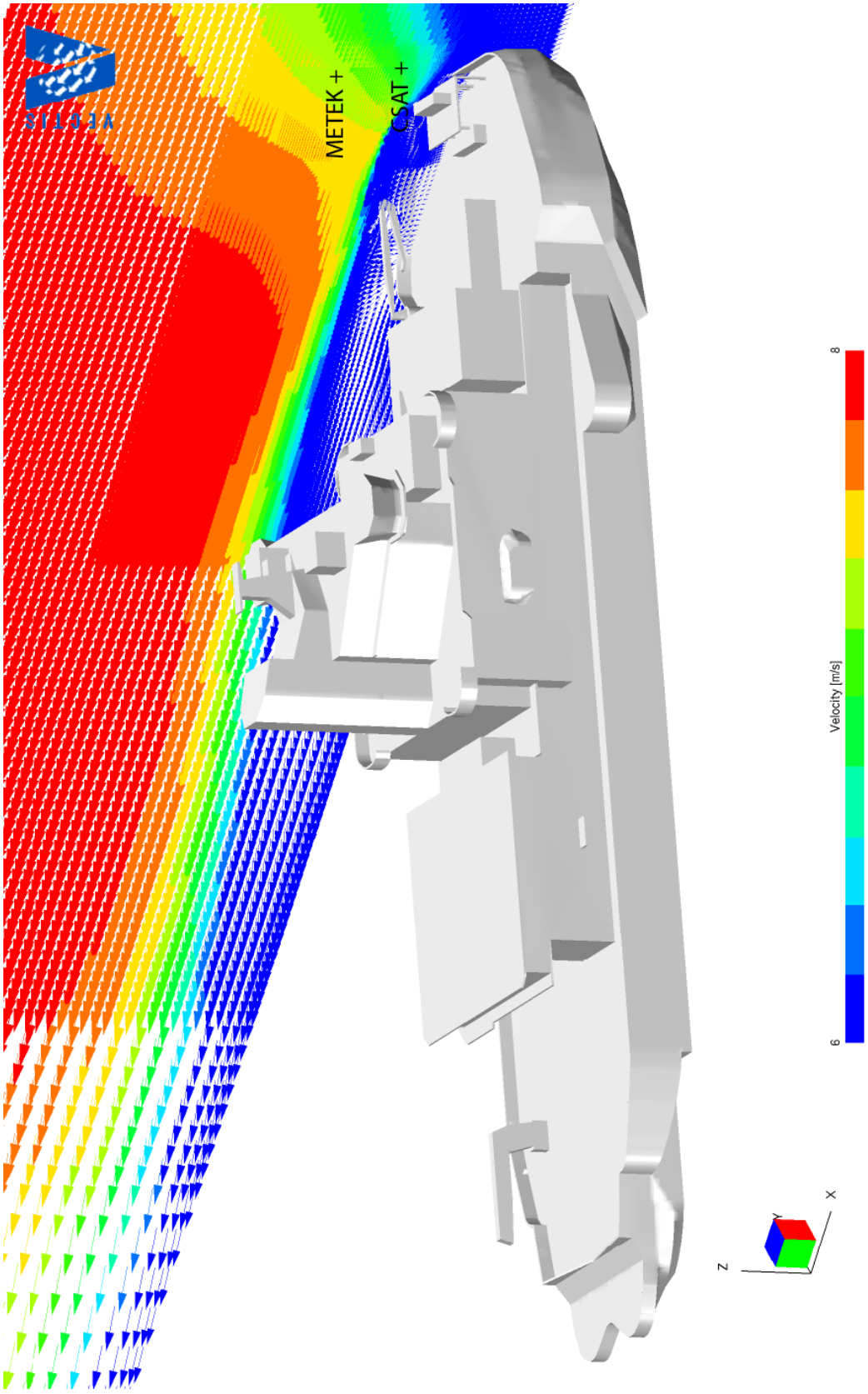

Figure A9 – METEK at 60 degree starboard flow

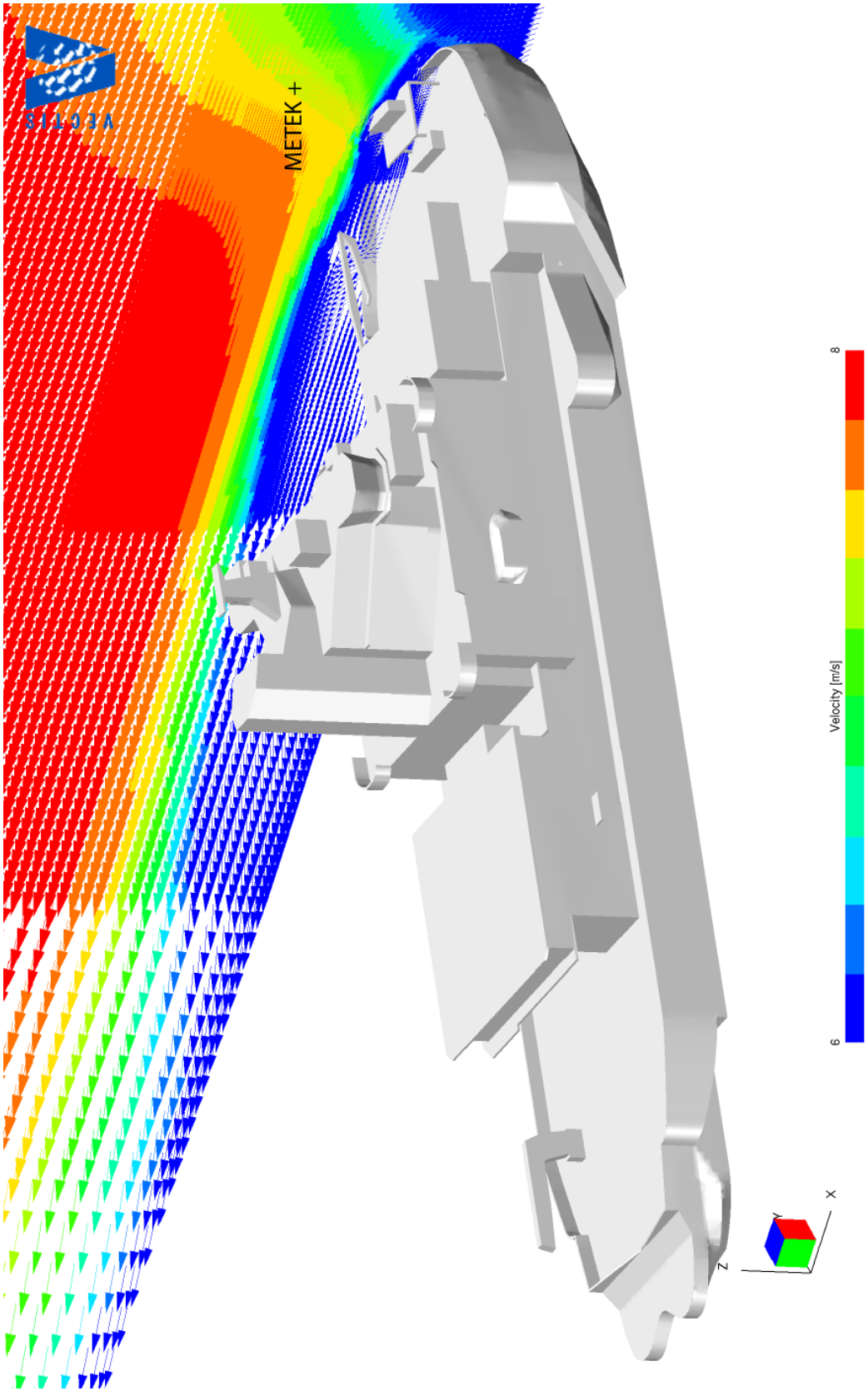

Figure A10 - CSAT at 60 degree starboard flow

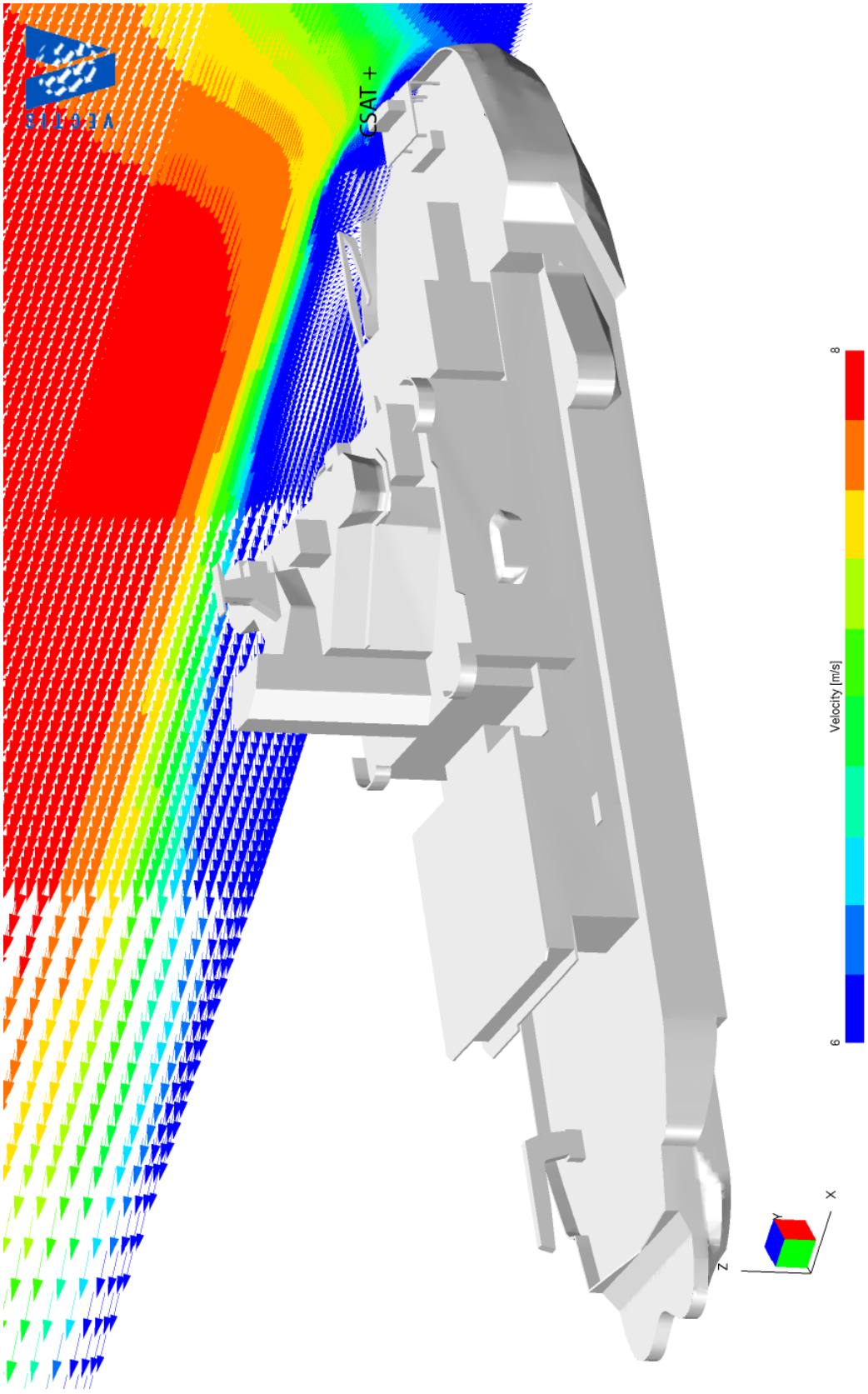

Figure A11 - METEK at 70 degree starboard flow

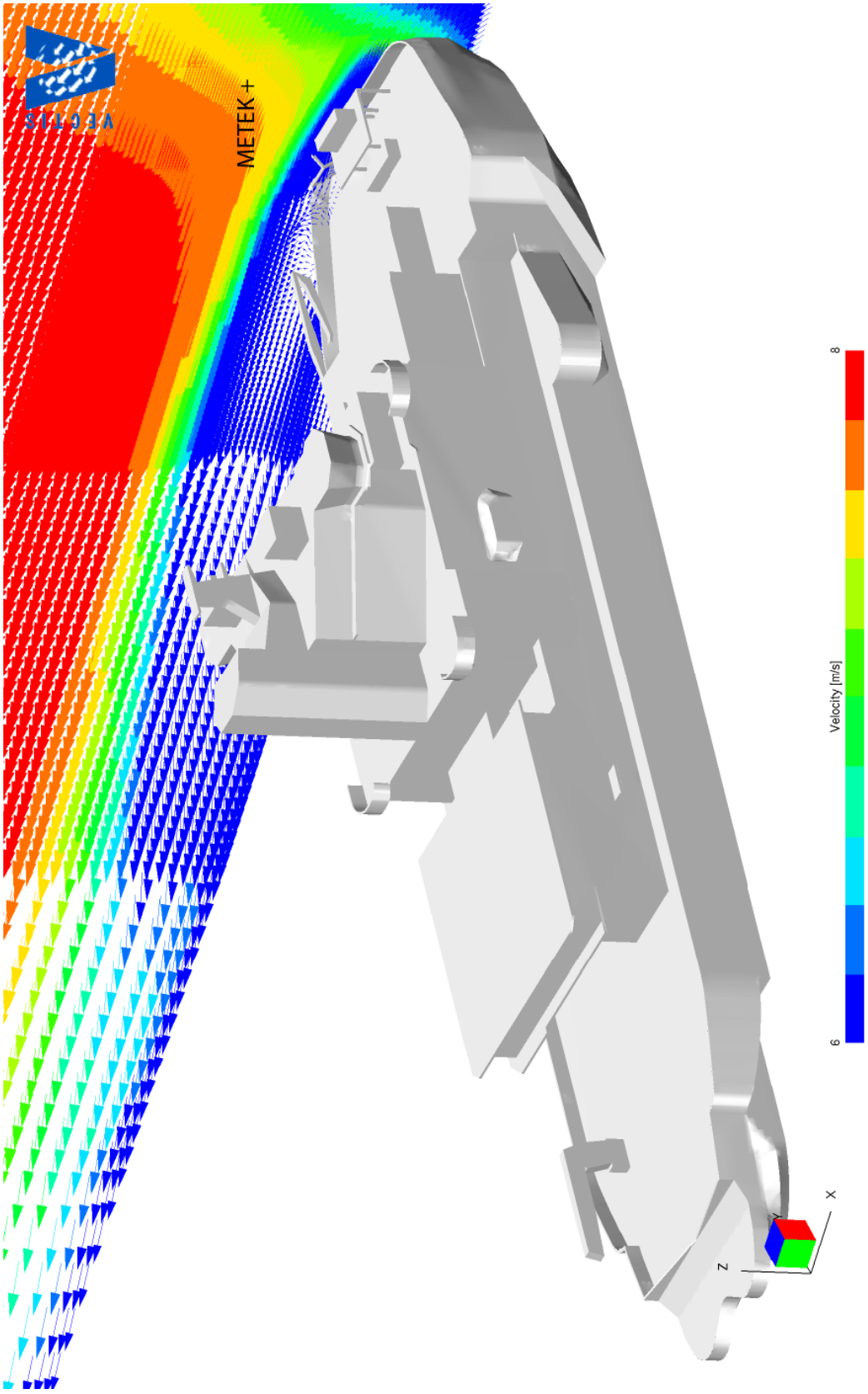

Figure A12 - CSAT at 70 degree starboard flow

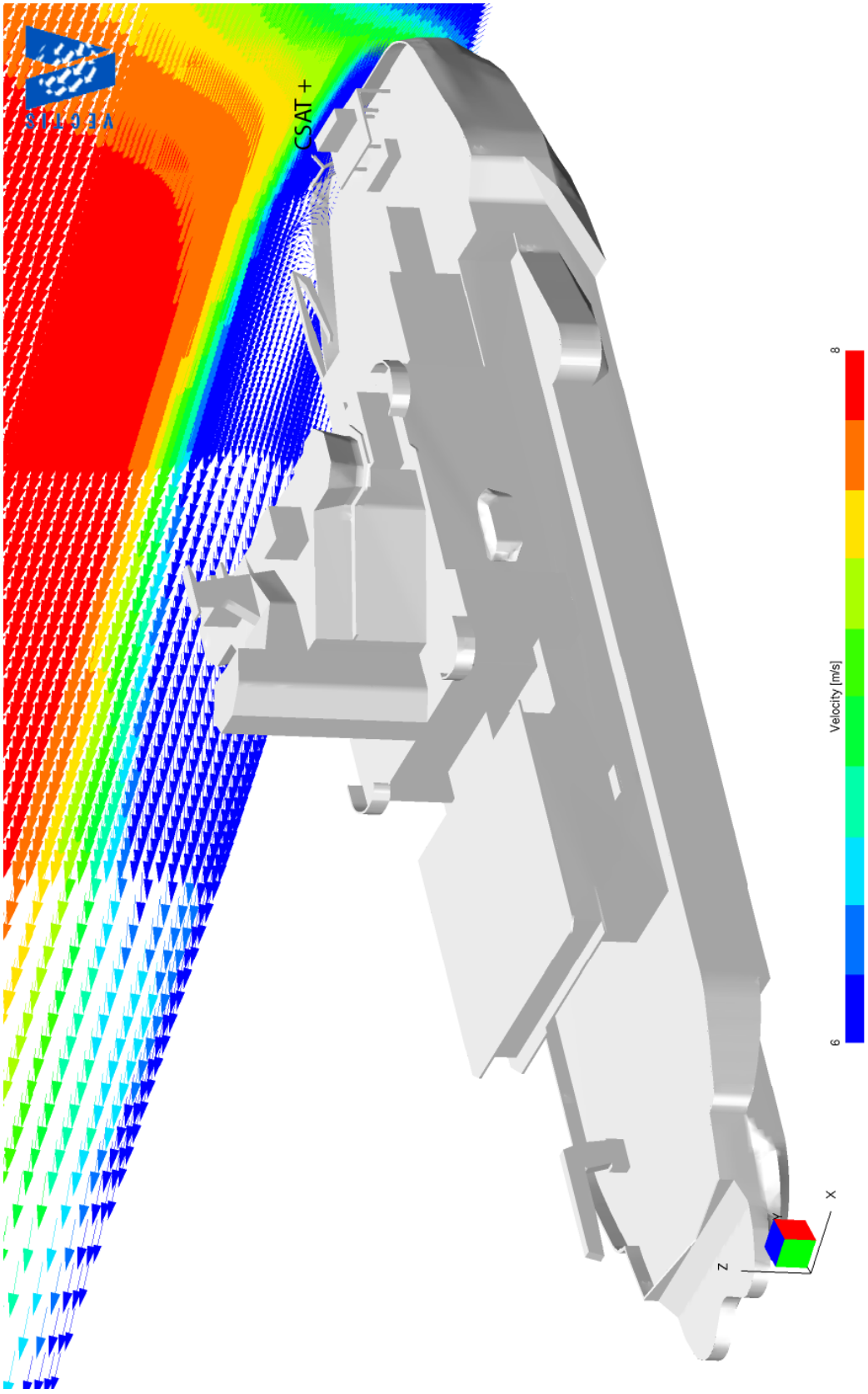

Figure A13 - METEK at 80 degree starboard flow

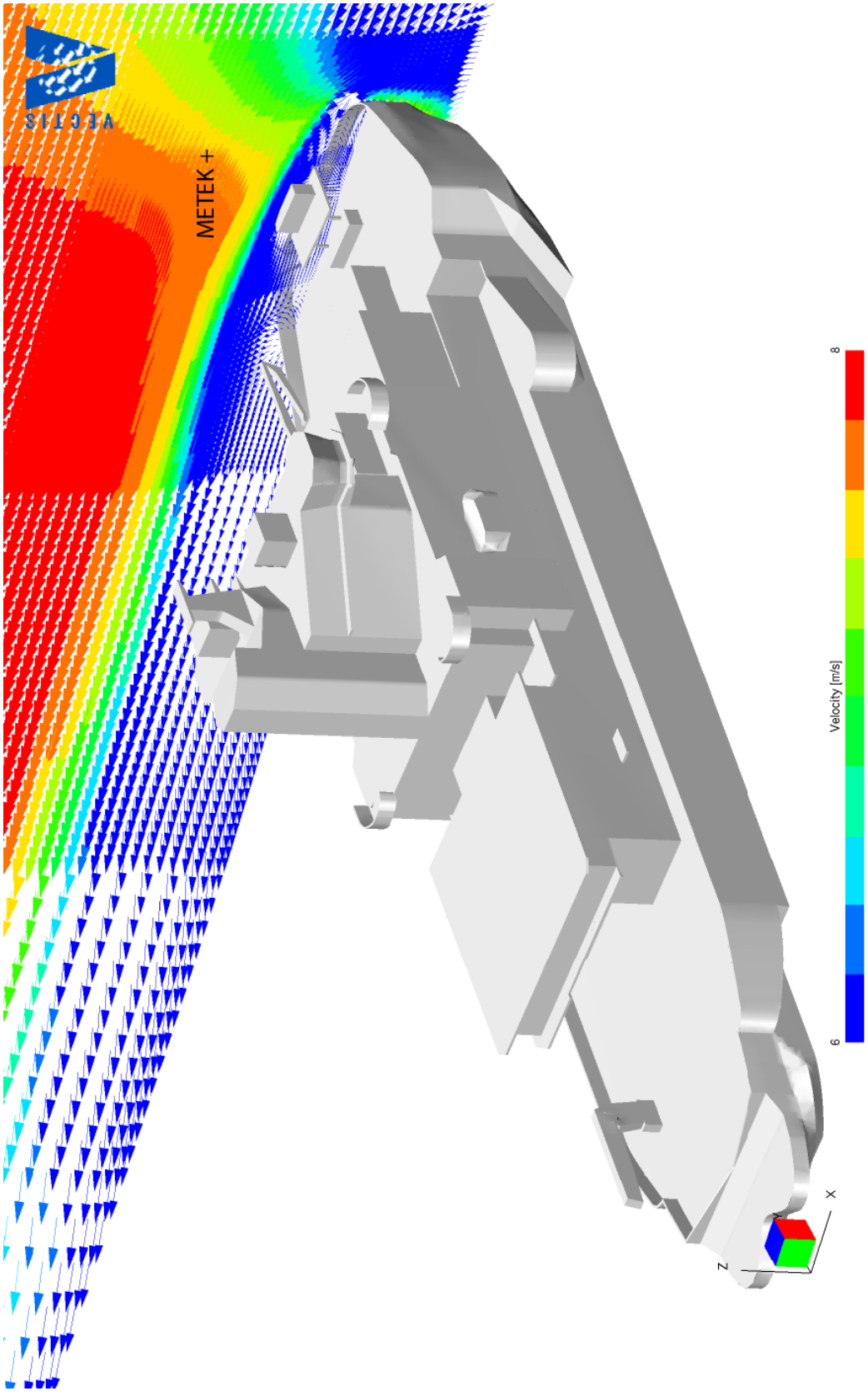

Figure A14 - CSAT at 80 degree starboard flow

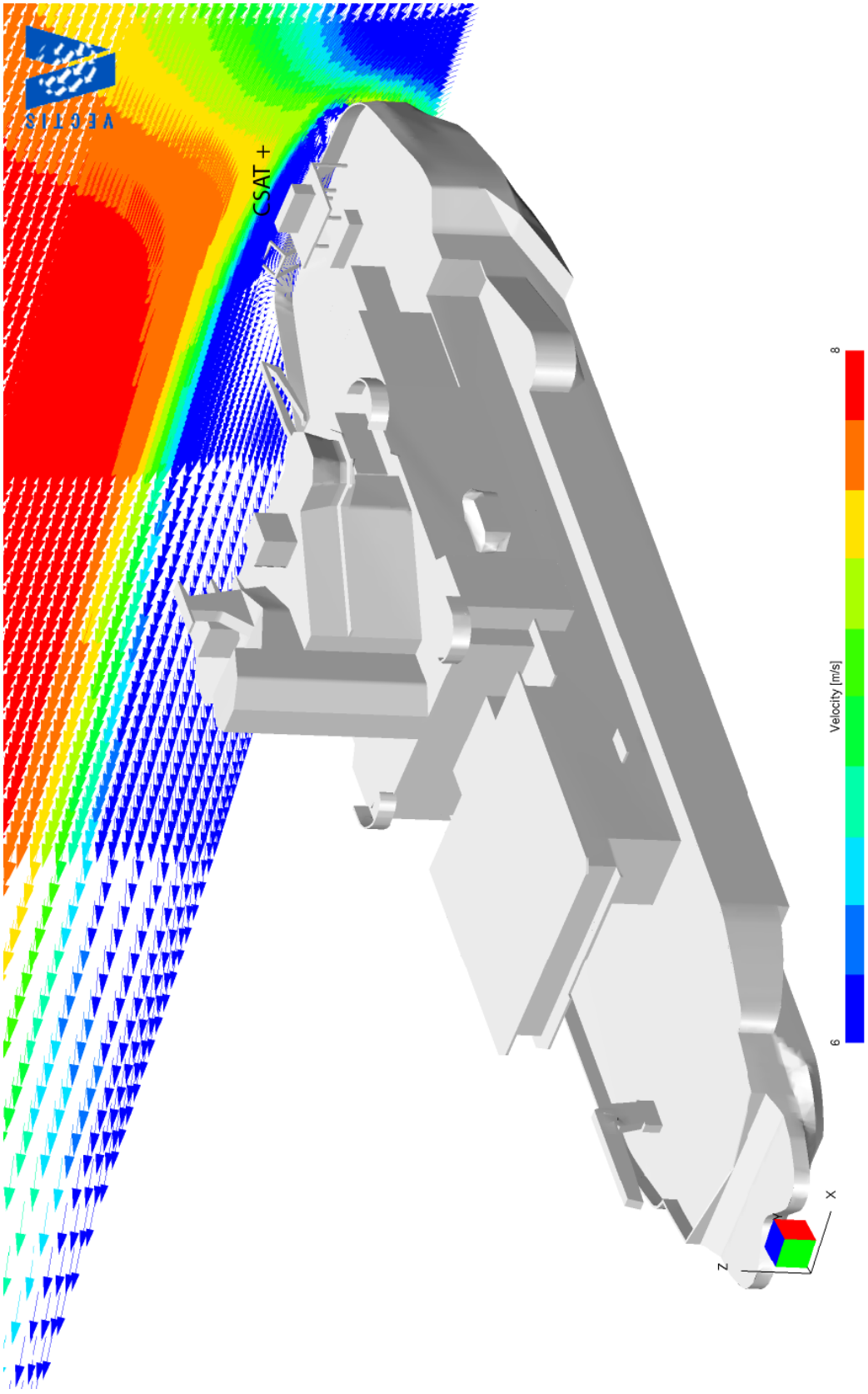

Figure A15 - METEK at 90 degree starboard flow

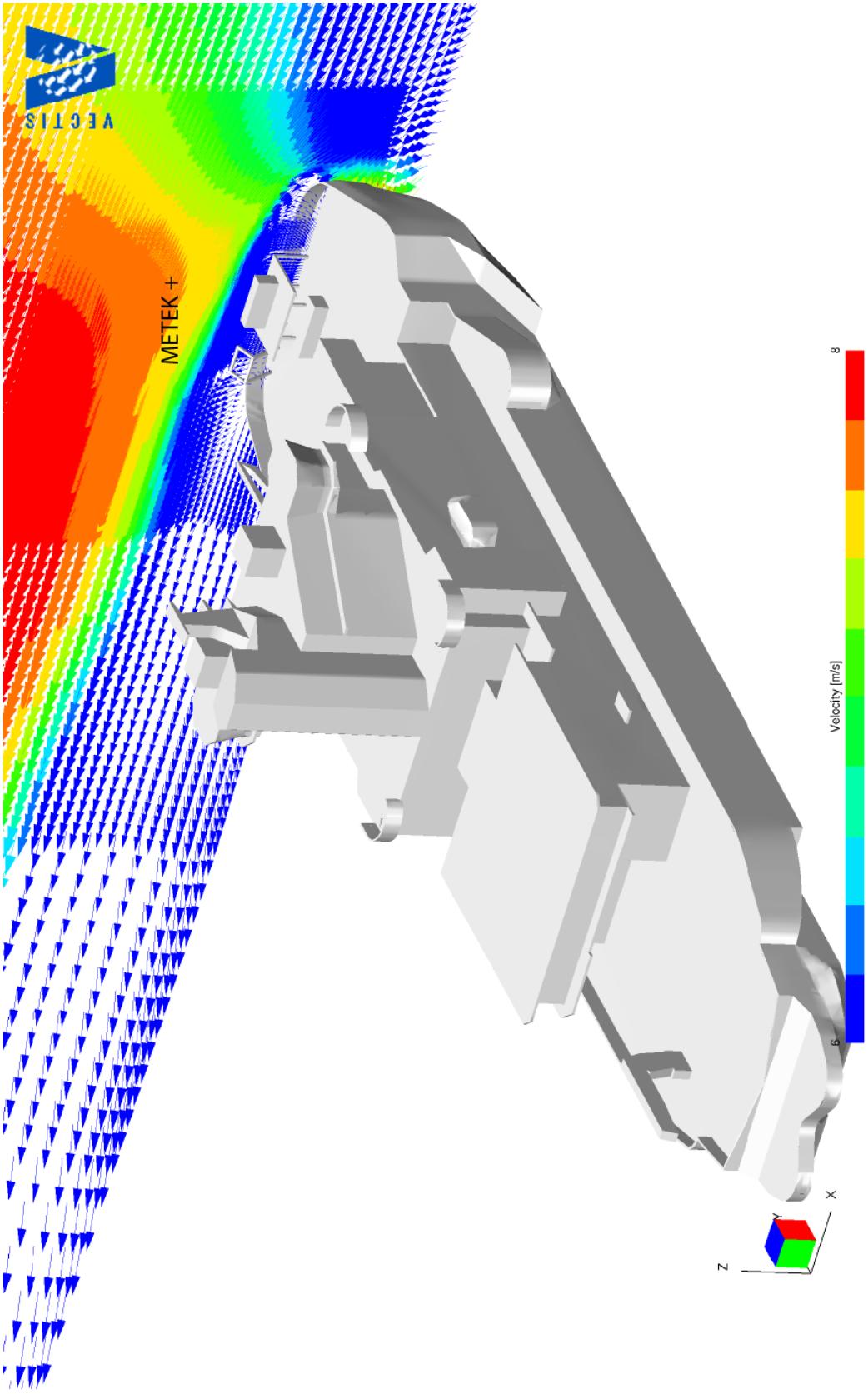

Figure A16 – CSAT at 90 degree starboard flow

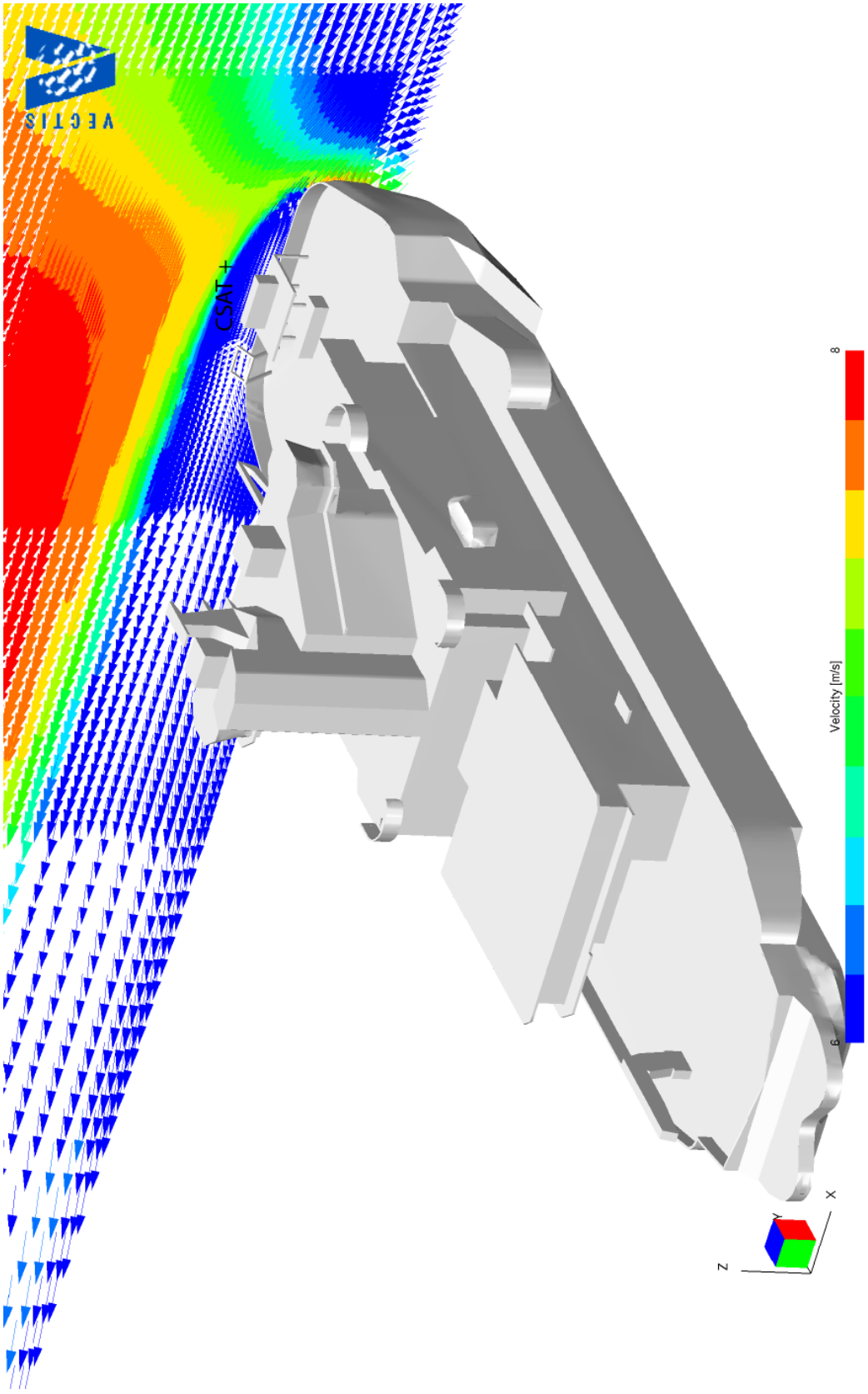

Figure A17 - METEK at 100 degree starboard flow

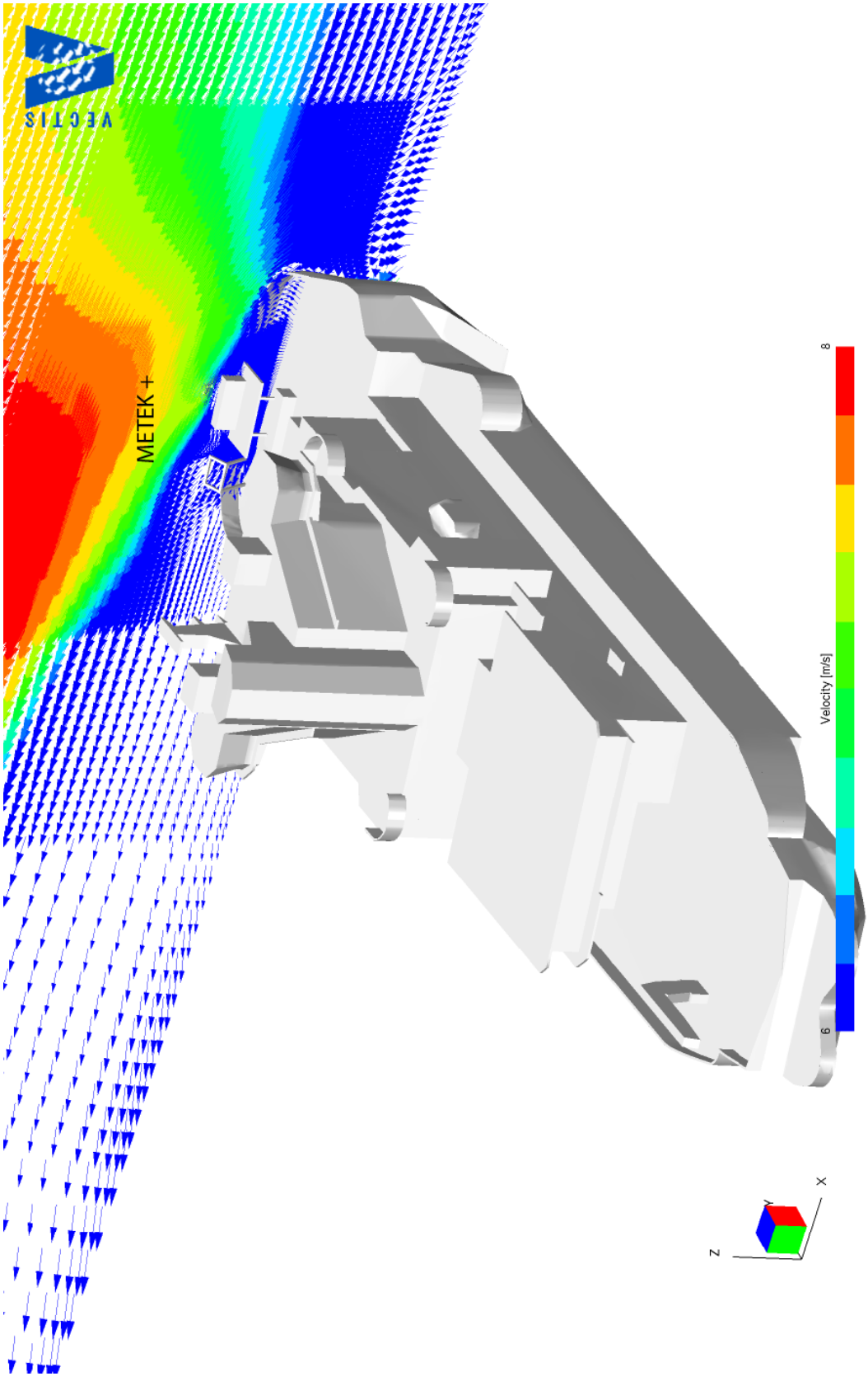

Figure A18 - CSAT at 100 degree starboard flow

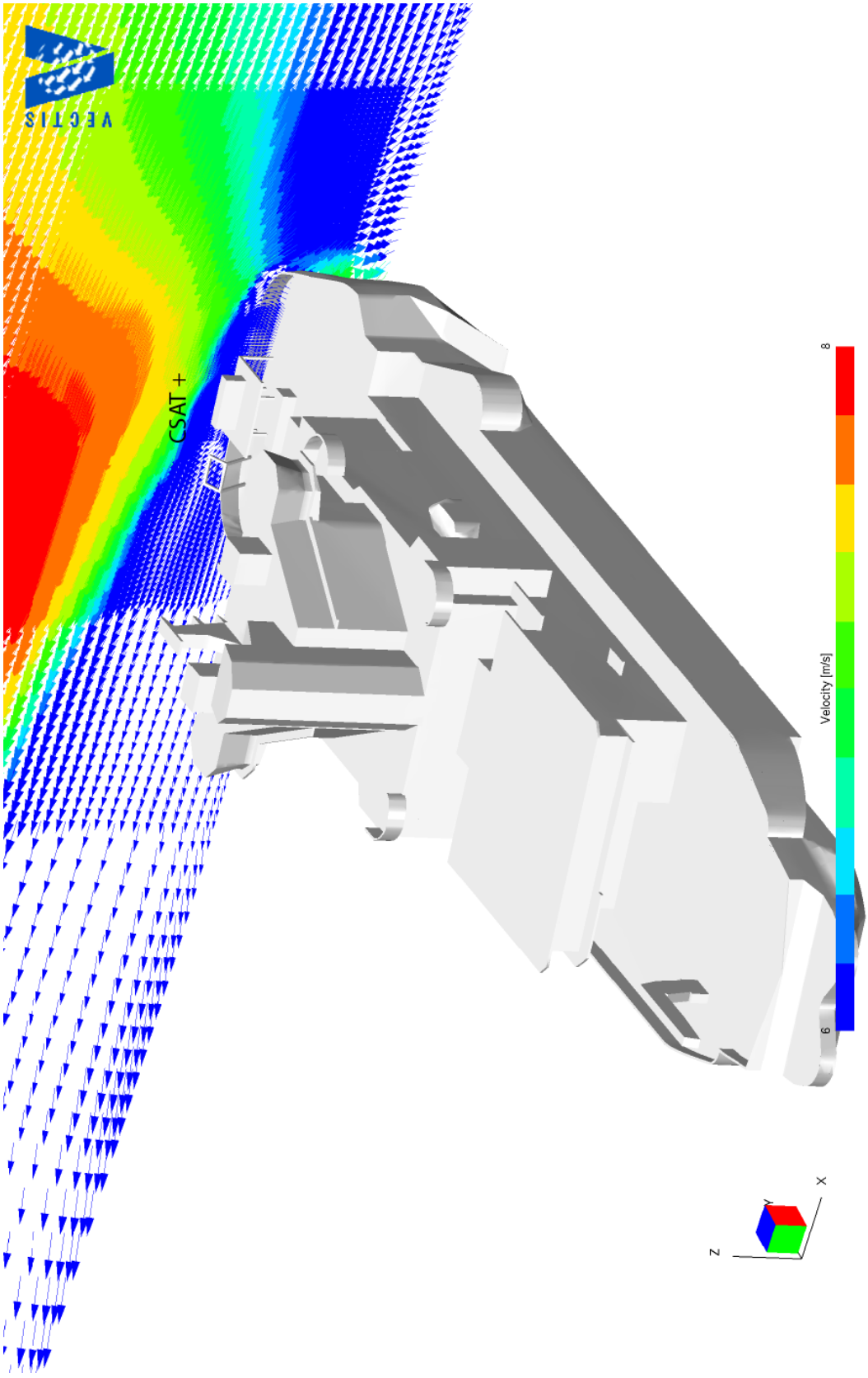

Figure A19 - METEK at 110 degree starboard flow

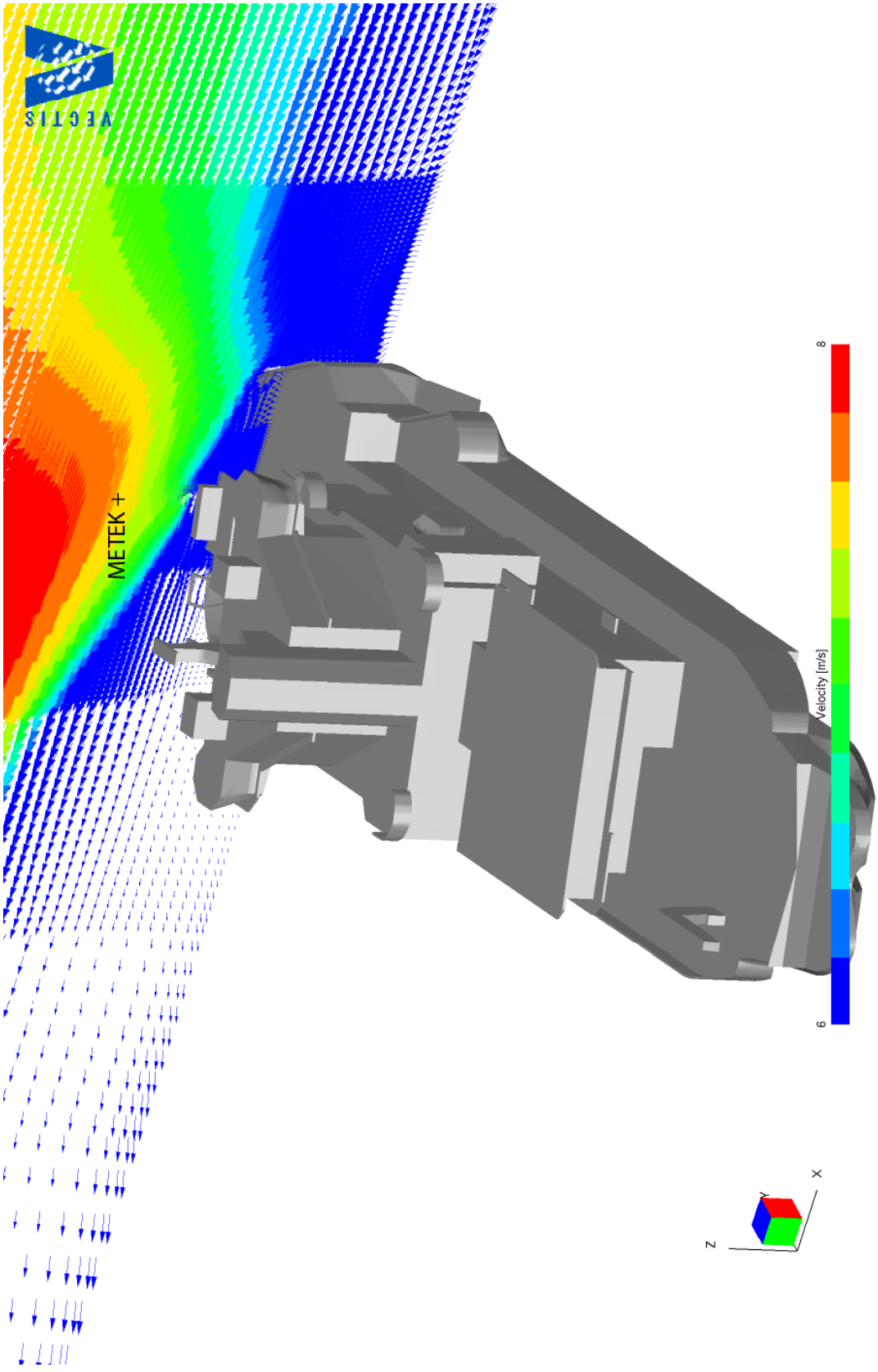

Figure A20 - CSAT at 110 degree starboard flow

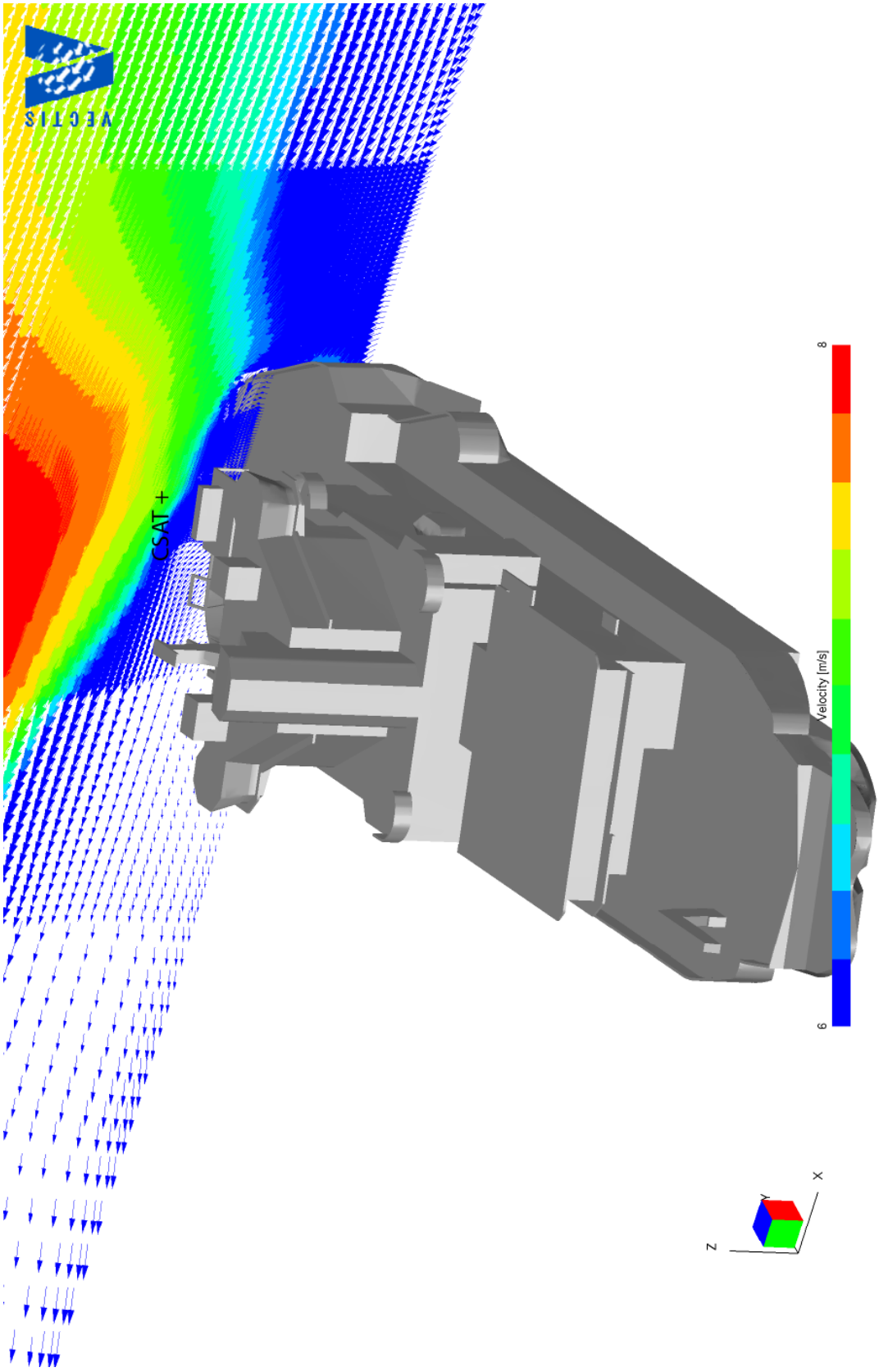

Figure A21 - METEK at 120 degree starboard flow

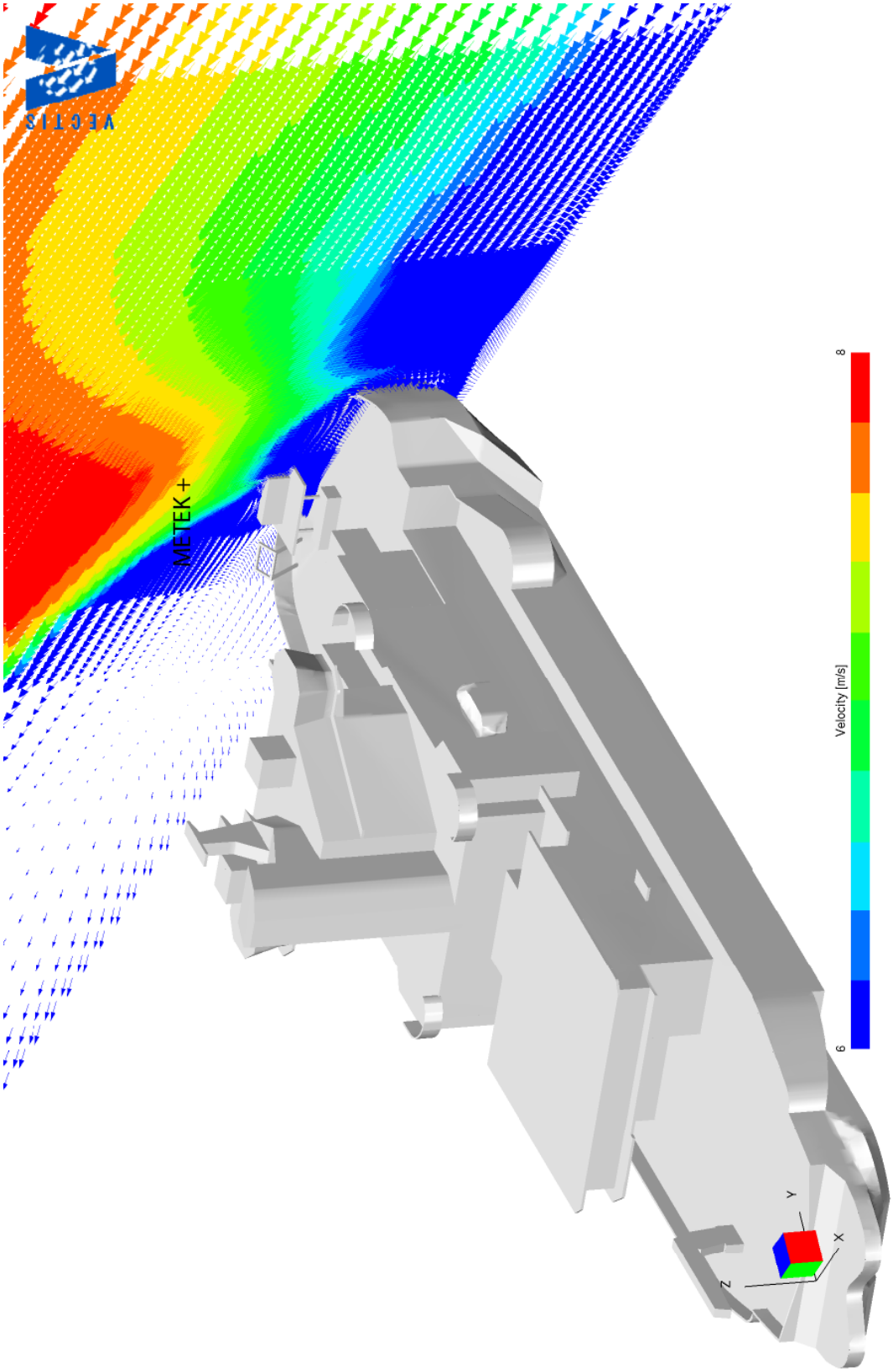

Figure A22 - CSAT at 120 degree starboard flow

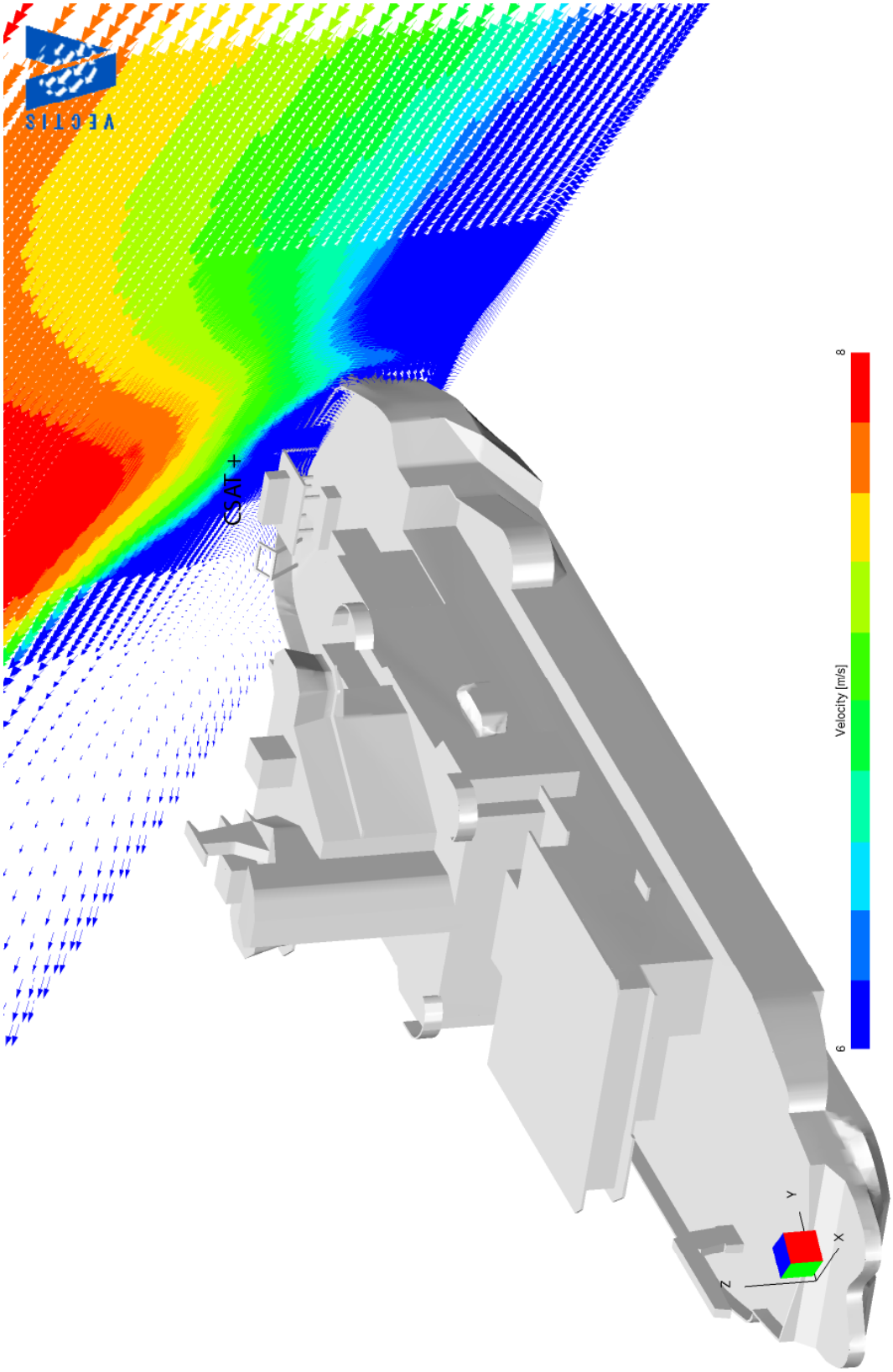

Figure A23 - METEK and CSAT at 150 degree starboard flow

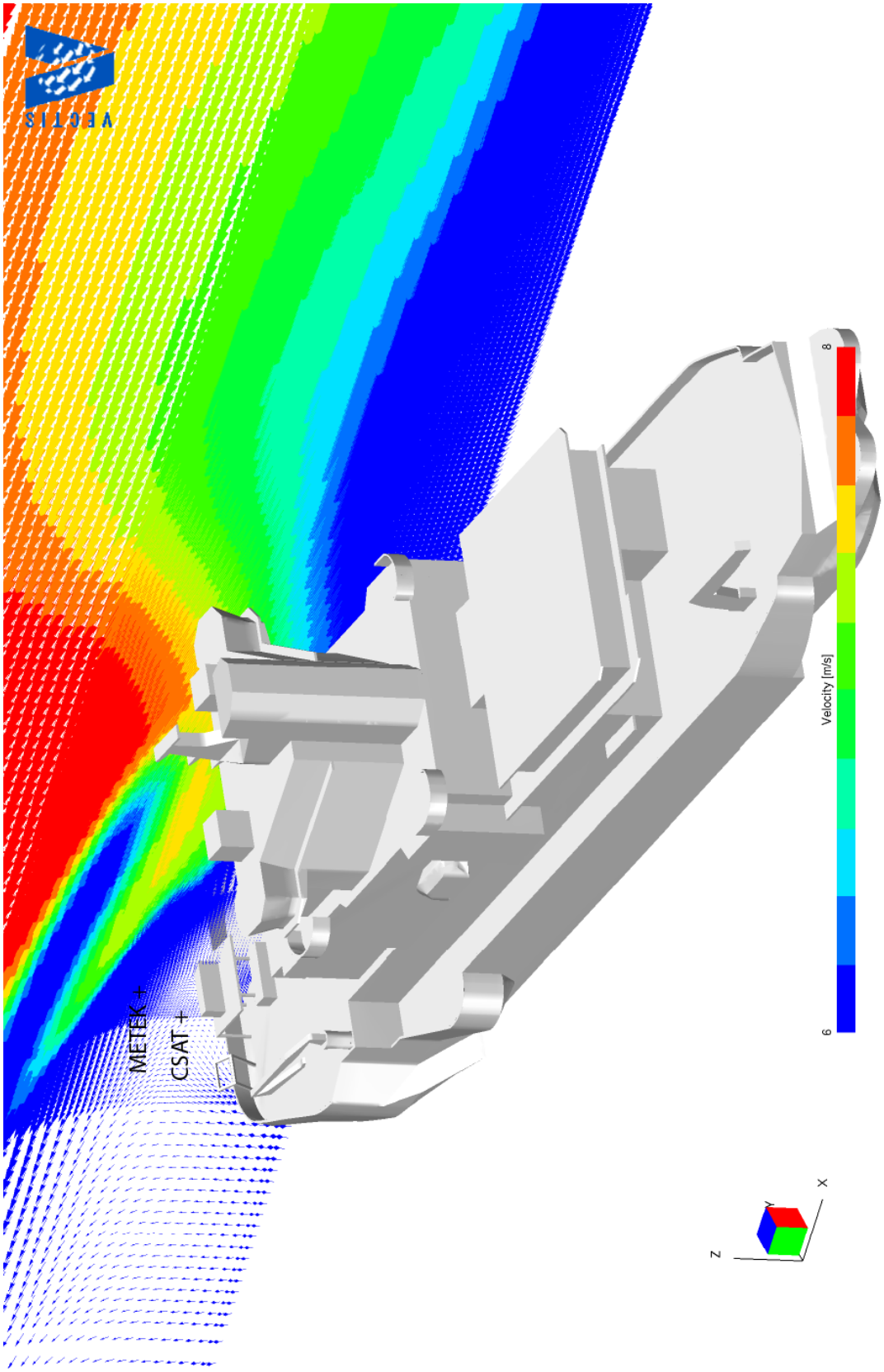

Figure A24 - METEK for a 0 degree bow-on flow

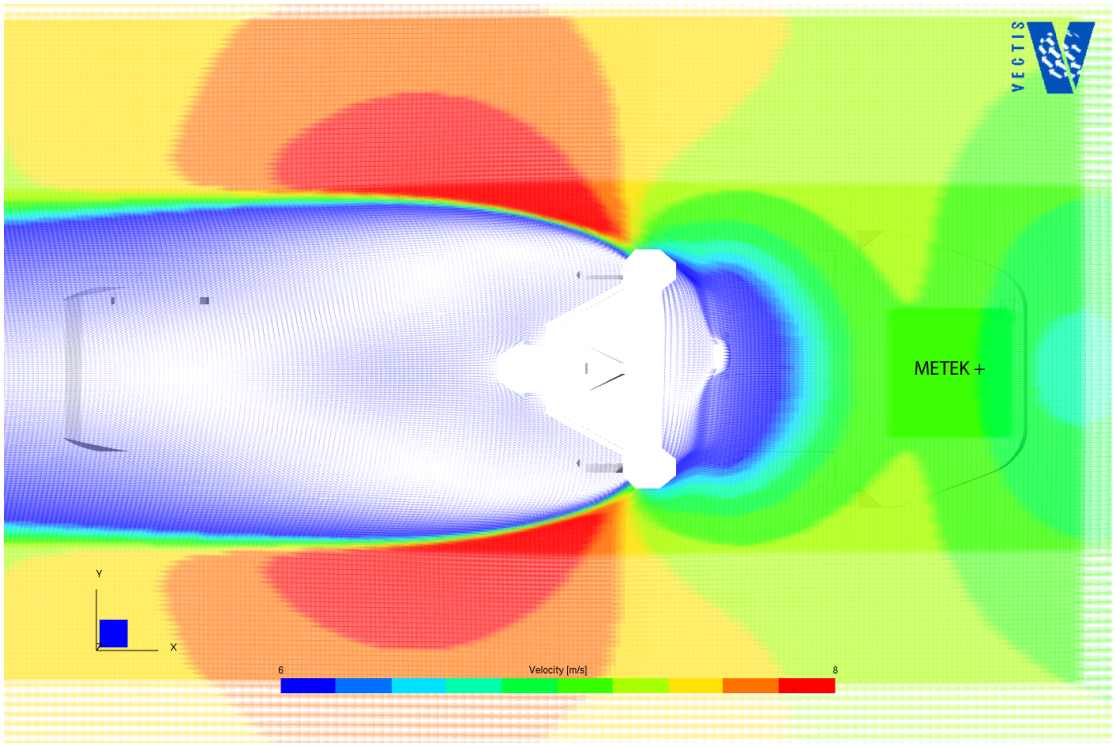

Figure A25 - CSAT for a 0 degree bow-on flow

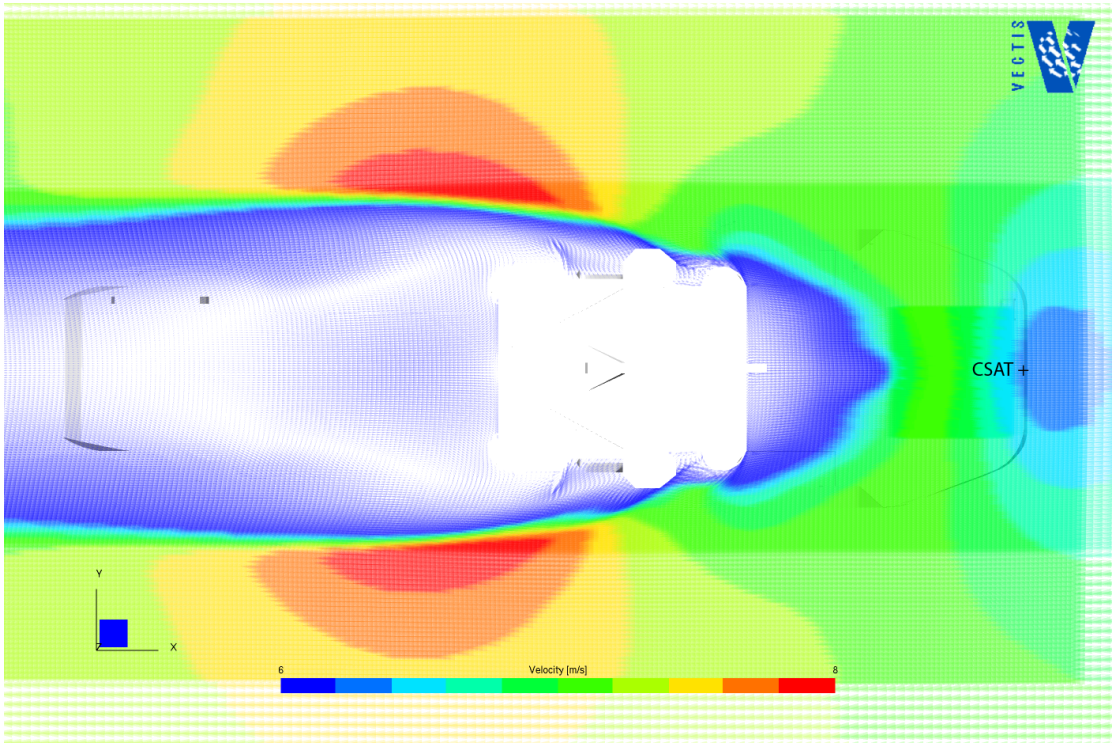

Figure A26 - METEK for a flow 10 degrees over the starboard side

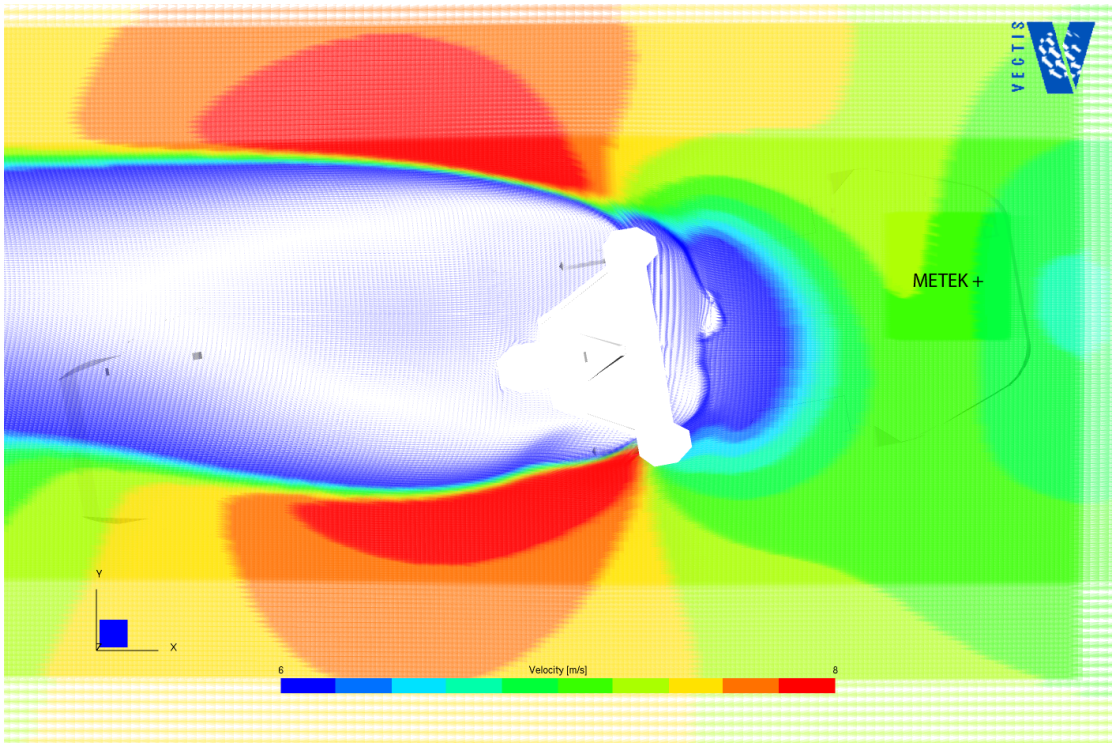

Figure A27 - CSAT for a flow 10 degrees over the starboard side

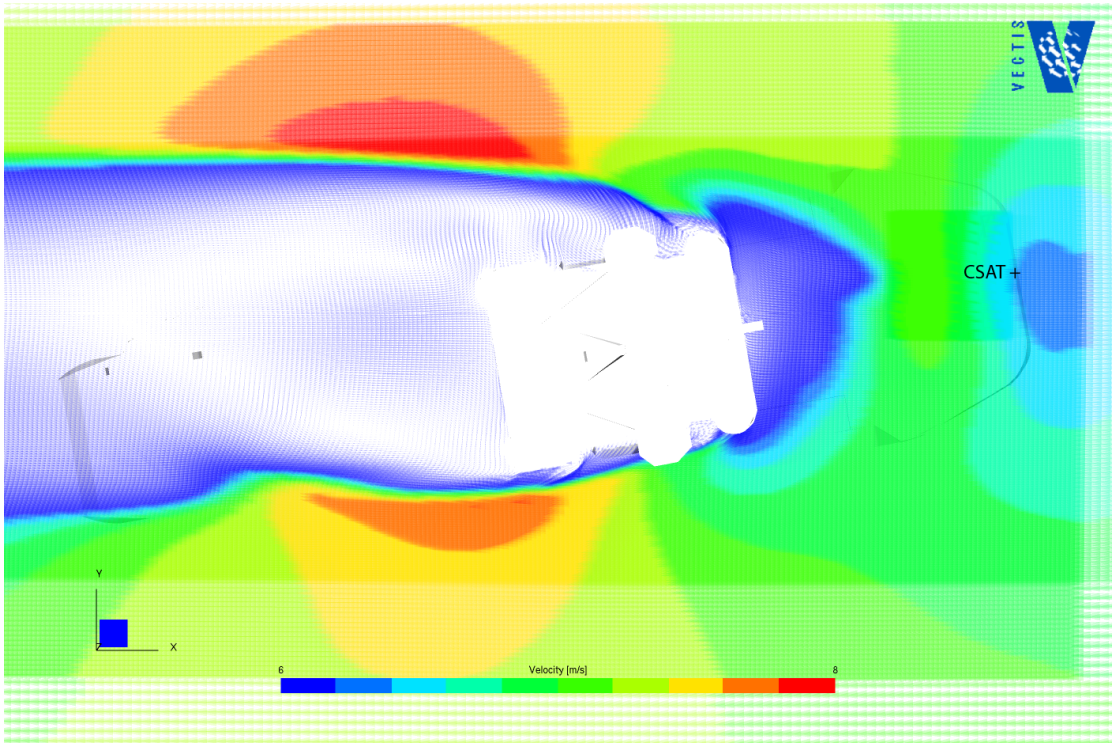

Figure A28 - METEK for a flow 20 degrees over the starboard side

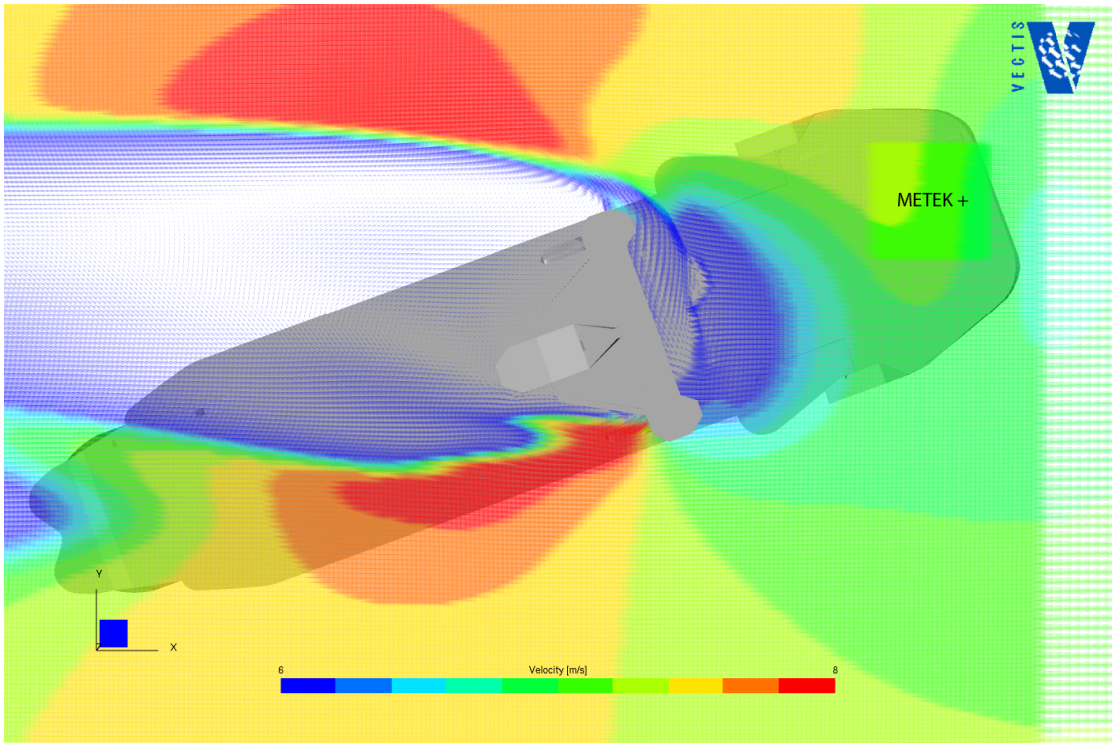

Figure A29 - CSAT for a flow 20 degrees over the starboard side

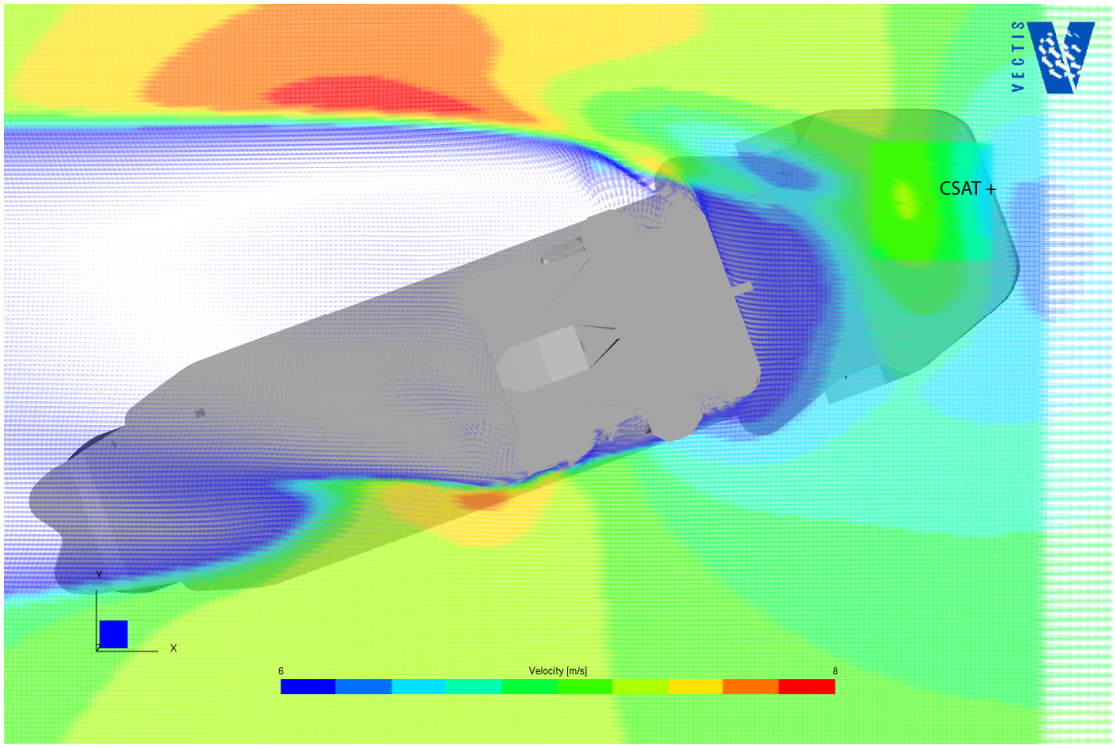

Figure A30 - METEK for a flow 30 degrees over the starboard side

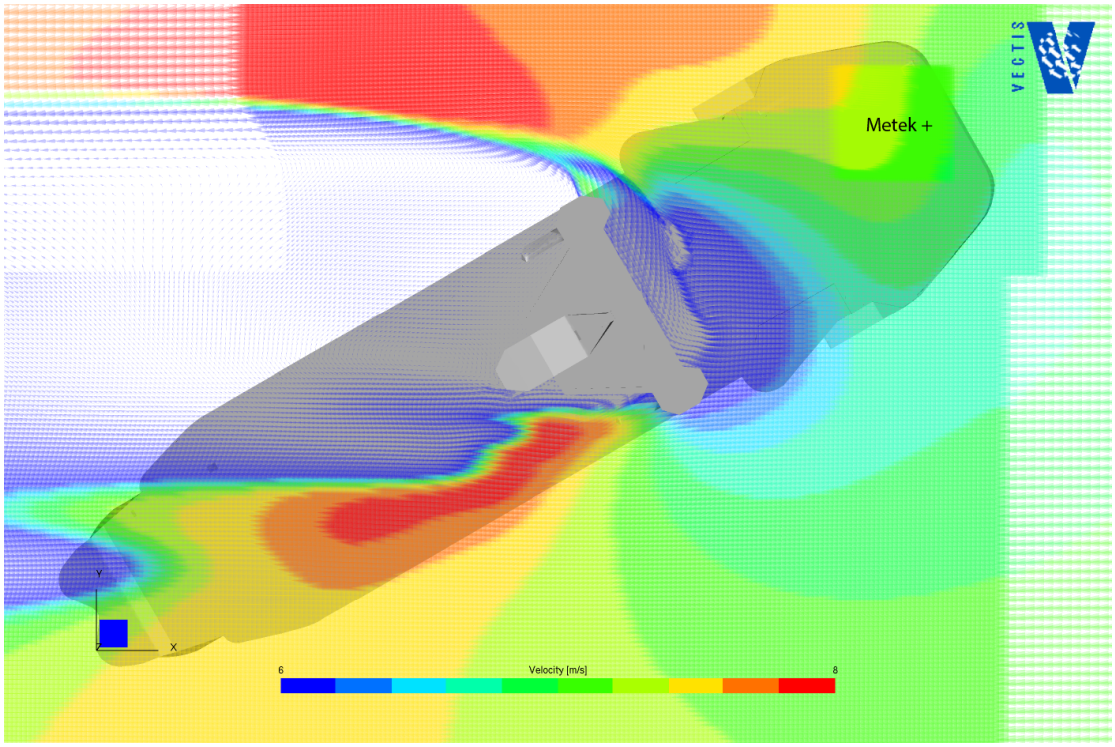

Figure A31 - CSAT for a flow 30 degrees over the starboard side

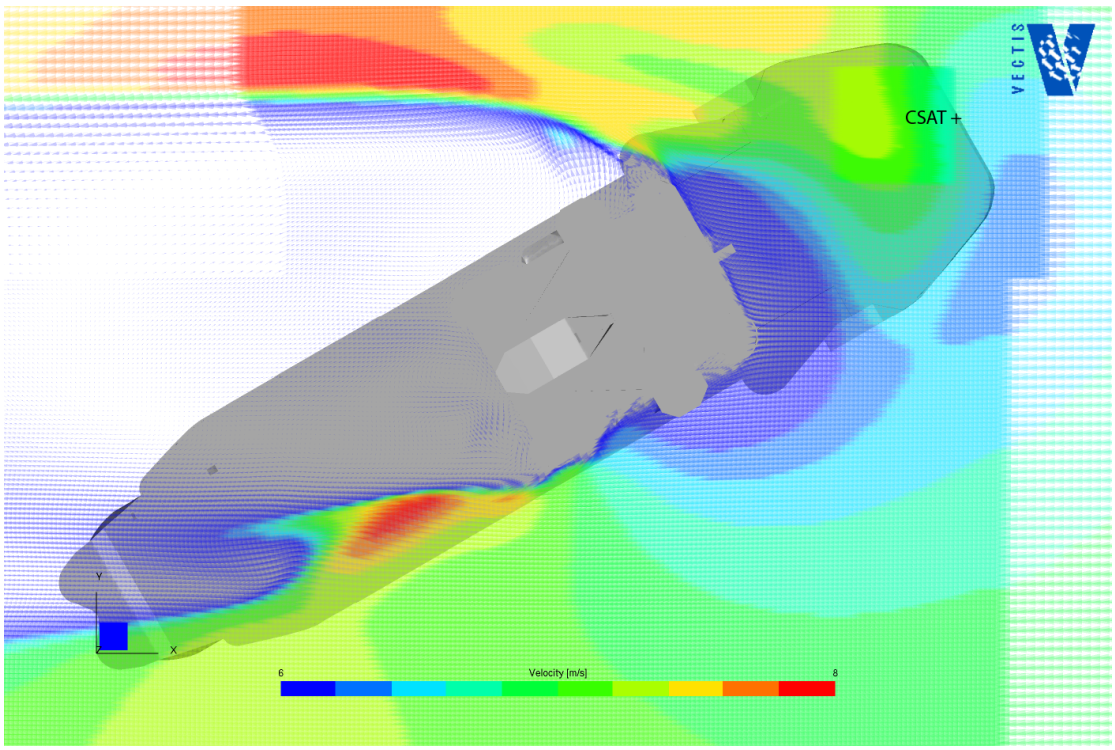

Figure A32 - METEK for a flow 40 degrees over the starboard side

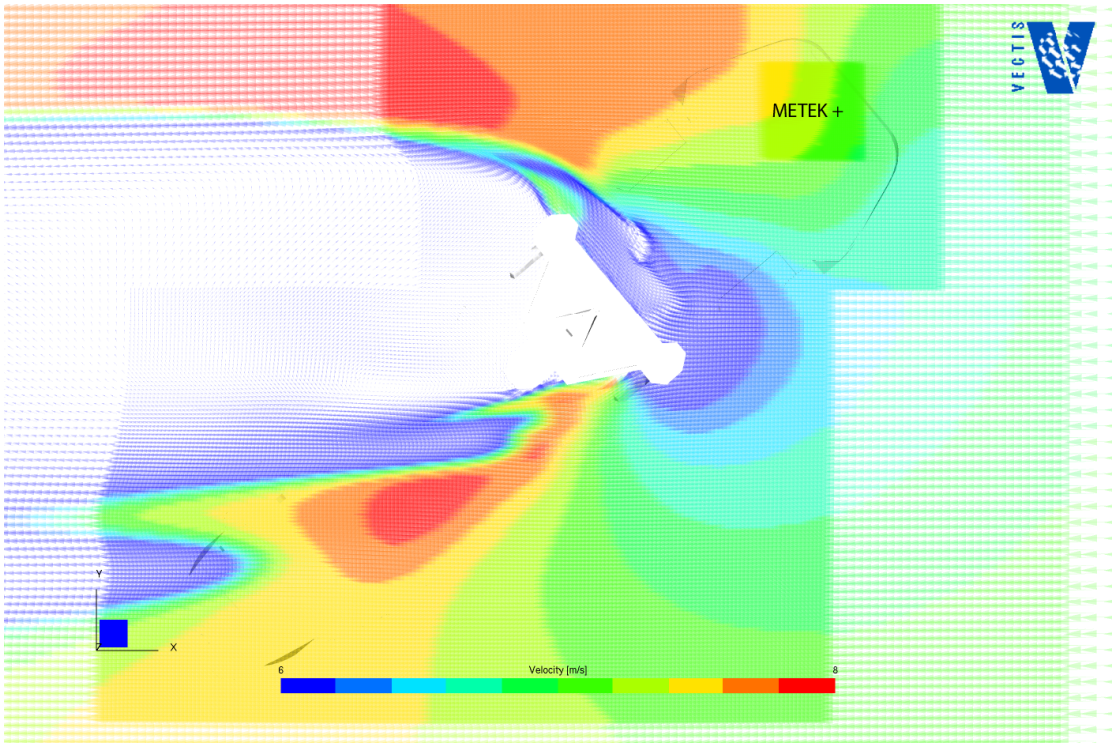

Figure A33 - CSAT for a flow 40 degrees over the starboard side

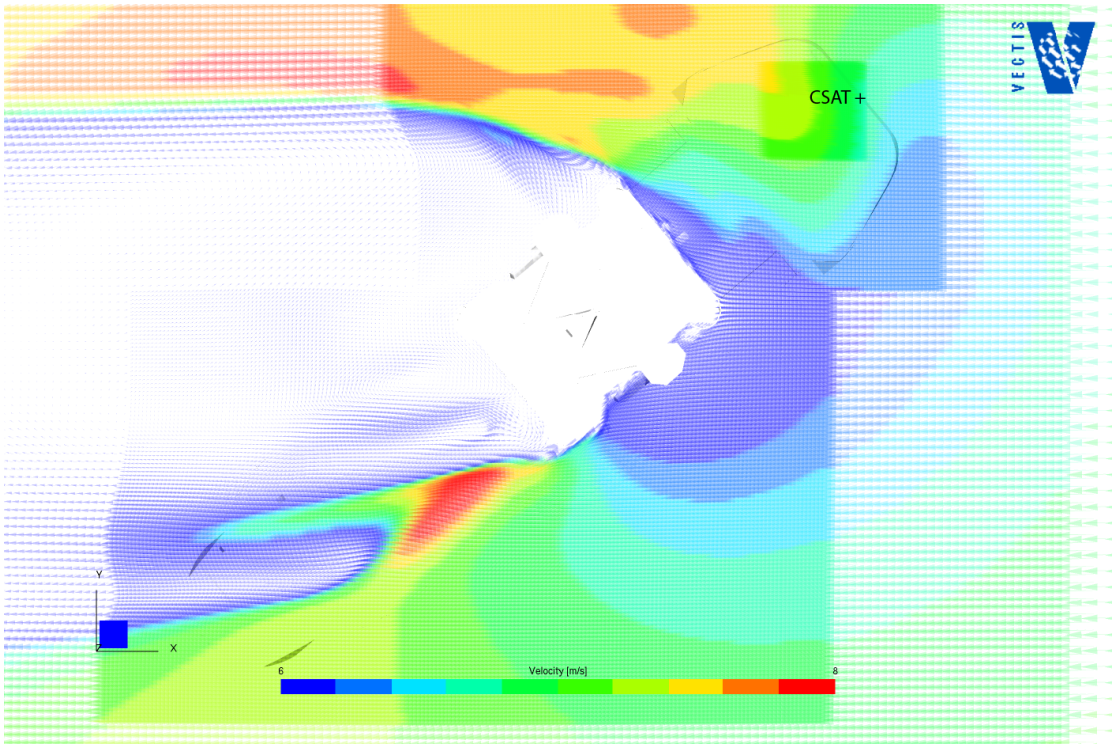

Figure A34 - METEK for a flow 50 degrees over the starboard side

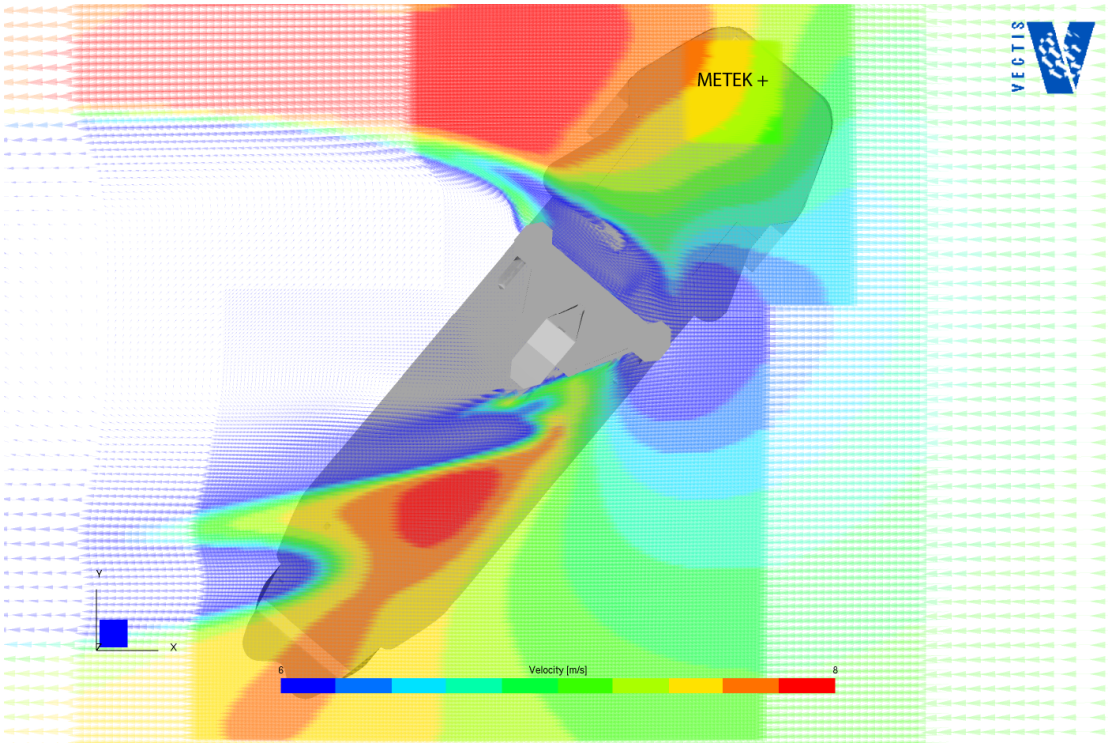

Figure A35 - CSAT for a flow 50 degrees over the starboard side

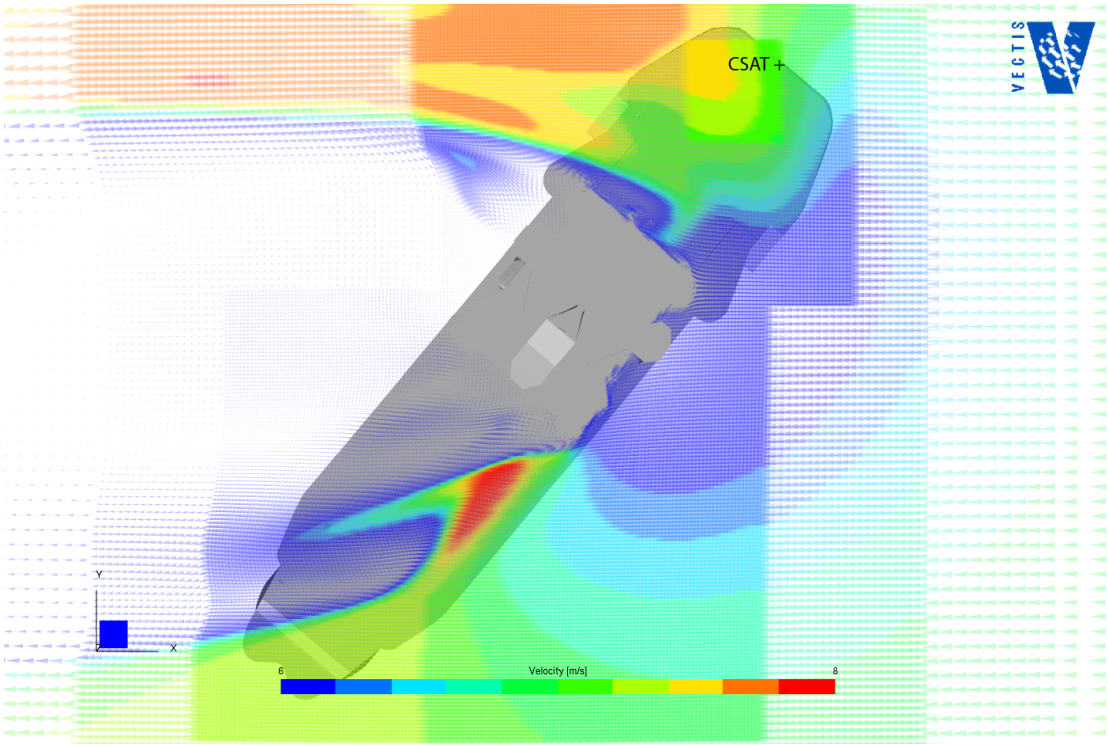

Figure A36 - METEK for a flow 60 degrees over the starboard side

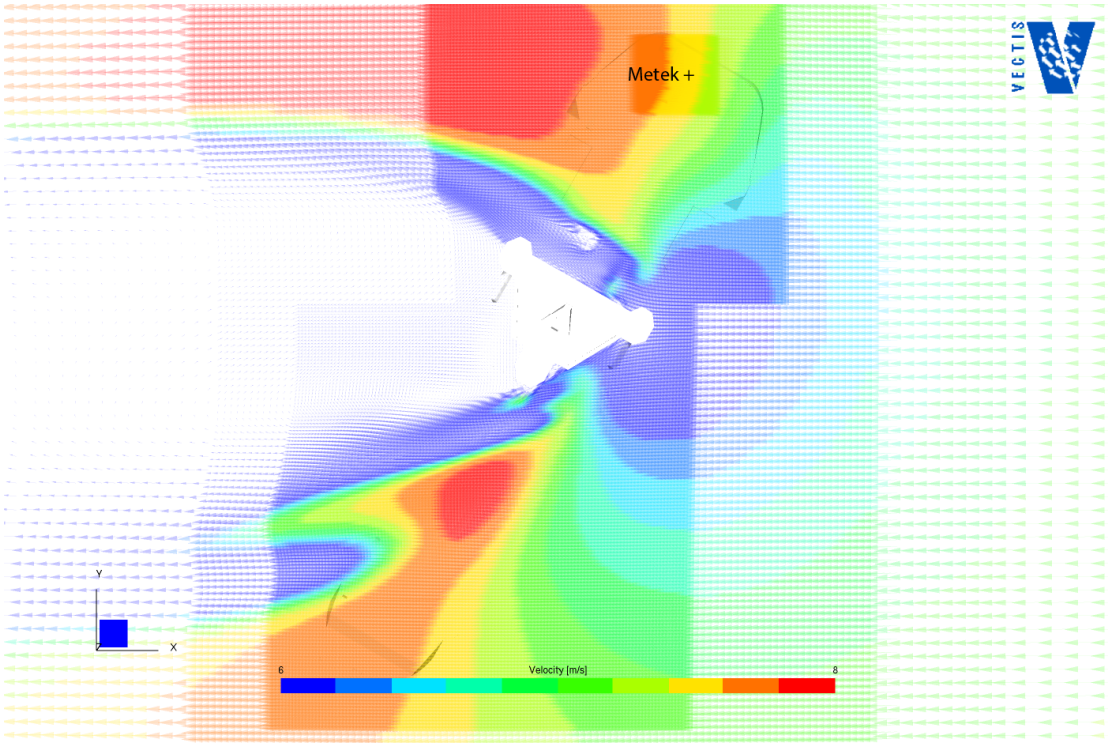

Figure A37 - CSAT for a flow 60 degrees over the starboard side

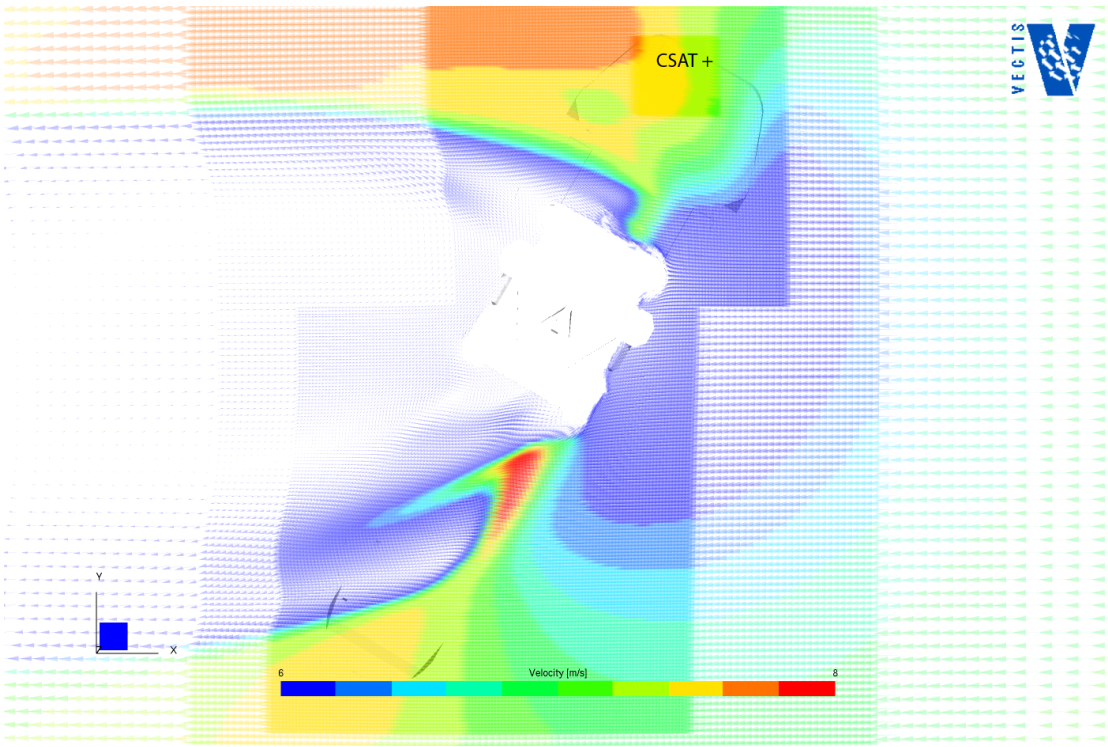

Figure A38 - METEK for a flow 70 degrees over the starboard side

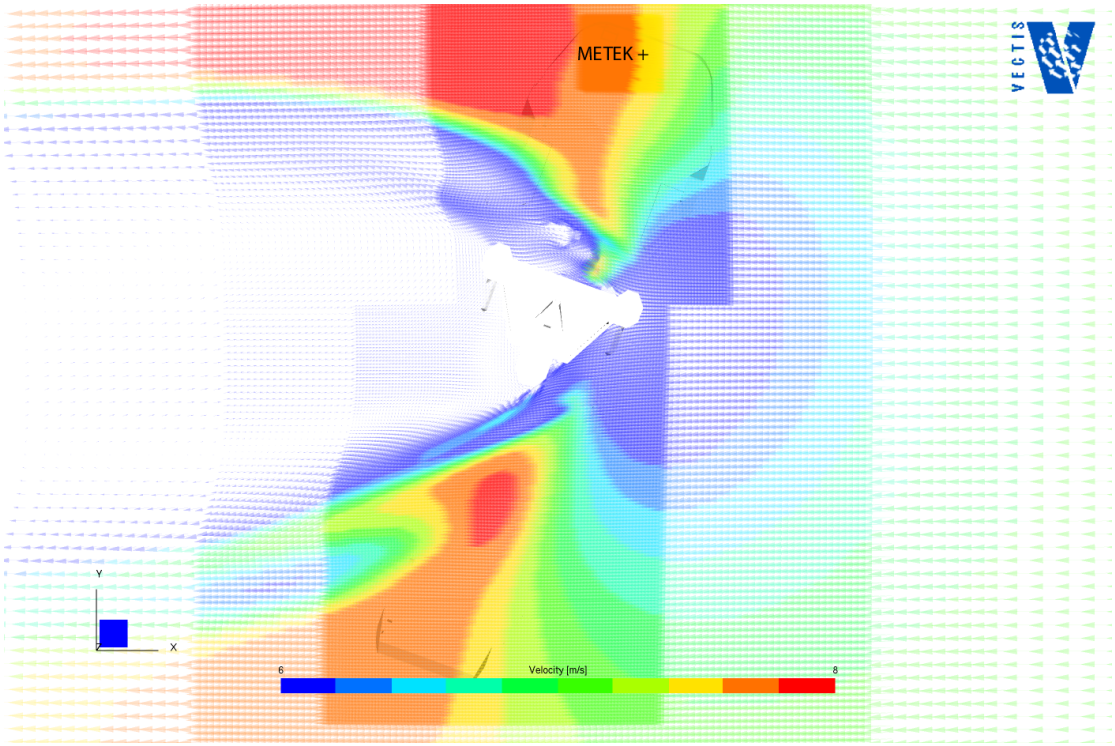

Figure A39 - CSAT for a flow 70 degrees over the starboard side

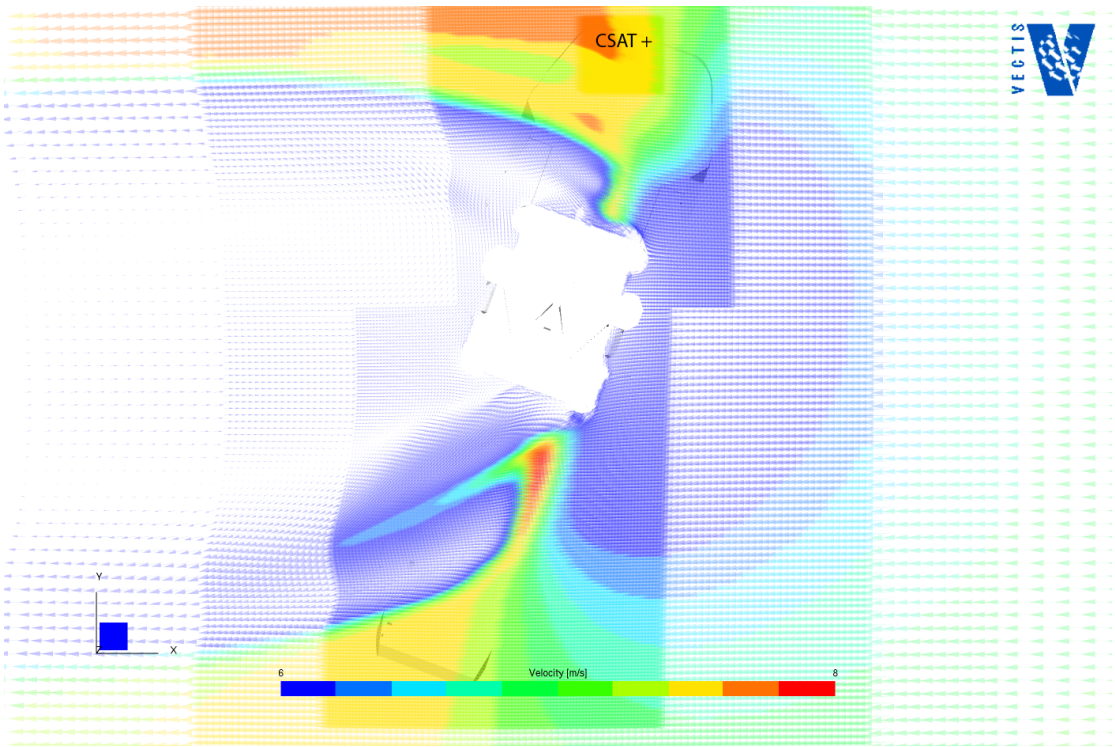

Figure A40 - METEK for a flow 80 degrees over the starboard side

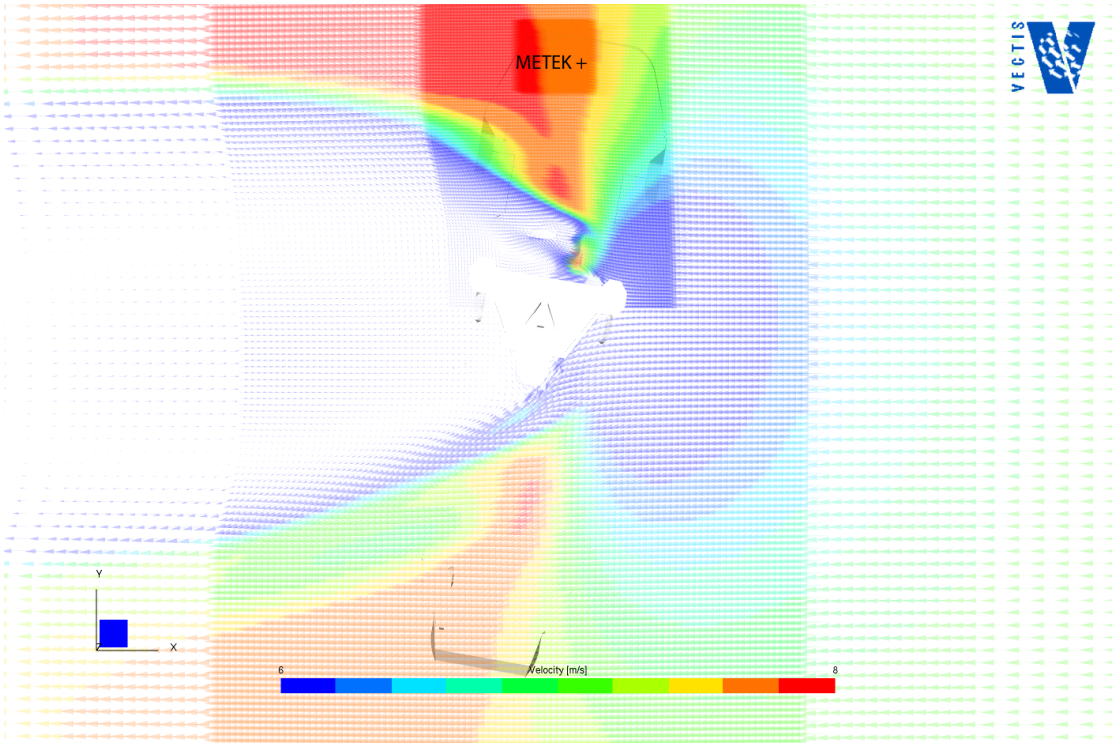

Figure A41 - CSAT for a flow 80 degrees over the starboard side

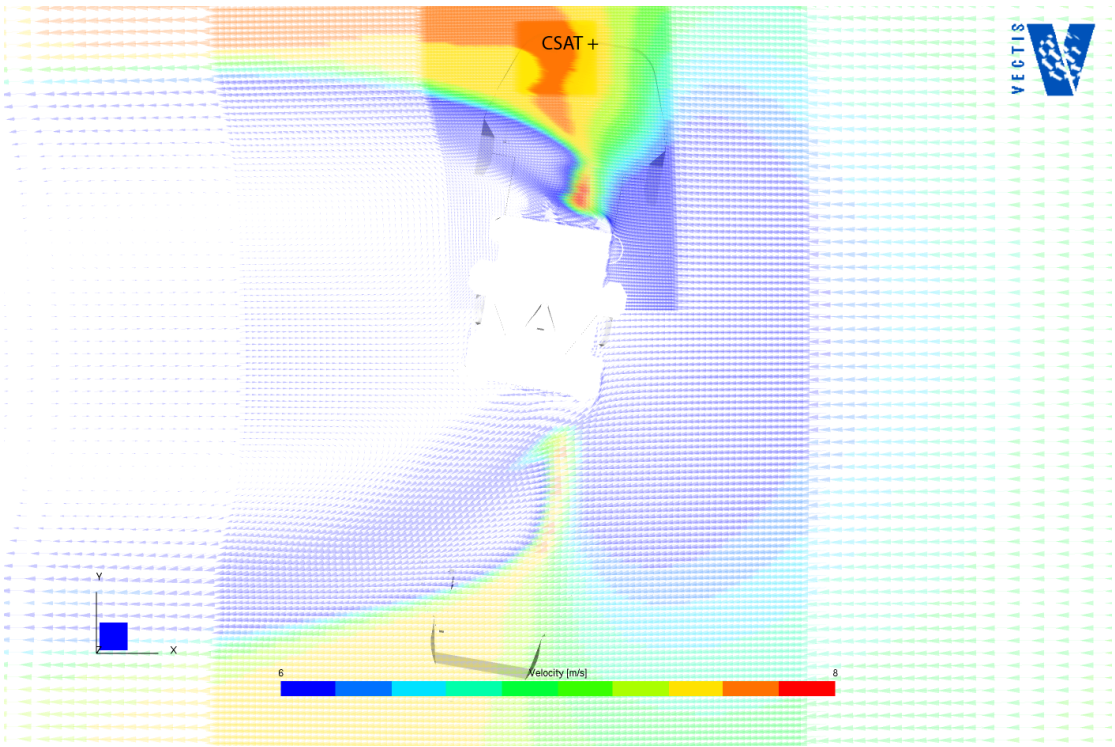

Figure A42 - METEK for a flow 90 degrees (beam-on) over the starboard side

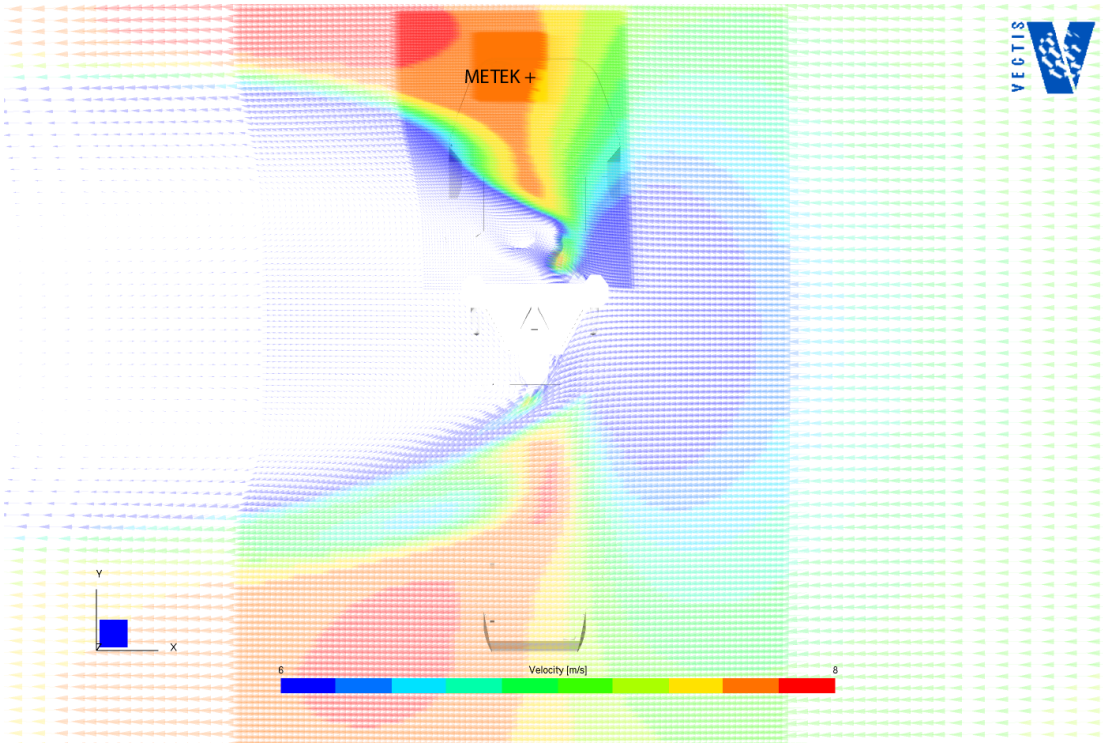

Figure A43 - CSAT for a flow 90 degrees (beam-on) over the starboard side

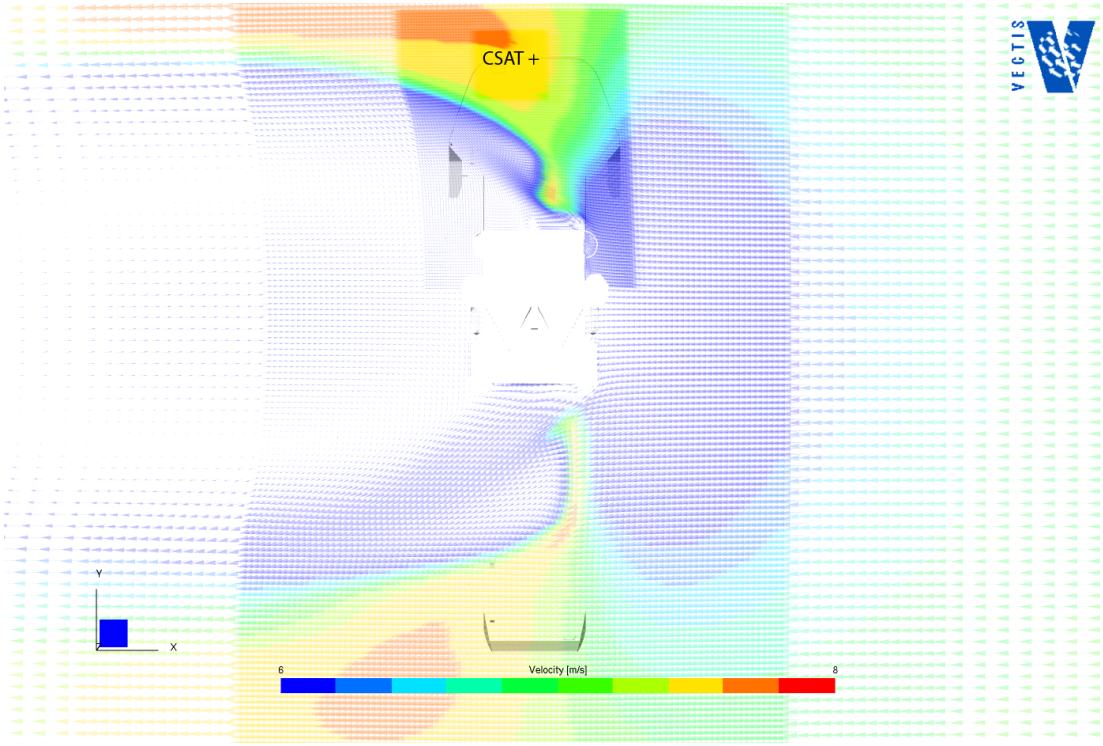

Figure A44 - METEK for a flow 100 degrees over the starboard side

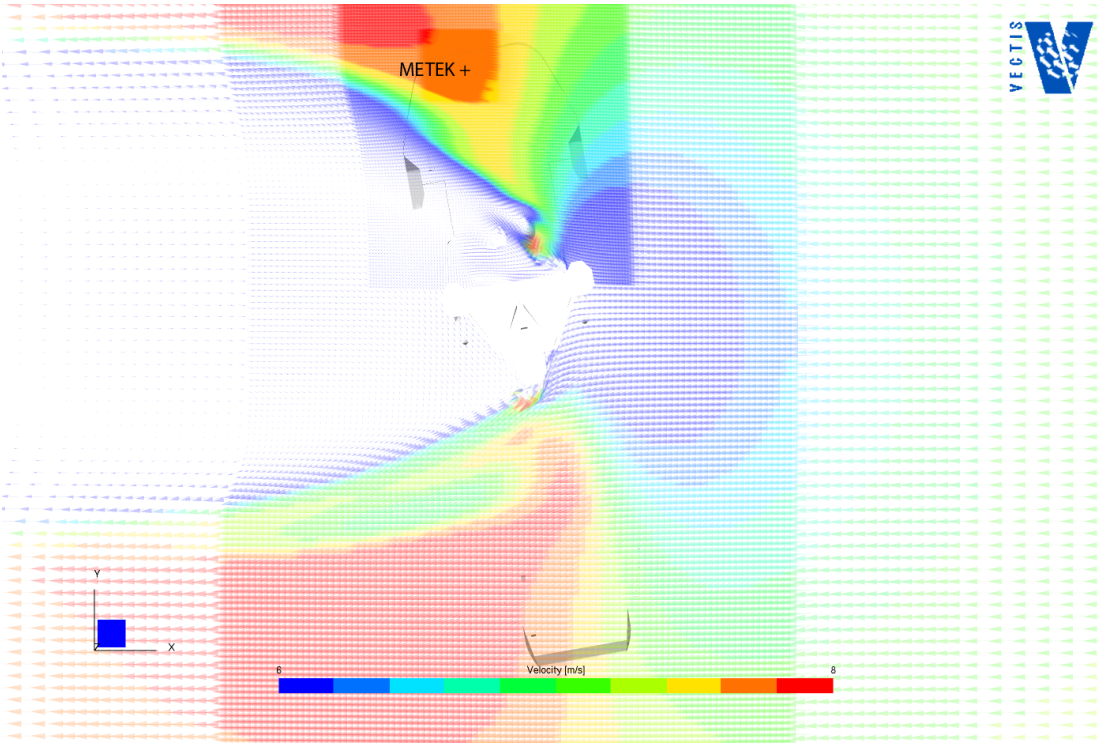

Figure A45 - CSAT for a flow 100 degrees over the starboard side

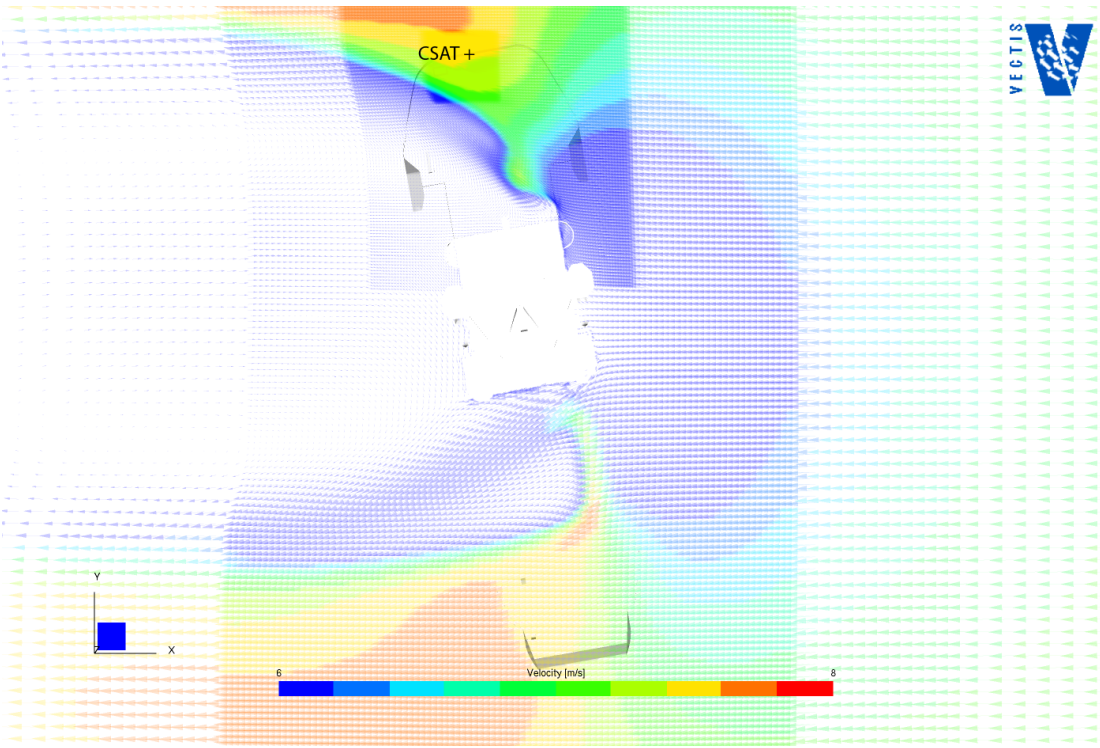

Figure A46 - METEK for a flow 110 degrees over the starboard side

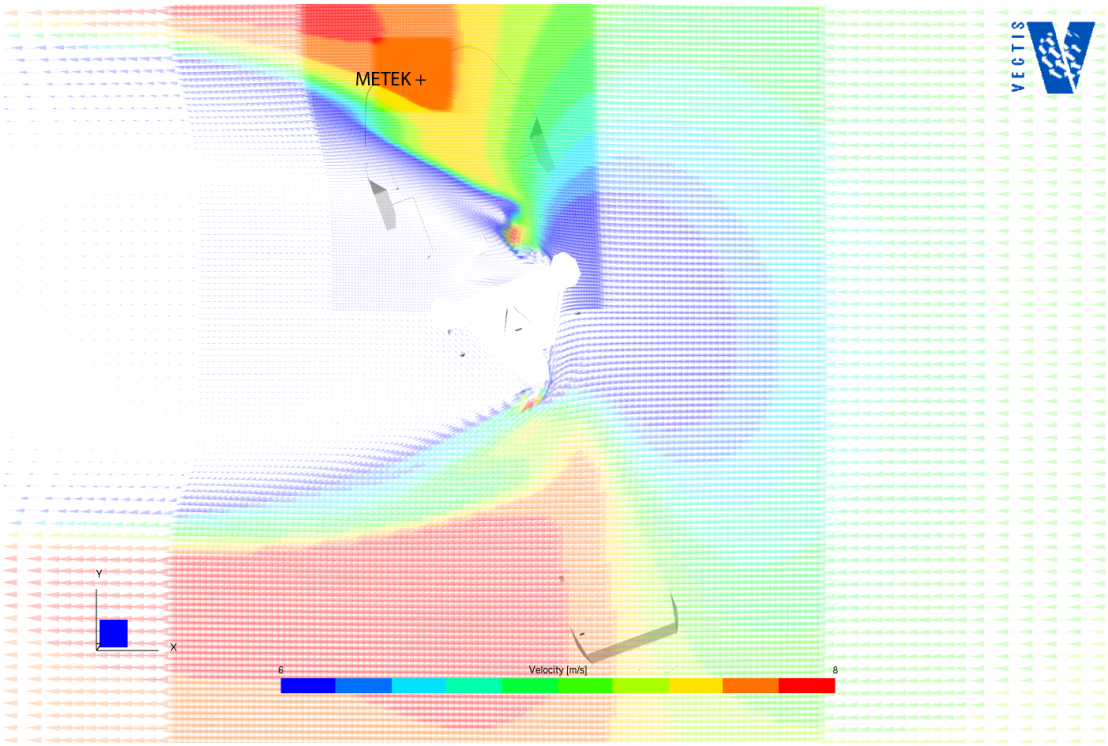

Figure A47 - CSAT for a flow 110 degrees over the starboard side

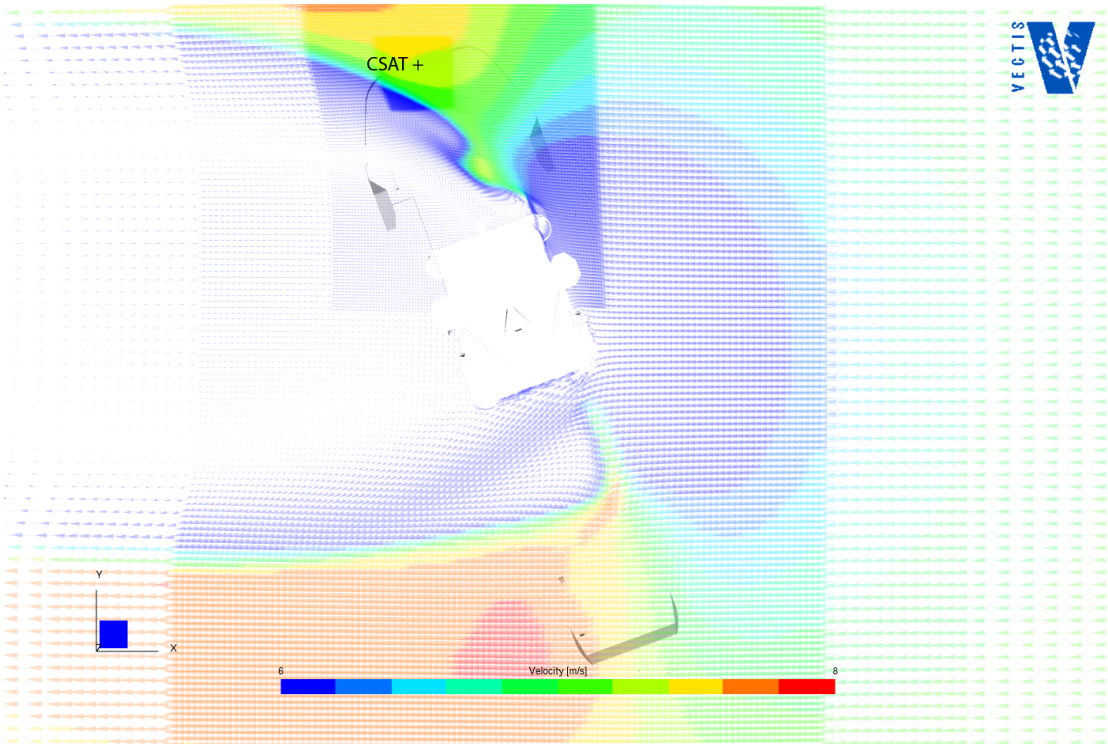

Figure A48 - METEK for a flow 120 degrees over the starboard side

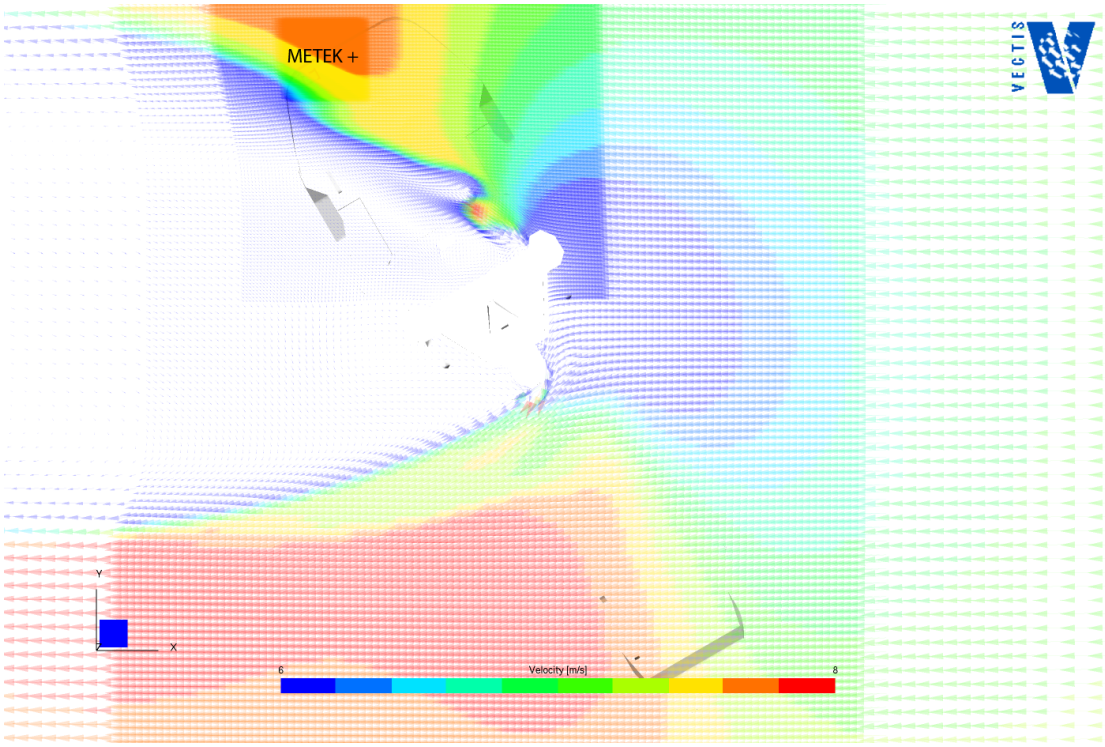

Figure A49 - CSAT for a flow 120 degrees over the starboard side

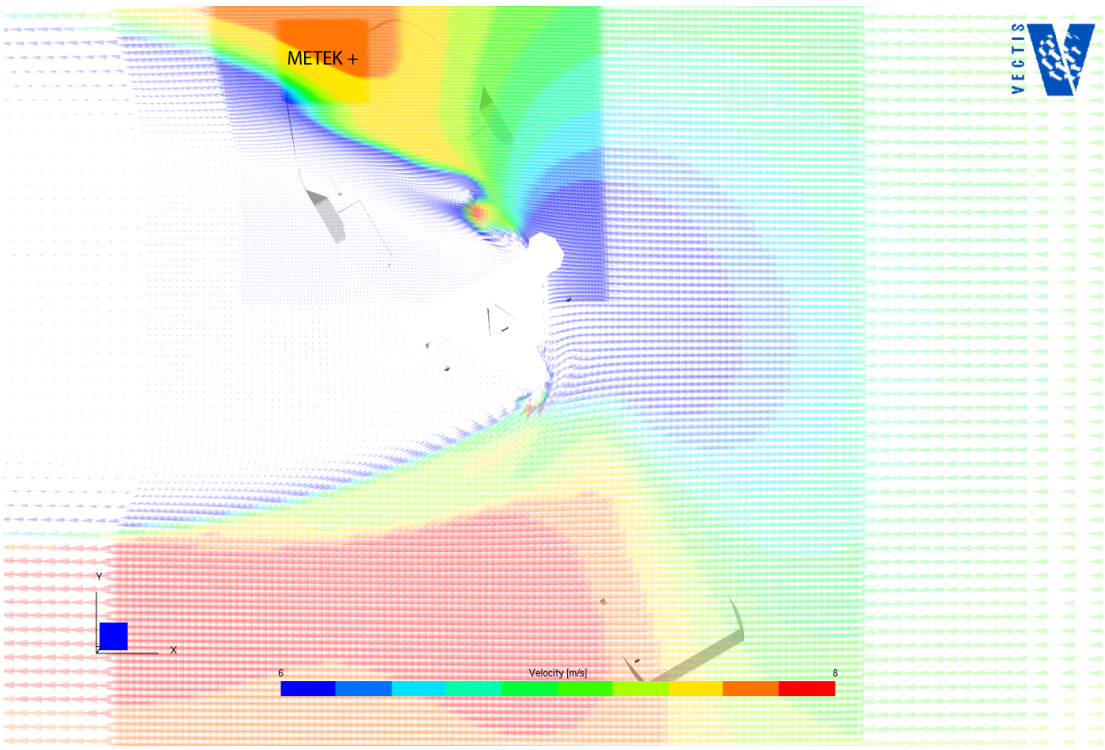

Figure A50 - METEK for a flow 150 degrees over the starboard side

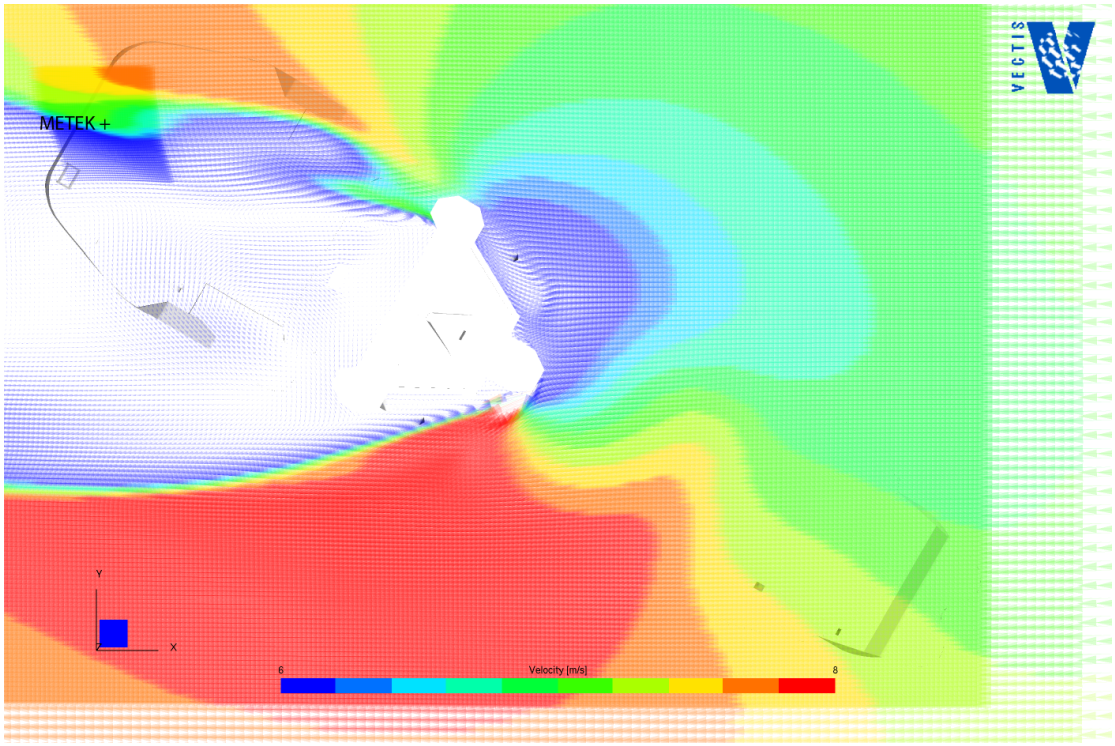

Figure A50 - CSAT for a flow 150 degrees over the starboard side

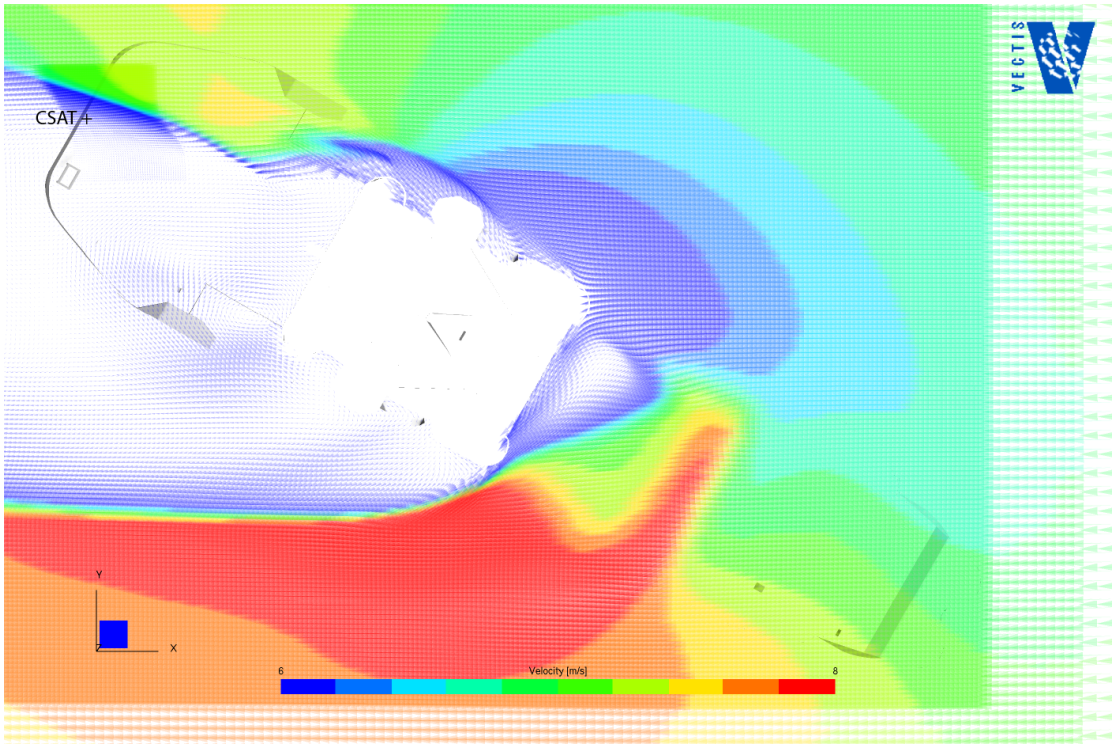

10. APPENDIX B: Summary table of results for each wind direction.

Table B.1. Summary of the effects of flow distortion. The values in brackets indicate the vertical displacement and the wind speed bias using a vertical displacement calculated from 2 seconds upstream, Δ_{zt}=2, of the anemometer site (after Yelland et al., 2002).

	Instrument height z (m)	Vertical displacement (m) Δz ($\Delta z_{t=2}$)	Velocity at instrument site (ms^{-1})	Free stream velocity at z (ms^{-1})	Free stream velocity at $z - \Delta z$ ($z - \Delta z_{t=2}$)	% velocity error at instrument site	% velocity error at instrument site at $z - \Delta z$ ($z - \Delta z_{t=2}$)	Angle of flow to the horizontal (degrees)	Horizontal twist (degrees)
150 degrees (flow over the port side)									
METEK	**20.58**	**-** (-)	**6.654**	**7.424**	**-** (-)	**-10.37**	**-** (-)	**11.11**	**-1.12**
CSAT	**16.03**	**-** (-)	**5.122**	**7.274**	**-** ()	**-29.58**	**-** (-)	**10.78**	**-0.60**
Weather station	**26.32**	**-** (-)	**-**	**-**	**-** (-)	**-**	**-** (-)	**-**	**-**
Port Ship's anemometer	**35.98**	**-**	**8.290**	**7.746**	**-**	**7.02**	**-**	**13.5**	**-4.3**
Stb. Ship's anemometer	**35.98**	**-**	**8.502**	**7.746**	**-**	**9.76**	**-**	**7.7**	**-11.8**
120 degrees (flow over the port side)									
METEK	**20.58**	**10.30** (2.17)	**7.750**	**7.425**	**6.896** (7.359)	**4.39**	**12.39** (5.32)	**6.53**	**-8.68**
CSAT	**16.03**	**10.34** (1.63)	**7.254**	**7.277**	**6.236** (7.210)	**-0.33**	**16.33** (0.61)	**4.95**	**-12.58**
Weather station	**26.32**	**-** (-)	**-**	**-**	**-** (-)	**-**	**-** (-)	**-**	**-**
Port Ship's anemometer	**35.98**	**-**	**8.055**	**7.748**	**-**	**3.96**	**-**	**17.6**	**3.9**
Stb. Ship's anemometer	**35.98**	**-**	**8.216**	**7.749**	**-**	**6.03**	**-**	**18.0**	**0.2**

Instrument	Instrument height z (m)	Vertical displacement ΔZ ($\Delta z_{t=2}$) (m)	Velocity at instrument site (ms^{-1})	Free stream velocity at z (ms^{-1})	Free stream velocity At z-ΔZ (z - $\Delta z_{t=2}$)	% velocity error at instrument site	% velocity error at instrument site at z-Δz (z - $\Delta z_{t=2}$)	Angle of flow to the horizontal (degrees)	Horizontal twist (degrees)
110 degrees (flow over the port side)									
METEK	20.58	8.77 (1.99)	7.813	7.424	7.060 (7.364)	5.24	10.67 (6.10)	5.95	-9.33
CSAT	16.03	8.35 (1.54)	7.456	7.277	6.541 (7.214)	2.47	13.99 (3.37)	3.92	-13.00
Weather station	26.32	- (-)	2.506	7.569	- (-)	-66.89	- (-)	-5.79	-68.90
Port Ship's anemometer	35.98	-	8.029	7.749	-	3.61	-	16.5	5.1
Stb. Ship's anemometer	35.98	-	8.214	7.749	-	6.00	-	16.9	4.4
100 degrees (flow over the port side)									
METEK	20.58	7.40 (1.79)	7.787	7.424	7.151 (7.369)	4.88	8.90 (5.67)	5.18	-9.93
CSAT	16.03	7.14 (1.58)	7.575	7.277	6.728 (7.213)	4.10	12.59 (5.02)	3.24	-12.82
Weather station	26.32	- (-)	2.788	7.569	- (-)	-63.17	- (-)	-16.36	59.03
Port Ship's anemometer	35.98	-	7.970	7.748	-	2.86	-	15.8	5.1
Stb. Ship's anemometer	35.98	-	8.299	7.748	-	7.11	-	14.3	4.9
90 degrees (flow over the port beam)									
METEK	20.58	6.03 (1.58)	7.746	7.405	7.142 (7.352)	4.60	8.46 (5.37)	4.22	-9.37
CSAT	16.03	5.96 (1.64)	7.608	7.224	6.809 (7.133)	5.31	11.73 (6.66)	2.93	-11.07
Weather station	26.32	13.42 (0.23)	3.610	7.560	7.038 (7.554)	-52.25	-48.71 ()	-0.41	-16.71
Port Ship's anemometer	35.98	-	8.034	7.744	-	3.74	-	13.8	5.5
Stb. Ship's anemometer	35.98	-	8.265	7.744	-	6.73	-	11.8	5.4

Instrument	Instrument height z (m)	Vertical displacement ΔZ ($\Delta z_{t=2}$) (m)	Velocity at instrument site (ms^{-1})	Free stream velocity at z (ms^{-1})	Free stream velocity At z-ΔZ (z - $\Delta z_{t=2}$)	% velocity error at instrument site	% velocity error at instrument site at z-Δz (z - $\Delta z_{t=2}$)	Angle of flow to the horizontal (degrees)	Horizontal twist (degrees)
80 degrees (flow over the port side)									
METEK	20.58	5.15 (1.52)	7.772	7.407	7.200 (7.357)	4.92	7.94 (5.65)	3.90	-8.14
CSAT	16.03	5.10 (1.64)	7.646	7.229	6.890 (7.229)	5.77	10.98 (7.11)	3.39	-9.47
Weather station	26.32	12.26 (0.48)	3.633	7.560	7.117 (7.550)	-51.95	-48.95 (-51.88)	6.67	-16.42
Port Ship's anemometer	35.98	-	7.947	7.745	-	2.61	-	13.2	5.8
Stb. Ship's anemometer	35.98	-	8.255	7.745	-	6.59	-	10.7	6.4
70 degrees (flow over the port side)									
METEK	20.58	4.43 (1.47)	7.701	7.406	7.234 (7.357)	3.98	6.45 (4.67)	4.14	-7.77
CSAT	16.03	4.35 (1.60)	7.581/90	7.229	6.955 (7.142)	4.87	9.00 (6.15)	4.05	-9.23
Weather station	26.32	- (-)	4.487	7.558	- -	-40.73	- (-)	11.9	-17.98
Port Ship's anemometer	35.98	-	7.958	7.743	-	2.78	-	12.2	5.2
Stb. Ship's anemometer	35.98	-	8.300	7.743	-	7.20	-	9.4	5.4
60 degrees (flow over the port side)									
METEK	20.58	3.93 (1.44)	7.581	7.406	7.259 (7.359)	2.37	4.44 (3.03)	4.63	-6.93
CSAT	16.03	3.90 (1.64)	7.429	7.230	6.991 (7.142)	2.74	6.27 (4.02)	5.56	-8.27
Weather station	26.32	12.98 (4.84)	6.614	7.558	7.072 (7.433)	-12.49	-6.47 (-11.02)	17.55	-16.03
Port Ship's anemometer	35.98	-	7.915	7.742	-	2.23	-	11.9	3.8
Stb. Ship's anemometer	35.98	-	8.290	7.743	-	7.07	-	9.8	4.3

Instrument	Instrument height z (m)	Vertical displacement ΔZ ($\Delta z_{t=2}$) (m)	Velocity at instrument site (ms^{-1})	Free stream velocity at z (ms^{-1})	Free stream velocity At z-ΔZ (z - $\Delta z_{t=2}$)	% velocity error at instrument site	% velocity error at instrument site at z-Δz (z - $\Delta z_{t=2}$)	Angle of flow to the horizontal (degrees)	Horizontal twist (degrees)
50 degrees (flow over the port side)									
METEK	20.58	3.60 (1.47)	7.451	7.407	7.276 (7.359)	0.59	2.41 (1.25)	5.31	-6.08
CSAT	16.03	3.68 (1.74)	7.253	7.233	7.011 (7.139)	0.28	3.46 (1.60)	7.27	-7.40
Weather station	26.32	12.87 (5.10)	7.171	7.559	7.081 (7.427)	-5.13	1.27 (-3.44)	21.46	-14.13
Port Ship's anemometer	35.98	-	7.959	7.744	-	2.78	-	10.8	1.6
Stb. Ship's anemometer	35.98	-	8.218	7.744	-	6.12	-	9.7	2.3
40 degrees (flow over the port side)									
METEK	20.58	3.32 (1.47)	7.322	7.406	7.287 (7.357)	-1.13	0.48 (-0.48)	5.92	-4.96
CSAT	16.03	3.51 (1.82)	7.086	7.233	7.023 (7.135)	-2.03	0.90 (-0.69)	8.93	-6.10
Weather station	26.32	12.21 (4.77)	7.243	7.557	7.119 (7.435)	-4.15	1.74 (-2.58)	26.19	-10.93
Port Ship's anemometer	35.98	-	7.964	7.742	-	2.88	-	10.8	0.2
Stb. Ship's anemometer	35.98	-	8.229	7.742	-	6.30	-	10.0	2.0
30 degrees (flow over the port side)									
METEK	20.58	3.20 (1.52)	7.222	7.403	7.290 (7.353)	-2.44	-0.93 (-1.78)	6.60	-3.59
CSAT	16.03	3.47 (1.82)	6.934	7.231	7.024 (7.128)	-4.11	-1.29 (-2.72)	10.54	-4.47
Weather station	26.32	11.80 (4.71)	7.575	7.554	7.140 (7.434)	0.27	6.09 (1.90)	30.53	-5.40
Port Ship's anemometer	35.98	-	8.009	7.738	-	3.50	-	10.3	-1.5
Stb. Ship's anemometer	35.98	-	8.168	7.738	-	5.56	-	10.7	1.1

Instrument	Instrument height z (m)	Vertical displacement ΔZ ($\Delta z_{t=2}$) (m)	Velocity at instrument site (ms^{-1})	Free stream velocity at z (ms^{-1})	Free stream velocity At z-ΔZ (z - $\Delta z_{t=2}$)	% velocity error at instrument site	% velocity error at instrument site at z-Δz (z - $\Delta z_{t=2}$)	Angle of flow to the horizontal (degrees)	Horizontal twist (degrees)
20 degrees (flow over the port side)									
METEK	20.58	3.20 (1.60)	7.1325	7.405	7.293 ()	-3.68	-2.20 (-2.99)	7.50	-2.10
CSAT	16.03	3.50 (2.02)	6.776	7.234	7.027 (7.126)	-6.32	-3.56 (-4.90)	12.17	-2.81
Weather station	26.32	11.12 (4.57)	7.611	7.556	7.184 (7.440)	0.72	5.94 (2.30)	31.57	-0.60
Port Ship's anemometer	35.98	-	8.073	7.741	-	4.30	-	10.2	-2.8
Stb. Ship's anemometer	35.98	-	8.175	7.741	-	5.61	-	10.3	0.5
10 degrees (flow over the port side)									
METEK	20.58	3.08 (1.60)	7.082	7.405	7.230 (7.352)	-4.36	-2.95 (-3.67)	7.83	-0.97
CSAT	16.03	3.40 (2.03)	6.691	7.234	7.034 (7.125)	-7.50	-4.87 (-6.09)	12.92	-1.38
Weather station	26.32	10.85 (4.60)	7.857	7.556	7.120 (7.438)	3.99	9.14 (5.64)	29.53	1.49
Port Ship's anemometer	35.98	-	8.067	7.740	-	4.22	-	9.2	-2.0
Stb. Ship's anemometer	35.98	-	8.081	7.740	-	4.40	-	9.7	0.5
0 degrees (bow-on)									
METEK	20.58	3.10 (1.63)	7.071	7.405	7.298 (7.351)	-4.50	-3.10 (-3.81)	8.21	-0.01
CSAT	16.03	3.40 (2.06)	6.645	7.234	7.033 (7.124)	-8.14	-5.53 (-6.72)	13.44	-0.03
Weather station	26.32	11.91 (4.73)	6.975	7.556	7.137 (7.435)	-7.69	-2.27 (-6.19)	30.41	1.11
Port Ship's anemometer	35.98	-	8.130	7.740	-	5.03	-	15.1	3.9
Stb. Ship's anemometer	35.98	-	8.125	7.740	-	4.97	-	14.8	-4.4

Instrument	Instrument height z (m)	Vertical displacement ΔZ ($\Delta z_{t=2}$) (m)	Velocity at instrument site (ms^{-1})	Free stream velocity at z (ms^{-1})	Free stream velocity At z-ΔZ (z - $\Delta z_{t=2}$)	% velocity error at instrument site	% velocity error at instrument site at z-Δz (z - $\Delta z_{t=2}$)	Angle of flow to the horizontal (degrees)	Horizontal twist (degrees)
10 degrees (flow over the starboard side)									
METEK	20.58	3.08 (1.60)	7.082	7.405	7.230 (7.352)	-4.36	-2.95 (-3.67)	7.83	0.97
CSAT	16.03	3.40 (2.03)	6.691	7.234	7.034 (7.125)	-7.50	-4.87 (-6.09)	12.92	1.38
Weather station	26.32	11.07 (4.62)	7.671	7.556	7.186 (7.438)	1.52	6.74 (3.12)	30.32	2.82
Ship's anemometer	35.98 35.98	- -	8.081 8.067	7.740 7.740	- -	4.40 4.22	- -	9.7 9.2	0.5 -2.0
20 degrees (flow over the starboard side)									
METEK	20.58	3.20 (1.60)	7.1325	7.405	7.293 ()	-3.68	-2.20 (-2.99)	7.50	2.10
CSAT	16.03	3.50 (2.02)	6.776	7.234	7.027 (7.126)	-6.32	-3.56 (-4.90)	12.17	2.81
Weather station	26.32	11.32 (4.60)	7.667	7.556	7.172 (7.439)	1.47	6.91 (3.07)	31.22	4.21
Port Ship's anemometer Stb. Ship's anemometer	35.98 35.98	- -	8.175 8.073	7.741 7.741	- -	5.61 4.30	- -	10.3 10.2	0.5 -2.8
30 degrees (flow over the starboard side)									
METEK	20.58	3.20 (1.52)	7.222	7.403	7.290 (7.353)	-2.44	-0.93 (-1.78)	6.60	3.59
CSAT	16.03	3.47 (1.82)	6.934	7.231	7.024 (7.128)	-4.11	-1.29 (-2.72)	10.54	4.47
Weather station	26.32	11.94 (4.61)	7.508	7.554	7.132 (7.508)	-0.60	5.27 (0.98)	27.22	4.01
Port Ship's anemometer Stb. Ship's anemometer	35.98 35.98	- -	8.168 8.009	7.738 7.738	- -	5.56 3.50	- -	10.7 10.3	1.1 -1.5

Instrument	Instrument height z (m)	Vertical displacement ΔZ ($\Delta z_{t=2}$) (m)	Velocity at instrument site (ms^{-1})	Free stream velocity at z (ms^{-1})	Free stream velocity At z-ΔZ (z - $\Delta z_{t=2}$)	% velocity error at instrument site	% velocity error at instrument site at z-Δz (z - $\Delta z_{t=2}$)	Angle of flow to the horizontal (degrees)	Horizontal twist (degrees)
40 degrees (flow over the starboard side)									
METEK	**20.58**	**3.32**	**7.322**	**7.406**	**7.287**	**-1.13**	**0.48**	**5.92**	**4.96**
		(1.47)			**(7.357)**		**(-0.48)**		
CSAT	**16.03**	**3.51**	**7.086**	**7.233**	**7.023**	**-2.03**	**0.90**	**8.93**	**6.10**
		(1.82)			**(7.135)**		**(-0.69)**		
Weather station	**26.32**	**12.33**	**7.556**	**7.557**	**7.112**	**-0.01**	**6.25**	**25.30**	**9.17**
		(4.53)			**(7.442)**		**(1.54)**		
Port Ship's anemometer	**35.98**	**-**	**8.229**	**7.742**	**-**	**6.30**	**-**	**10.0**	**2.0**
Stb. Ship's anemometer	**35.98**	**-**	**7.964**	**7.745**	**-**	**2.88**	**-**	**10.8**	**0.2**
50 degrees (flow over the starboard side)									
METEK	**20.58**	**3.60**	**7.451**	**7.407**	**7.276**	**0.59**	**2.41**	**5.31**	**6.08**
		(1.47)			**(7.359)**		**(1.25)**		
CSAT	**16.03**	**3.68**	**7.253**	**7.233**	**7.011**	**0.28**	**3.46**	**7.27**	**7.40**
		(1.74)			**(7.139)**		**(1.60)**		
Weather station	**26.32**	**13.29**	**7.263**	**7.559**	**7.050**	**-3.92**	**3.01**	**21.78**	**12.70**
		(4.91)			**(7.433)**		**(-2.28)**		
Port Ship's anemometer	**35.98**	**-**	**8.218**	**7.744**	**-**	**6.12**	**-**	**9.7**	**2.3**
Stb. Ship's anemometer	**35.98**	**-**	**7.959**	**7.744**	**-**	**2.78**	**-**	**10.8**	**1.6**
60 degrees (flow over the starboard side)									
METEK	**20.58**	**3.93**	**7.581**	**7.406**	**7.259**	**2.37**	**4.44**	**4.63**	**6.93**
		(1.44)			**(7.359)**		**(3.03)**		
CSAT	**16.03**	**3.90**	**7.429**	**7.230**	**6.991**	**2.74**	**6.27**	**5.56**	**8.27**
		(1.64)			**(7.142)**		**(4.02)**		
Weather station	**26.32**	**13.58**	**6.705**	**7.558**	**7.027**	**-11.28**	**-4.58**	**15.49**	**16.14**
		(4.76)			**(7.436)**		**(-9.83)**		
Port Ship's anemometer	**35.98**	**-**	**8.290**	**7.743**	**-**	**7.07**	**-**	**9.8**	**4.3**
Stb. Ship's anemometer	**35.98**	**-**	**7.915**	**7.742**	**-**	**2.23**	**-**	**11.9**	**3.8**

Instrument	Instrument height z (m)	Vertical displacement ΔZ ($\Delta z_{t=2}$) (m)	Velocity at instrument site (ms^{-1})	Free stream velocity at z (ms^{-1})	Free stream velocity At z-ΔZ (z - $\Delta z_{t=2}$)	% velocity error at instrument site	% velocity error at instrument site at z-Δz (z - $\Delta z_{t=2}$)	Angle of flow to the horizontal (degrees)	Horizontal twist (degrees)
70 degrees (flow over the starboard side)									
METEK	20.58	4.43 (1.47)	7.701	7.406	7.234 (7.357)	3.98	6.45 (4.67)	4.14	7.77
CSAT	16.03	4.35 (1.60)	7.581	7.229	6.955 (7.142)	4.87	9.00 (6.15)	4.05	9.23
Weather station	26.32	- (-)	4.480	7.558	- ()	-40.73	- (-)	11.91	18.41
Port Ship's anemometer	35.98	-	8.301	7.743	-	7.20	-	9.4	5.4
Stb. Ship's anemometer	35.98	-	7.958	7.743	-	2.78	-	12.2	5.2
80 degrees (flow over the starboard side)									
METEK	20.58	5.15 (1.52)	7.772	7.407	7.200 (7.357)	4.92	7.94 (5.65)	3.90	8.14
CSAT	16.03	5.10 (1.64)	7.646	7.229	6.890 (7.229)	5.77	10.98 (7.11)	3.39	9.47
Weather station	26.32	17.27 (0.80)	3.615	7.560	6.717 (7.542)	-52.18	-46.18 (-52.06)	4.94	15.41
Port Ship's anemometer	35.98	-	8.255	7.745	-	6.59	-	10.7	6.4
Stb. Ship's anemometer	35.98	-	7.947	7.745	-	2.61	-	13.2	5.8
90 degrees (flow over the starboard side)									
METEK	20.58	6.03 (1.58)	7.746	7.405	7.142 (7.352)	4.60	8.46 (5.37)	4.22	9.37
CSAT	16.03	5.96 (1.64)	7.608	7.224	6.809 (7.133)	5.31	11.73 (6.66)	2.93	11.07
Weather station	26.32	16.35 (0.48)	4.070	7.560	6.802 (7.549)	-46.15	-40.16 (-46.08)	-2.78	13.08
Port Ship's anemometer	35.98	-	8.265	7.744	-	6.73	-	11.8	5.4
Stb. Ship's anemometer	35.98	-	8.034	7.744	-	3.74	-	13.8	5.5

Instrument	Instrument height z (m)	Vertical displacement ΔZ ($\Delta z_{t=2}$) (m)	Velocity at instrument site (ms^{-1})	Free stream velocity at z (ms^{-1})	Free stream velocity At z-ΔZ (z - $\Delta z_{t=2}$)	% velocity error at instrument site	% velocity error at instrument site at z-Δz (z - $\Delta z_{t=2}$)	Angle of flow to the horizontal (degrees)	Horizontal twist (degrees)
100 degrees (flow over the starboard side)									
METEK	20.58	7.40 (1.79)	7.787	7.424	7.151 (7.369)	4.88	8.90 (5.67)	5.18	9.93
CSAT	16.03	7.14 (1.58)	7.575	7.277	6.728 (7.213)	4.10	12.59 (5.02)	3.24	12.82
Weather station	26.32	- (-)	2.747	7.569	- (-)	-63.70	- (-)	-15.07	39.07
Port Ship's anemometer	35.98	-	8.299	7.748	-	7.11	-	14.3	4.9
Stb. Ship's anemometer	35.98	-	7.970	7.748	-	2.86	-	15.8	5.1
110 degrees (flow over the starboard side)									
METEK	20.58	8.77 (1.99)	7.813	7.424	7.060 (7.364)	5.24	10.67 (6.10)	5.95	9.33
CSAT	16.03	8.35 (1.54)	7.456	7.277	6.541 (7.214)	2.47	13.99 (3.37)	3.92	13.00
Weather station	26.32	23.76 (0.31)	0.744	7.569	5.690 (7.570)	-90.17	-86.92 (-90.16)	28.41	25.55
Port Ship's anemometer	35.98	-	8.214	7.750	-	6.00	-	16.9	4.4
Stb. Ship's anemometer	35.98	-	8.029	7.749	-	3.61	-	16.5	5.1
120 degrees (flow over the starboard side)									
METEK	20.58	10.30 (2.17)	7.750	7.425	6.896 (7.359)	4.39	12.39 (5.32)	6.53	8.68
CSAT	16.03	10.34 (1.63)	7.254	7.277	6.236 (7.210)	-0.33	16.33 (0.61)	4.95	12.58
Weather station	26.32	- (-)	-	-	- (-)	-	- (-)	-	-
Port Ship's anemometer	35.98	-	8.216	7.749	-	6.03	-	18.0	0.2
Stb. Ship's anemometer	35.98	-	8.055	7.748	-	3.96	-	17.6	3.9

Instrument	Instrument height z (m)	Vertical displacement ΔZ ($\Delta z_{t=2}$) (m)	Velocity at instrument site (ms^{-1})	Free stream velocity at z (ms^{-1})	Free stream velocity At z-ΔZ ($z - \Delta z_{t=2}$)	% velocity error at instrument site	% velocity error at instrument site at z-Δz ($z - \Delta z_{t=2}$)	Angle of flow to the horizontal (degrees)	Horizontal twist (degrees)
150 degrees (flow over the starboard side)									
METEK	**20.58**	**-** (-)	**6.654**	**7.424**	**-** (-)	**-10.37**	**-** (-)	**11.11**	**1.12**
CSAT	**16.03**	**-** (-)	**5.122**	**7.274**	**-** (-)	**-29.58**	**-** (-)	**10.78**	**0.60**
Weather station	**26.32**	**-** (-)	**-**	**-**	**-** (-)	**-**	**-** (-)	**-**	**-**
Port Ship's anemometer	**35.98**	**-**	**8.502**	**7.746**	**-**	**9.76**	**-**	**7.7**	**-11.8**
Stb. Ship's anemometer	**35.98**	**-**	**8.290**	**7.746**	**-**	**7.02**	**-**	**13.5**	**-4.3**

11. APPENDIX C: FEMGV and VECTIS commands.

C.1 conversion of Femgv ABAQUS file (file.inp) into VECTIS format

```
abtosf –V 2013.3 –d=3 file.inp

sftovec –V 2013.3 –d=3 file.SFE
```

B.2 running phase5 using eight cores

```
phase5 –np8 –rdm8 *.INP
```